PARTICLE-IN-CELL SIMULATIONS FOR LASER-DRIVEN EXPERIMENTS

Emmanuel d'Humières
CELIA - Université de Bordeaux

Outline

Part 1

- Introduction to plasma simulation
- The Particle In Cell method
- Parallelization and supercomputers
- How to launch a Particle in Cell simulation

Part 2

- Additional physical modules
- Examples of PIC simulations of high intensity LPI
- Available tutorials
- Prospects for the near future

PW laser generates high energy particles

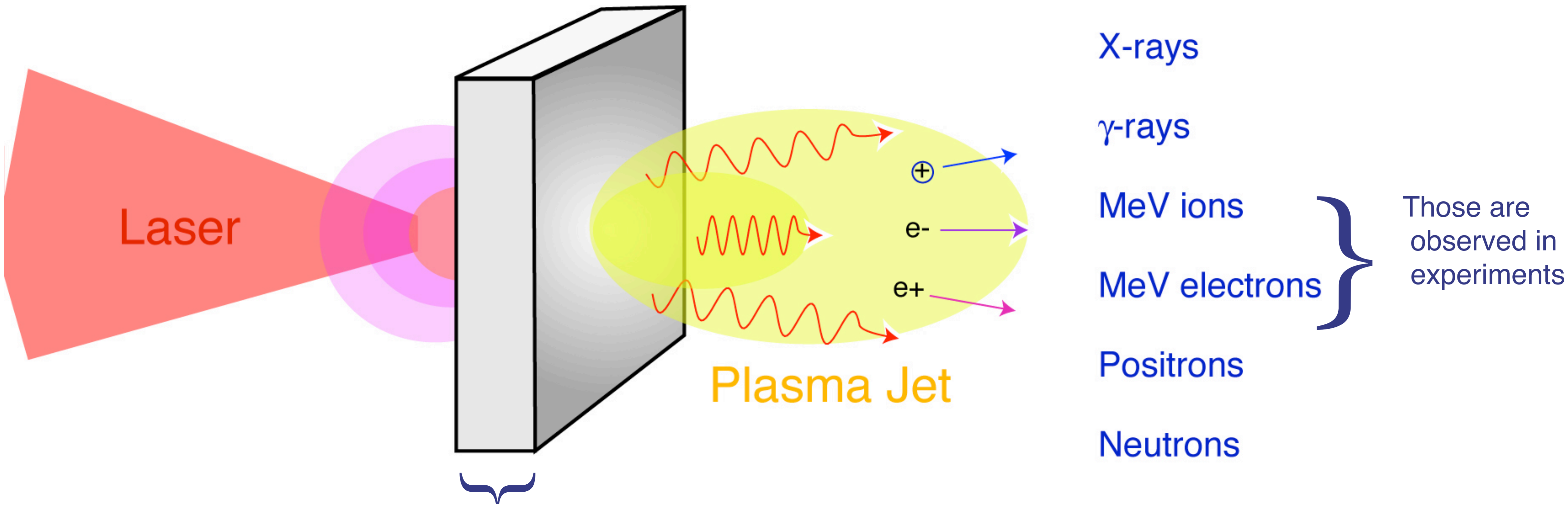

Everything happens in less than a picosecond (10^{-12}s).
(no way to see inside the target)

To understand what's going on, numerical simulation on supercomputer is necessary!

Laser intensity increase and computing power increase versus time

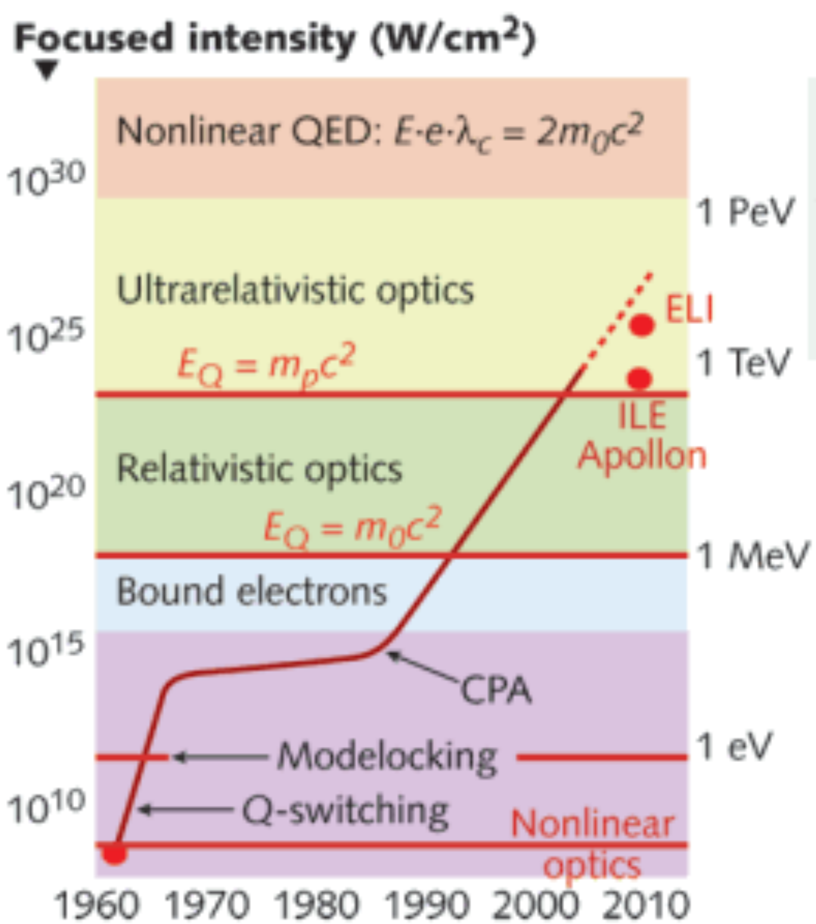

Ultrarelativistic intensity is defined with respect to the proton $E_Q = m_pc^2$, intensity ~10^{24} W/cm^2

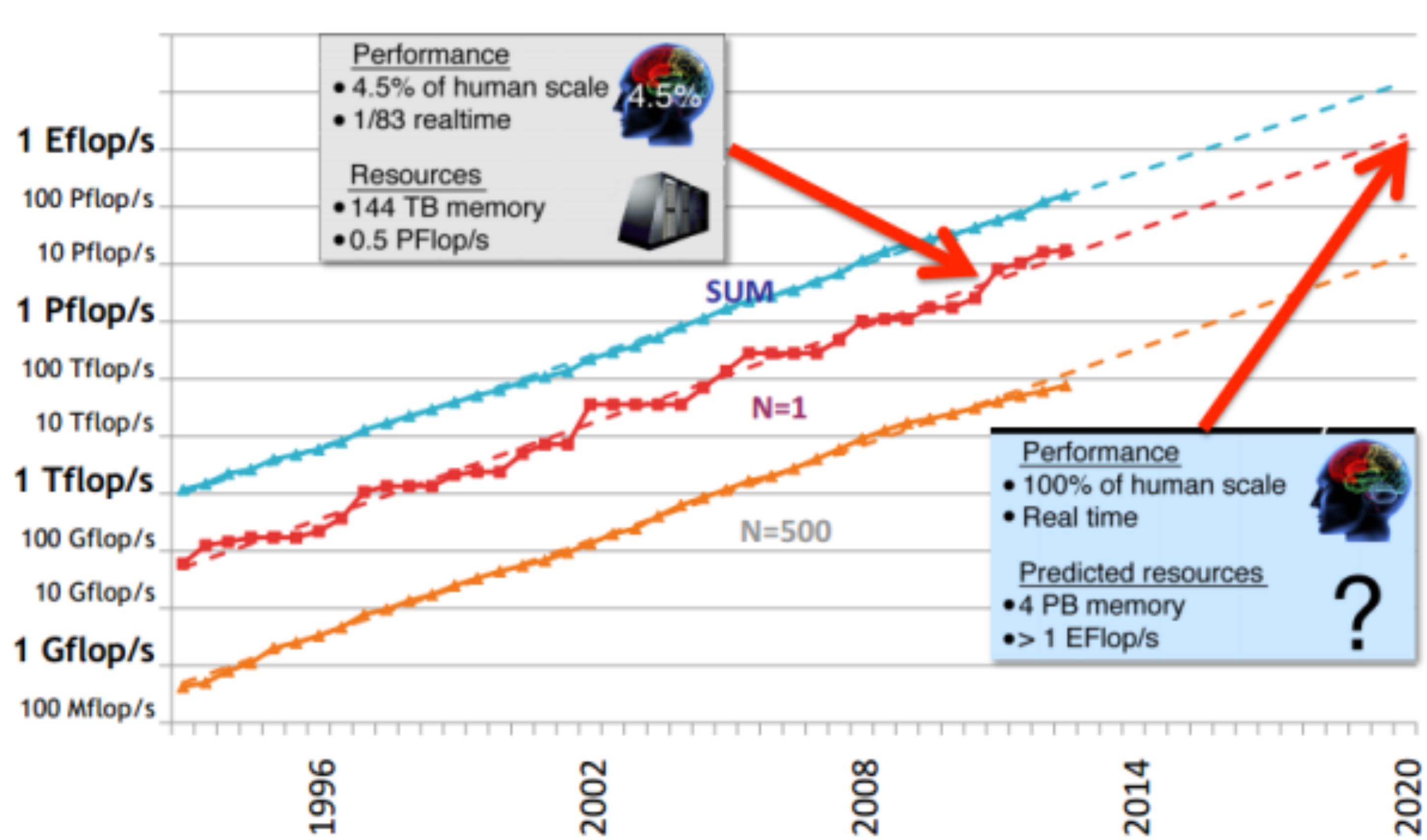

Introduction to plasma simulation

Laser generated plasmas simulation

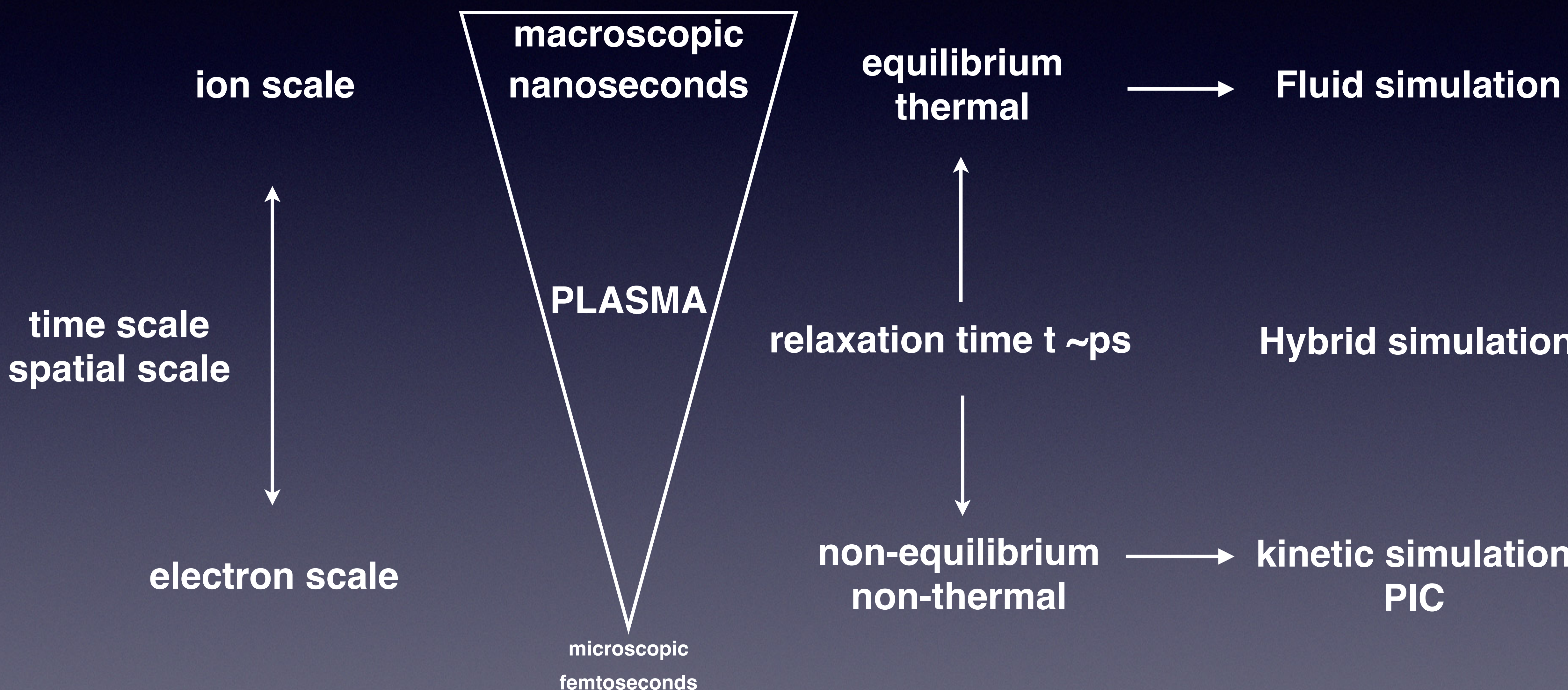

From hydro to PIC simulations

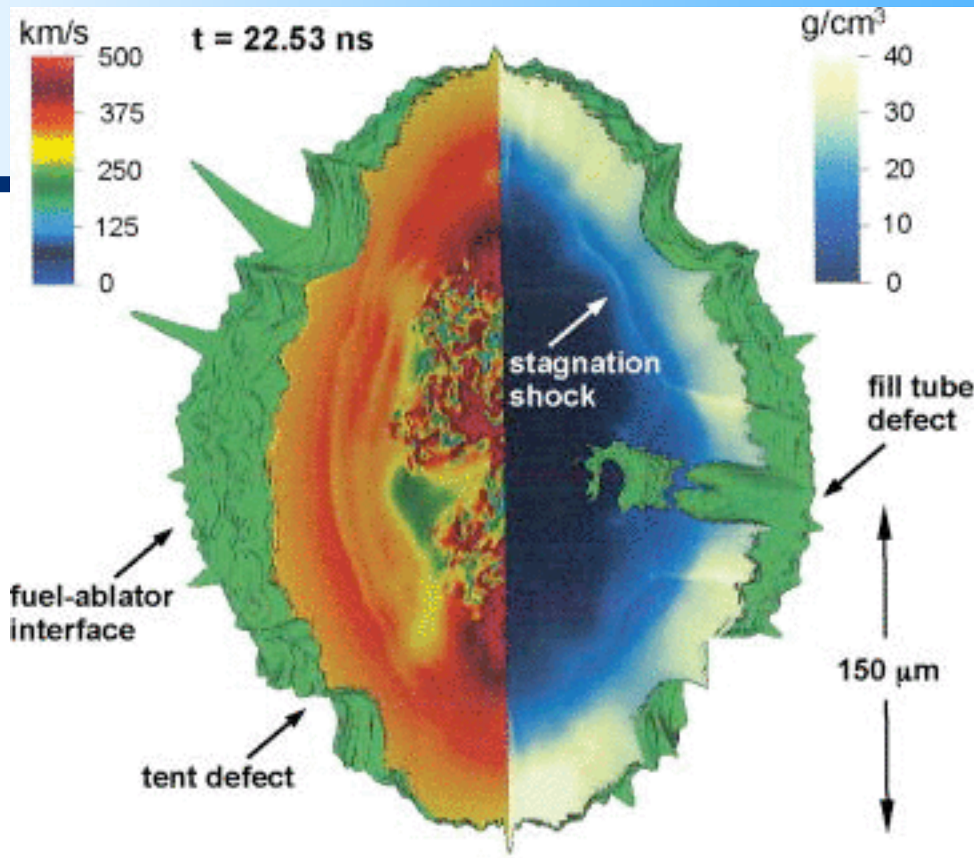

HYDRA (LLNL) D.S. Clark et al. Physics of Plasmas 22, 022703 (2015)

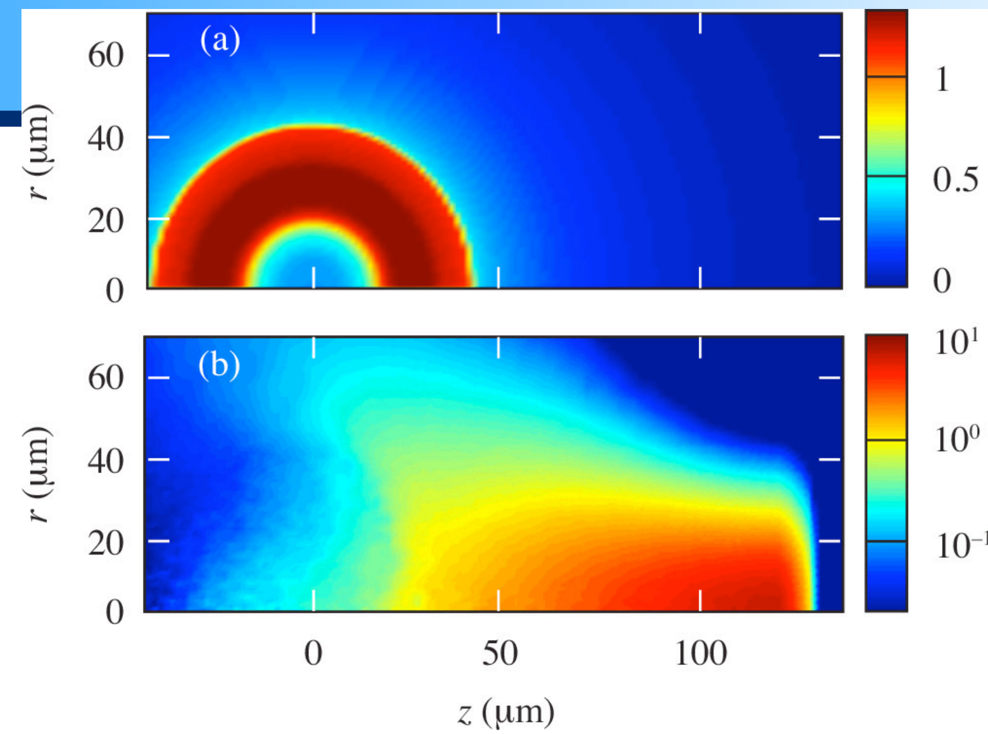

Hybrid code LSP A.A. Solodov et al. Physics of Plasmas 15, 112702 (2008)

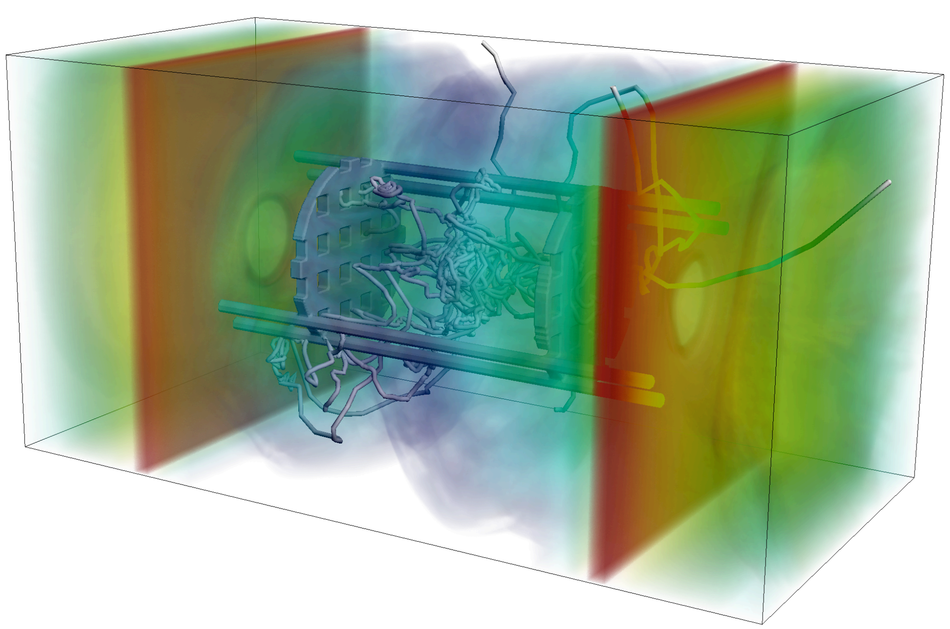

https://flash.rochester.edu/site/flashcode/

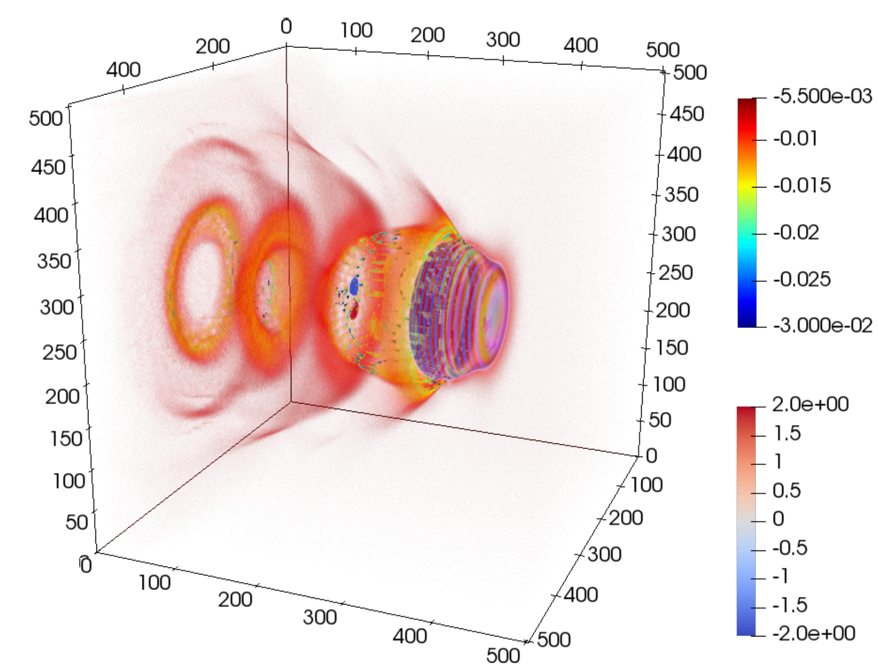

source: SMILEI dev-team

Plasma (1)
Plasma is a group of charged particles

Charge neutral

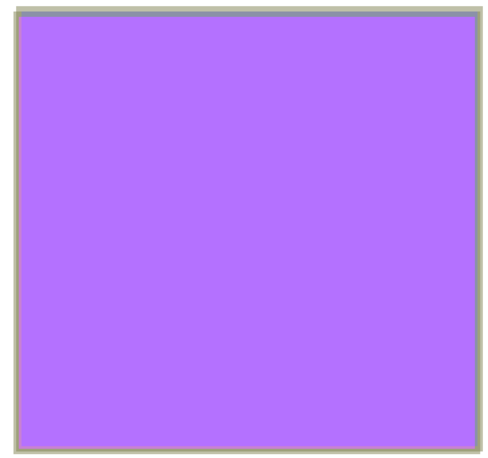

Charge separation

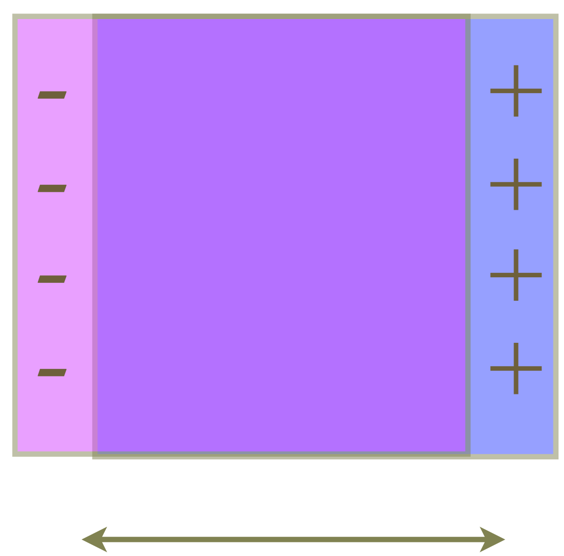

Plasma frequency

$$\omega_{pe} = \sqrt{\frac{4\pi e^2 n_e}{m_e}}$$

Electrons are oscillating with ω_{pe}.

Plasma (2)
Charge shielding in plasma

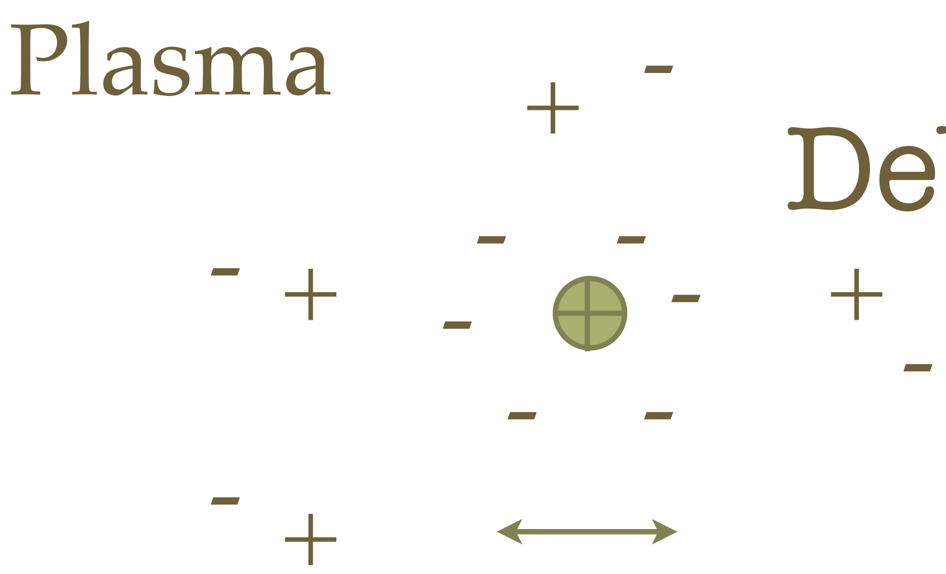

Debye shielding

~Debye length

$$\lambda_D = \frac{v_e}{\omega_{pe}} \propto \frac{v_e}{\sqrt{n_e}}$$

v_e: electron's thermal velocity

Particle Simulation

Courtesy of Y. Sentoku

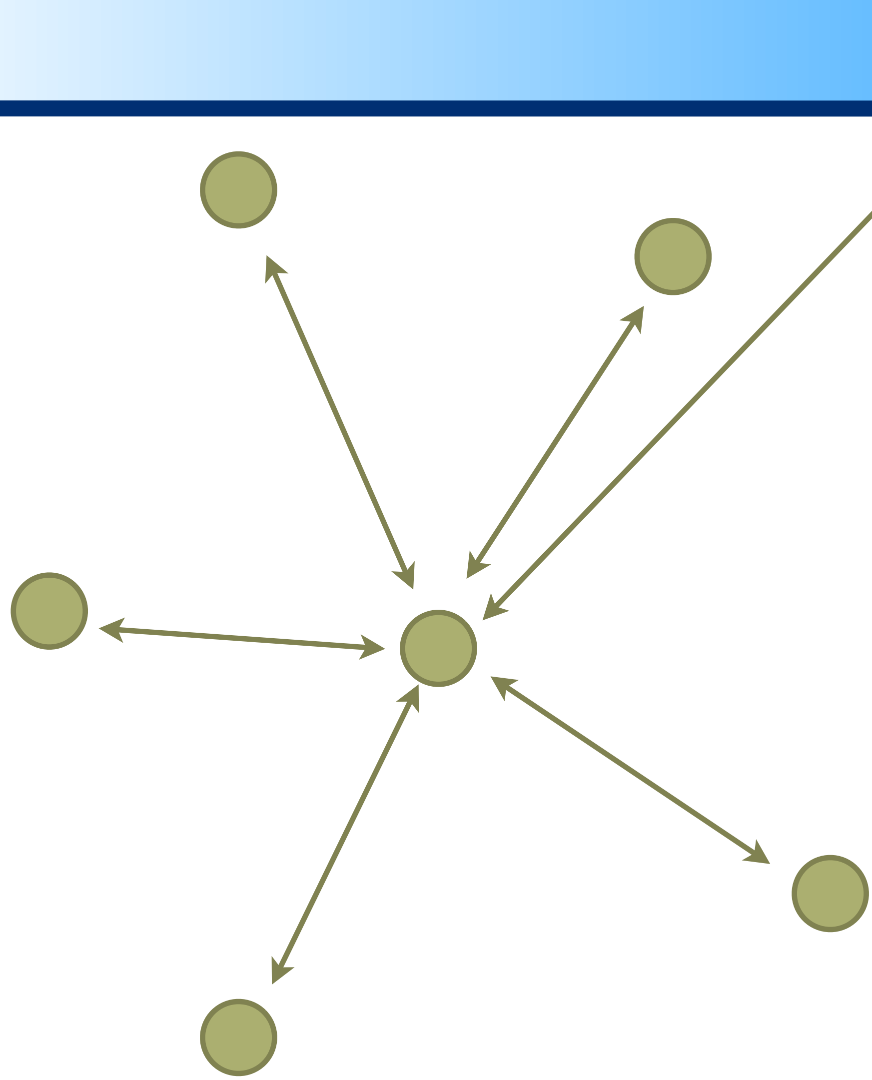

Astrophysics

need to calculate gravity from all the other stars.

Debye shielding

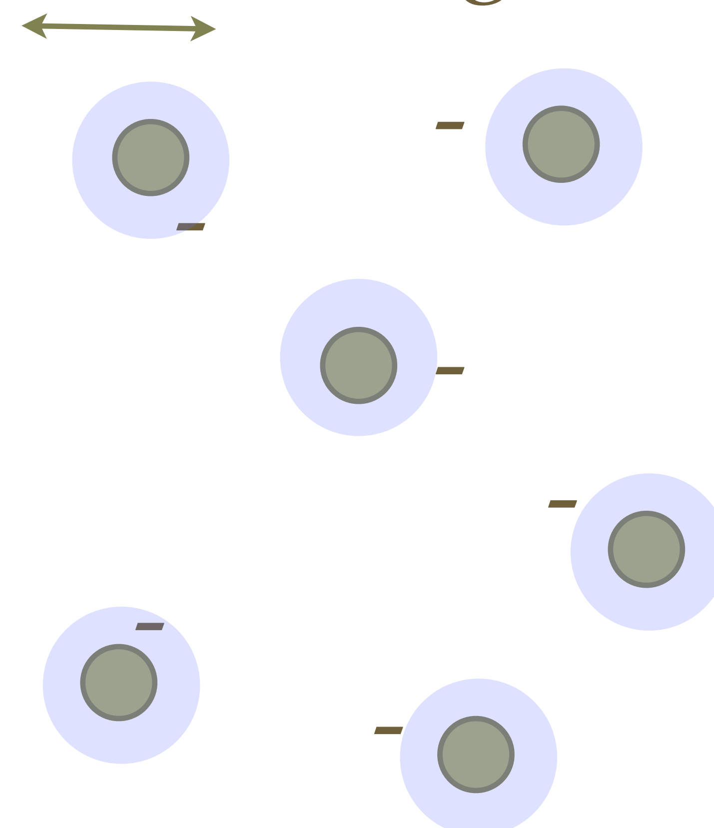

Plasma physics

calculate the Coulomb force only from inside the Debye sphere.

The Particle In Cell method

The Vlasov-Maxwell system of equations

Plasma (all species are represented by their dist. function)

$$\partial_t f_s + \frac{\mathbf{p}}{m_s \gamma} \cdot \nabla f_s + \mathbf{F}_L \cdot \nabla_{\mathbf{p}} f_s = 0$$

$$\mathbf{F}_L = q_s \left(\mathbf{E} + \frac{\mathbf{p}}{m_s \gamma} \times \mathbf{B} \right)$$

$$\rho(t, \mathbf{x}) = \int d\mathbf{p} f_s(t, \mathbf{x}, \mathbf{p})$$

$$J(t, \mathbf{x}) = q_s \int d\mathbf{p} \, \frac{\mathbf{p}}{m_s \gamma} \, f_s(t, \mathbf{x}, \mathbf{p})$$

Electromagnetic Field

$$\nabla \cdot \mathbf{E} = \frac{\rho}{\epsilon_0} \qquad \partial_t \mathbf{E} = -\frac{1}{\epsilon_0} \mathbf{J} + c^2 \nabla \times \mathbf{B}$$

$$\nabla \cdot \mathbf{B} = 0 \qquad \partial_t \mathbf{B} = -\nabla \times \mathbf{E}$$

Introduction to Plasma Theory
D. R. Nicholson

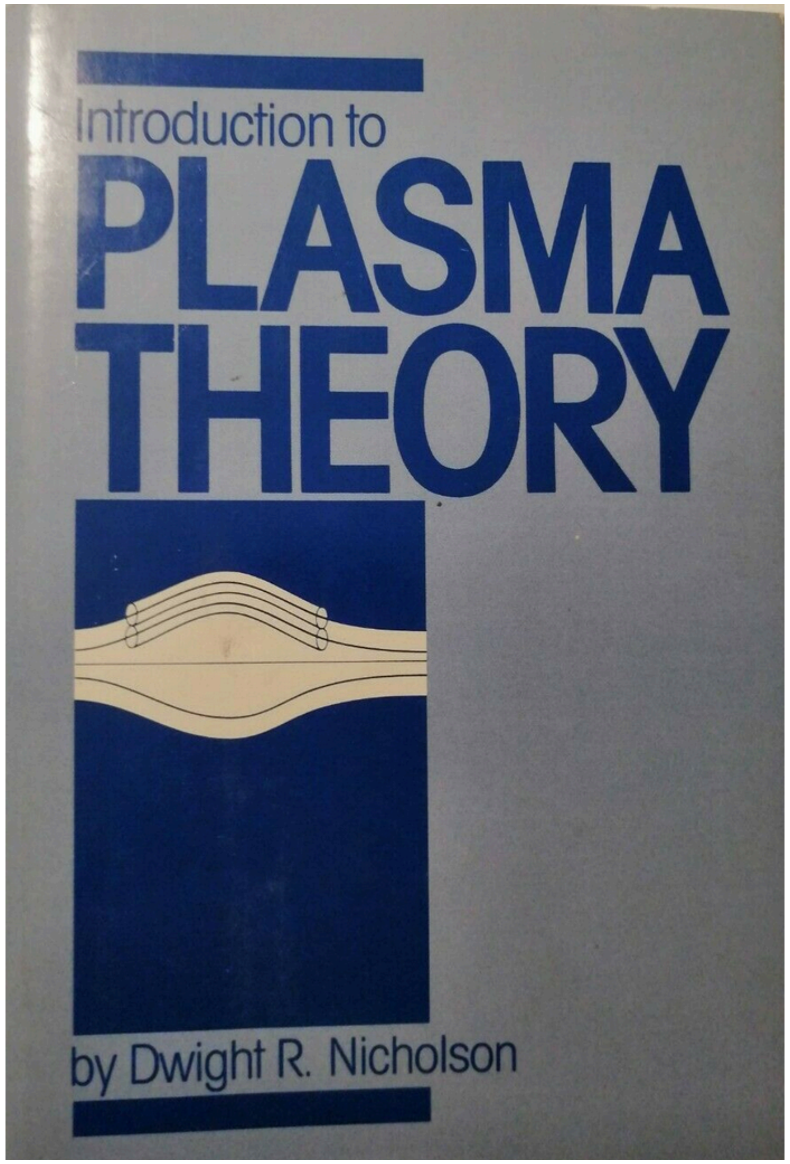

Courtesy of M. Grech

Vlasov equation in a nutshell

Starting point : Klimontovich's exact picture

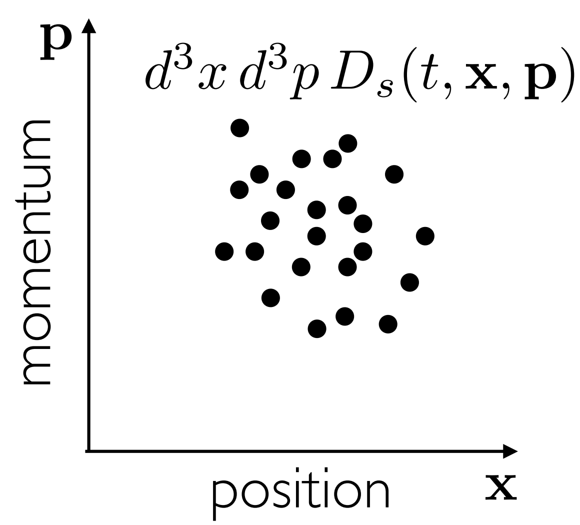

If the exact state of the system is know at a time t_0

Ds ≡ Phase space density

$$D_s(t_0, \mathbf{x}, \mathbf{p}) = \sum_p \delta(\mathbf{x} - \mathbf{x}_p(t_0))\, \delta(\mathbf{p} - \mathbf{p}_p(t_0))$$

the evolution of the system at later times is known exactly and satisfies the Klimontovich equation:

$$\boxed{\partial_t D_s + \mathbf{p} \cdot \nabla\, D_s + q_s(\mathbf{E}_{\rm tot} + \mathbf{v} \times \mathbf{B}_{\rm tot}) \cdot \nabla_p\, D_s = 0\,.}$$

Ensemble averaging : towards the plasma kinetic equation and Vlasov equation

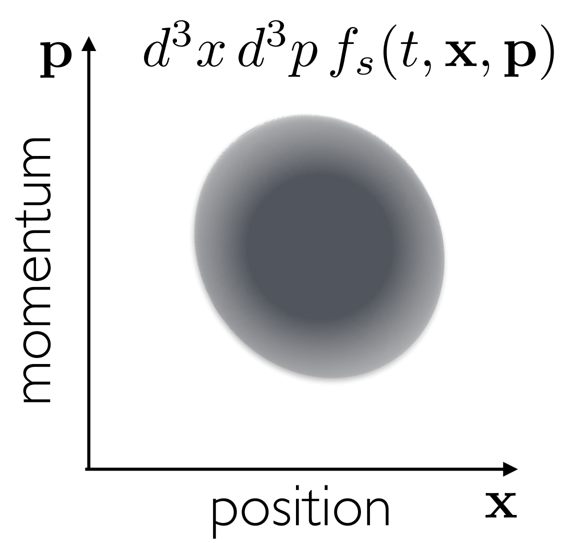

$$\begin{aligned}
\overbrace{D_s(\mathbf{x}, \mathbf{v}, t)}^{\text{total}} &= \overbrace{f_s(\mathbf{x}, \mathbf{v}, t)}^{\text{smooth, average}} + \overbrace{\delta D_s(\mathbf{x}, \mathbf{v}, t)}^{\text{microscopic fluctuations}} \\
\mathbf{E}_{\rm tot}(\mathbf{x}, t) &= \mathbf{E}(\mathbf{x}, t) + \delta\mathbf{E}(\mathbf{x}, t) \\
\mathbf{B}_{\rm tot}(\mathbf{x}, t) &= \mathbf{B}(\mathbf{x}, t) + \delta\mathbf{B}(\mathbf{x}, t)\rangle
\end{aligned}$$

Pluging this in Klimontovich equation and ensemble averaging leads:

$$\boxed{\partial_t f_s + \mathbf{p} \cdot \nabla\, f_s + q_s(\mathbf{E} + \mathbf{v} \times \mathbf{B}) \cdot \nabla_p\, f_s = -q_s \left\langle (\delta\mathbf{E} + \mathbf{v} \times \delta\mathbf{B})\, \delta f_s \right\rangle\,.}$$

collective behavior microscopic/collisions

Courtesy of M. Grech

Our starting point is the Vlasov-Maxwell description for a *collisionless* plasma

Plasma (all species are represented by their dist. function)

$$\partial_t f_s + \frac{\mathbf{p}}{m_s \gamma} \cdot \nabla f_s + \mathbf{F}_L \cdot \nabla_{\mathbf{p}} f_s = 0$$

$$\mathbf{F}_L = q_s \left(\mathbf{E} + \frac{\mathbf{p}}{m_s \gamma} \times \mathbf{B} \right)$$

$$\rho(t, \mathbf{x}) = \int d\mathbf{p} f_s(t, \mathbf{x}, \mathbf{p})$$

$$J(t, \mathbf{x}) = q_s \int d\mathbf{p} \frac{\mathbf{p}}{m_s \gamma} f_s(t, \mathbf{x}, \mathbf{p})$$

Electromagnetic Field

$$\nabla \cdot \mathbf{E} = \frac{\rho}{\epsilon_0} \qquad \partial_t \mathbf{E} = -\frac{1}{\epsilon_0} \mathbf{J} + c^2 \nabla \times \mathbf{B}$$

$$\nabla \cdot \mathbf{B} = 0 \qquad \partial_t \mathbf{B} = -\nabla \times \mathbf{E}$$

The standard electromagnetic PIC code solves this set of equation !

Courtesy of M. Grech

References

Plasma Physics via Computer Simulation
C. K. Birdsall & A. B. Langdon

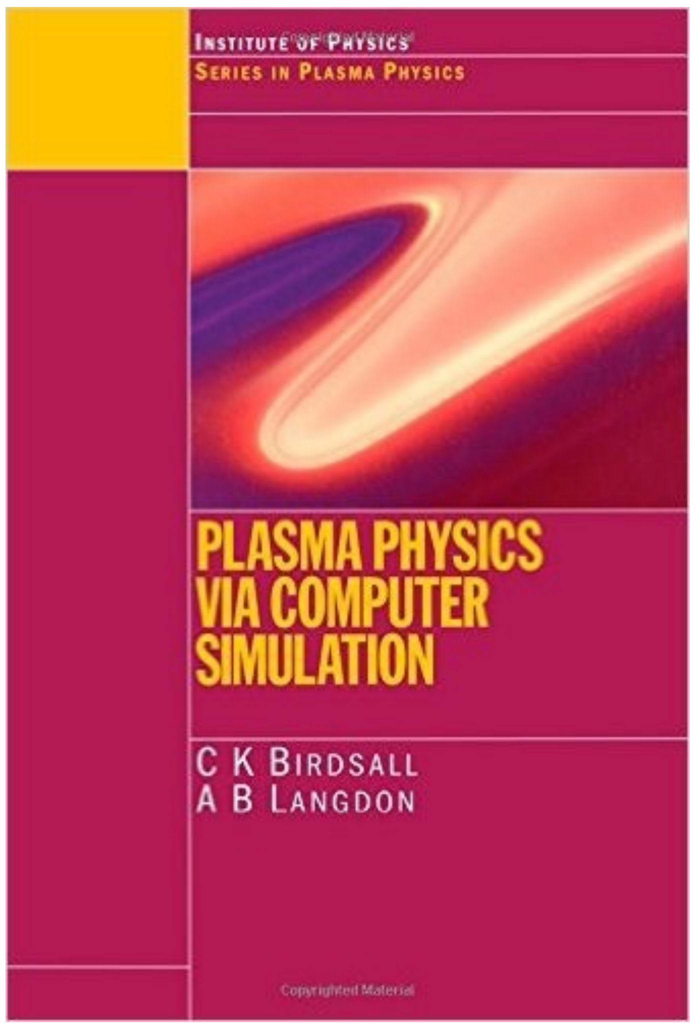

Computational Electrodynamics
A. Taflove

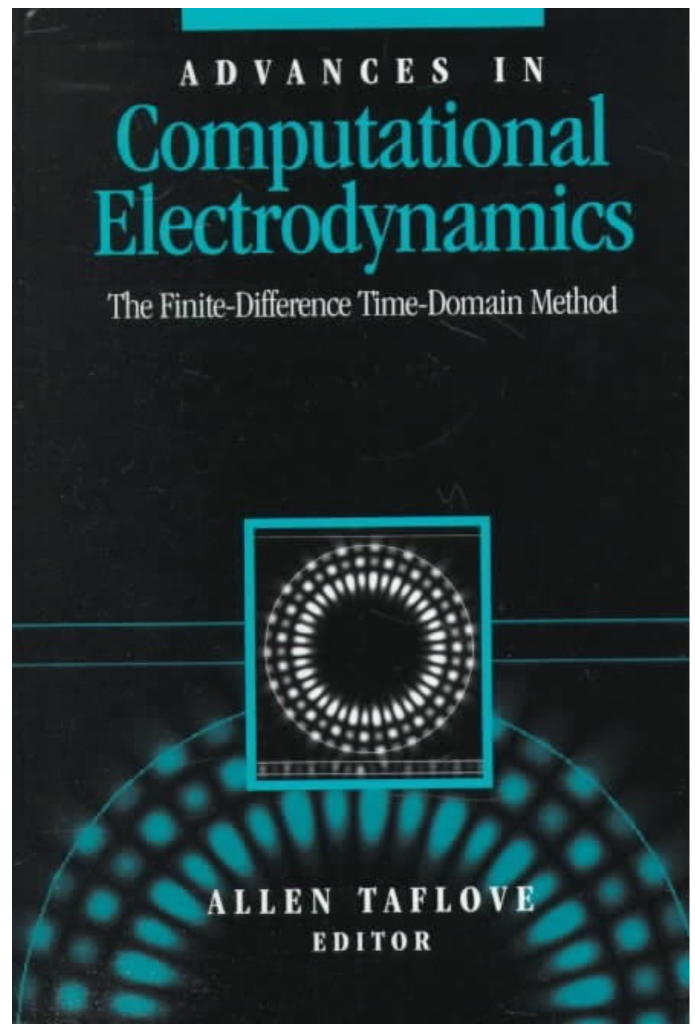

Numerical Recipies
W. H. Press *et al.*

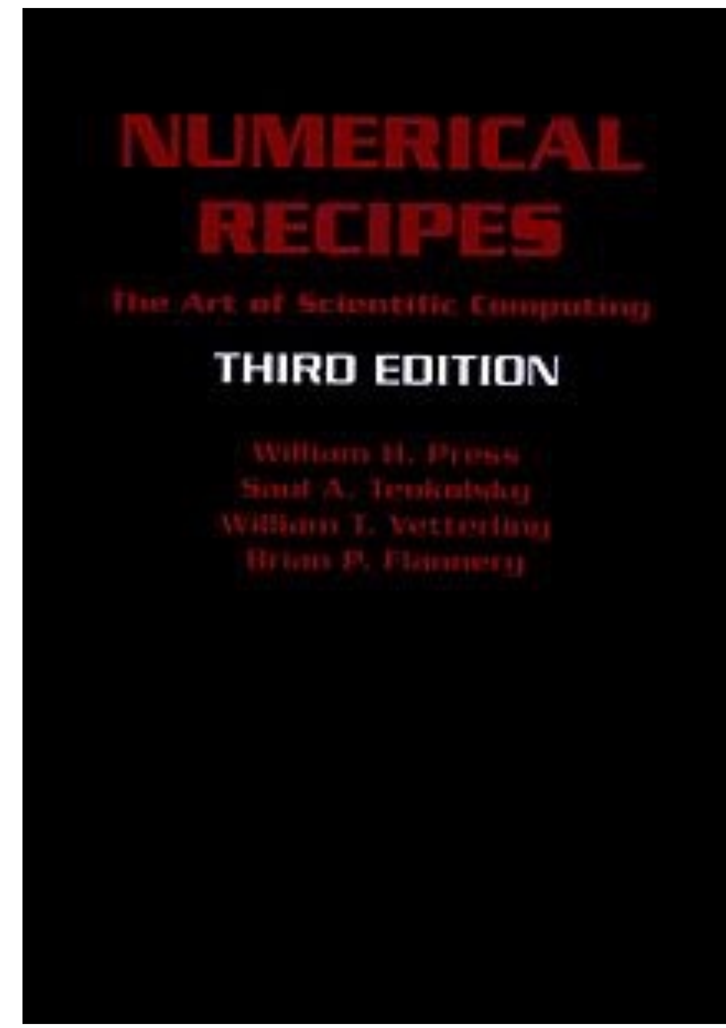

1st Remark

Normalization: the Vlasov-Maxwell (relativistic) description provides us with a set of natural units

Plasma

$$\partial_t f_s + \frac{\mathbf{p}}{m_s \gamma} \cdot \nabla f_s + \mathbf{F}_L \cdot \nabla_{\mathbf{p}} f_s = 0$$

Electromagnetic Field

$$\nabla \cdot \mathbf{E} = \rho \qquad \partial_t \mathbf{E} = -\mathbf{J} + \nabla \times \mathbf{B}$$

$$\nabla \cdot \mathbf{B} = 0 \qquad \partial_t \mathbf{B} = -\nabla \times \mathbf{E}$$

Velocity	c
Charge	e
Mass	m_e
Momentum	$m_e\, c$
Energy, Temperature	$m_e c^2$
Time	ω_r^{-1}
Length	c/ω_r
Number density	$n_r = \epsilon_0\, m_e\, \omega_r^2/e^2$
Current density	$e\, c\, n_r$
Pressure	$m_e\, c^2\, n_r$
Electric field	$m_e\, c\, \omega_r/e$
Magnetic field	$m_e\, \omega_r/e$
Poynting flux	$m_e\, c^3\, n_r/2$

The value of ω_r is not defined *a priori*, and acts as a *scaling factor*.

Courtesy of M. Grech

Laser and plasma units in the code

- Laser electric field amplitude: $m_e\omega_0 c/e$ (3.2 TV/m for λ=1 µm)
- Magnetic fields: $m_e\omega_0/e$ (110 MG for λ=1 µm)
- Laser intensity related to a_0: $a_0=0.85*\mathrm{sqrt}(I_{18}\lambda^2)$
- Relation between laser frequency and critical density: $\omega_0/\omega_{pe}=1/\mathrm{sqrt}(n_e/n_c)$
- Lengths are in c/ω_0 or in wavelengths and times ω_0^{-1} or in laser periods.

2nd Remark

The Particle-In-Cell method integrates Vlasov Equation along the trajectories of so-called *quasi-particles*

Vlasov Eq. is a **partial differential equation** (PDE) in *Ns*+*Nv* phase-space:

$$\partial_t f_s + \frac{\mathbf{p}}{m_s \gamma} \cdot \nabla f_s + \mathbf{F}_L \cdot \nabla_{\mathbf{p}} f_s = 0$$

Direct integration (*Vlasov codes*) has tremendous computational cost!

The **PIC ansatz** consists in decomposing the distribution fct:

$$f_s(t, \mathbf{x}, \mathbf{p}) = \sum_{p=1}^{N} w_p \, S(\mathbf{x} - \mathbf{x}_p(t)) \, \delta(\mathbf{p} - \mathbf{p}_p(t))$$

Shape-function

Dirac-distribution

Courtesy of M. Grech

Initializing your PIC simulation

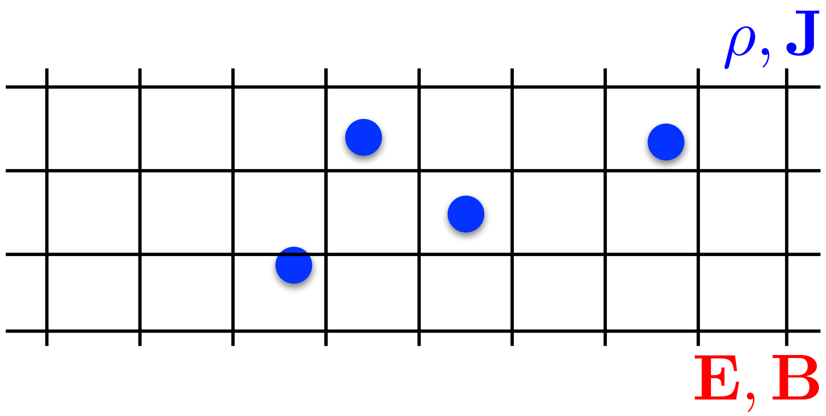

1) for each species of your plasma, create your quasi-particles
   e.g. defining the species density, velocity and temperature profiles

2) loop over all particles and project charge and current density onto the grid

3) knowing the charge density solve Poisson's Eq. to get the electrostatic field

4) add any (user defined) external fields provided they are divergence-free

Courtesy of M. Grech

The Particle-In-Cell loop

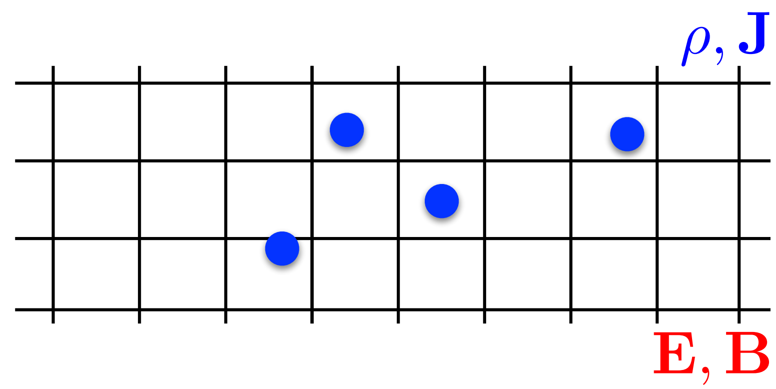

Gather fields at particle position

$$[\mathbf{E}, \mathbf{B}] \rightarrow [\mathbf{E}_p, \mathbf{B}_p]$$

Solve Maxwell's Eqs.

$$\partial_t \mathbf{E} = -\mathbf{J} + \nabla \times \mathbf{B}$$

$$\partial_t \mathbf{B} = -\nabla \times \mathbf{E}$$

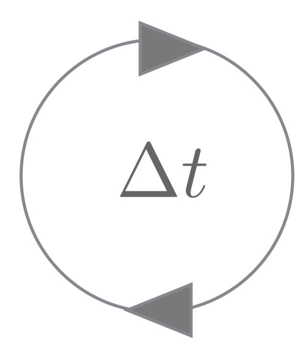

Push all particles

$$\forall p \quad d_t \mathbf{u}_p = \frac{q_s}{m_s} \mathbf{F}_L, \qquad d_t \mathbf{x}_p = \mathbf{u}_p / \gamma_p$$

Project current densities on grid*

$$[\mathbf{x}_p, \mathbf{p}_p] \rightarrow [\rho, \mathbf{J}]$$

* using a charge conserving scheme

Courtesy of M. Grech

Step 1

Field gathering: interpolation at particle position

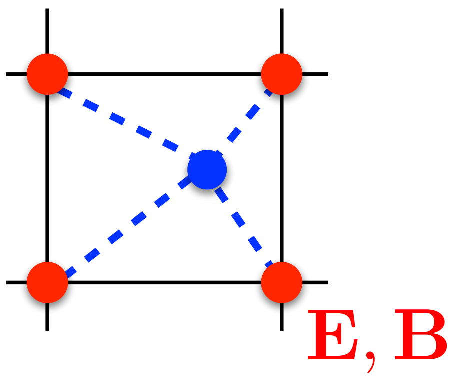

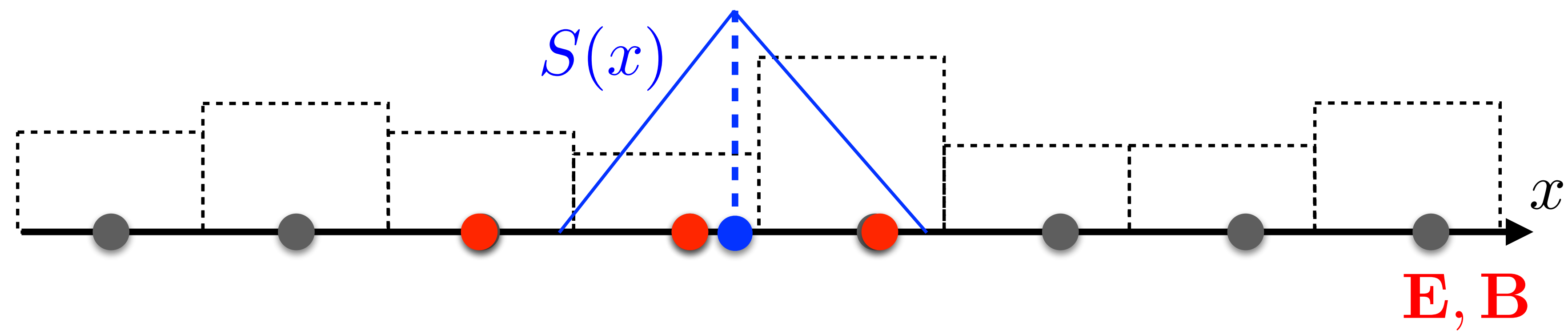

$$(\mathbf{E},\mathbf{B})_p \equiv \int d\mathbf{x}\,(\mathbf{E},\mathbf{B})(\mathbf{x})\,S(\mathbf{x}-\mathbf{x}_p)$$

$$\hat{s}^{(0)}(x) = \Delta x\,\delta(x),$$

$$\hat{s}^{(1)}(x) = \begin{cases} 1 \text{ if } |x| \le \frac{1}{2}\,\Delta x, \\ 0 \text{ otherwise,} \end{cases}$$

$$\boxed{\hat{s}^{(2)}(x) = \begin{cases} \left(1 - \left|\frac{x}{\Delta x}\right|\right) & \text{if } |x| \le \Delta x, \\ 0 & \text{otherwise,} \end{cases}}$$

$$\hat{s}^{(3)}(x) = \begin{cases} \frac{3}{4}\left[1 - \frac{4}{3}\left(\frac{x}{\Delta x}\right)^2\right] & \text{if } |x| \le \frac{1}{2}\,\Delta x, \\ \frac{9}{8}\left(1 - \frac{2}{3}\left|\frac{x}{\Delta x}\right|\right)^2 & \text{if } \frac{1}{2}\,\Delta x < |x| \le \frac{3}{2}\,\Delta x, \\ 0 & \text{otherwise,} \end{cases}$$

$$\hat{s}^{(4)}(x) = \begin{cases} \frac{2}{3}\left[1 - \frac{3}{2}\left(\frac{x}{\Delta x}\right)^2 + \frac{3}{4}\left|\frac{x}{\Delta x}\right|^3\right] & \text{if } |x| \le \Delta x, \\ \frac{4}{3}\left(1 - \frac{1}{2}\left|\frac{x}{\Delta x}\right|\right)^3 & \text{if } \Delta x < |x| \le 2\,\Delta x, \\ 0 & \text{otherwise.} \end{cases}$$

Courtesy of M. Grech

II. High order interpolation scheme

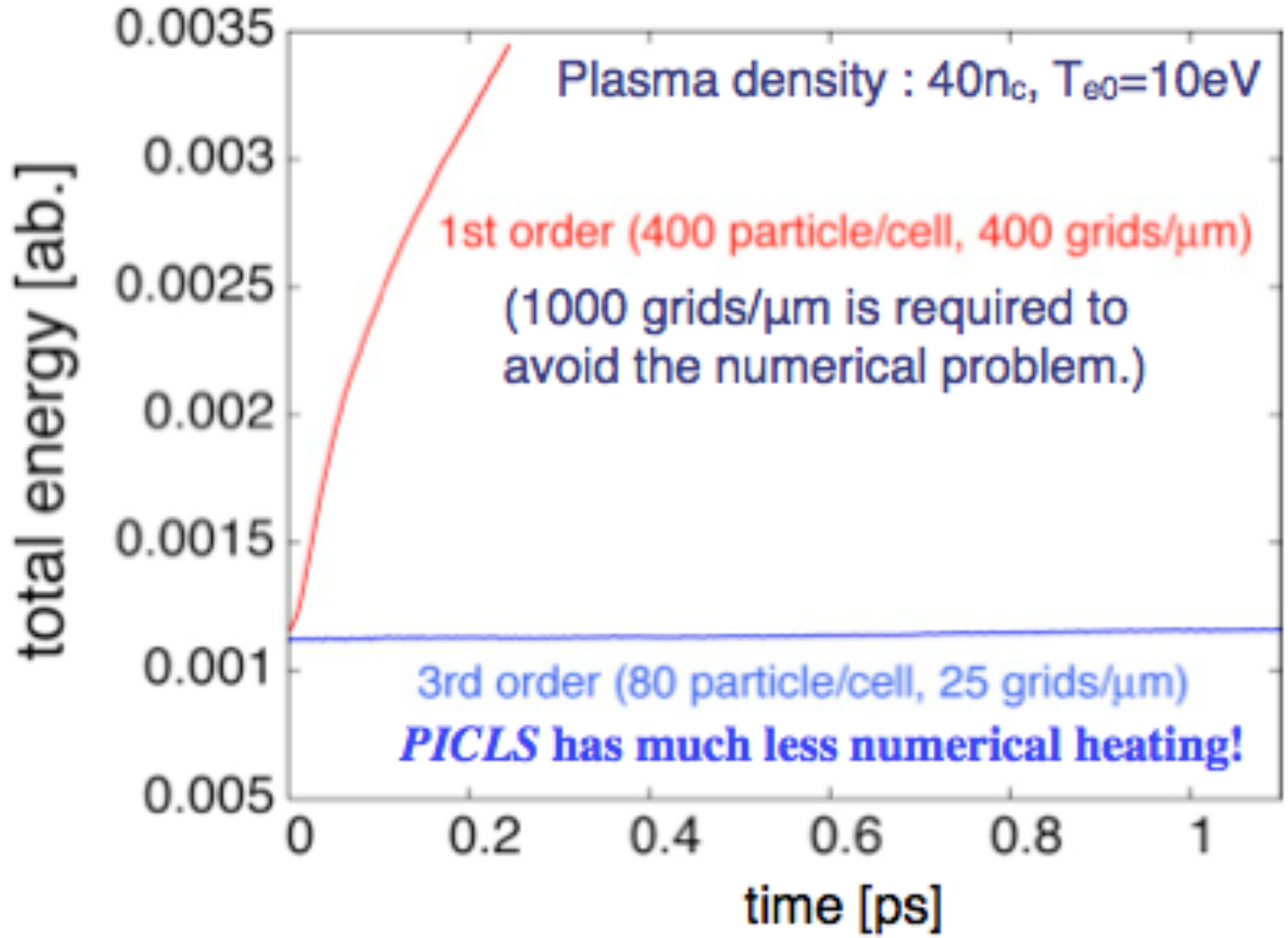

Adopting the high order interpolation, PICLS has much less numerical heating with even 40 times larger mesh of Debye length. Drastically reducing PIC cost.

Step 2

The Boris leap-frog *pusher* is a very popular method to advance particles

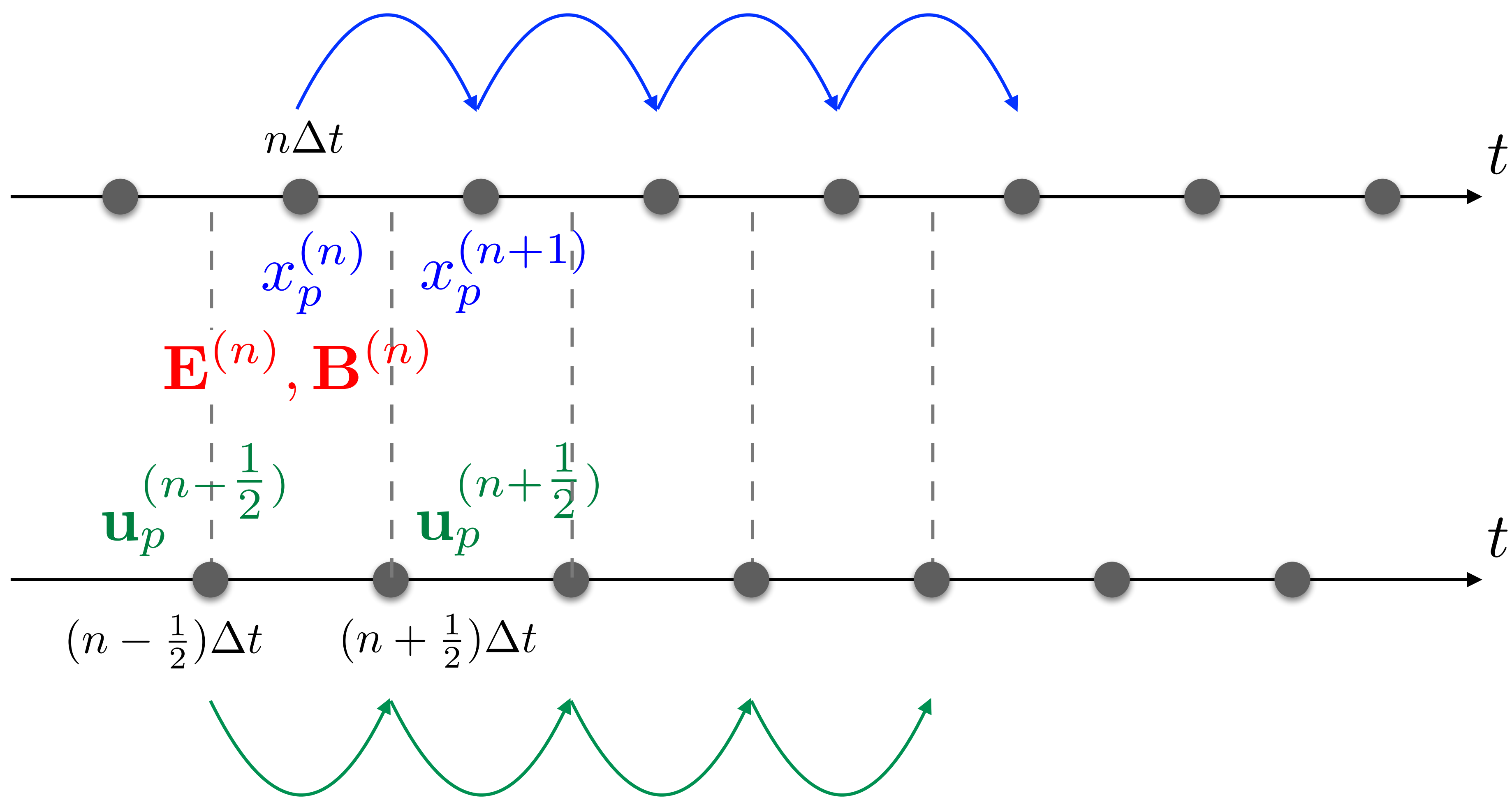

$$\mathbf{u}_m = \mathbf{u}_p^{(n-\frac{1}{2})} + \frac{q_s}{m_s}\frac{\Delta t}{2}\mathbf{E}_p$$

$$\mathbf{u}_p = \mathbf{u}_p^{(n-\frac{1}{2})} + \frac{q_s}{m_s}\Delta t\,\mathcal{M}(\mathbf{B}_p)\,\mathbf{u}_m$$

$$\mathbf{u}_p^{(n+\frac{1}{2})} = \mathbf{u}_p + \frac{q_s}{m_s}\frac{\Delta t}{2}\mathbf{E}_p$$

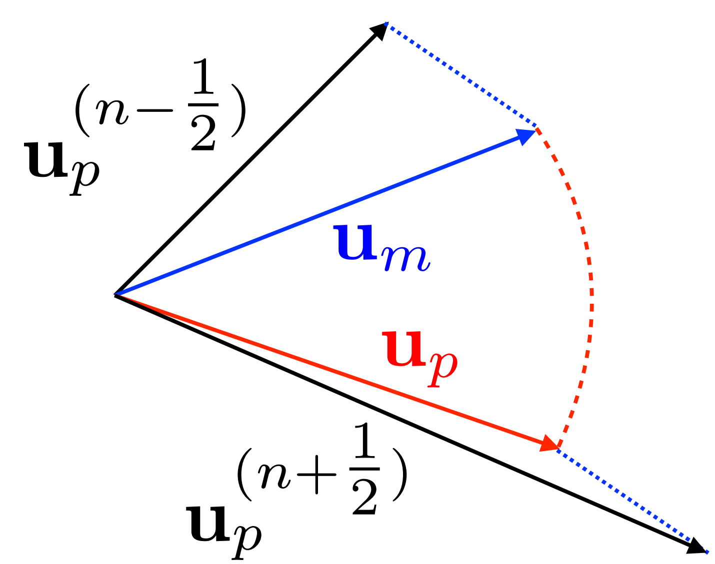

Step 3

Charge-conserving current deposition scheme are available among which Esirkepov's is 'most' popular

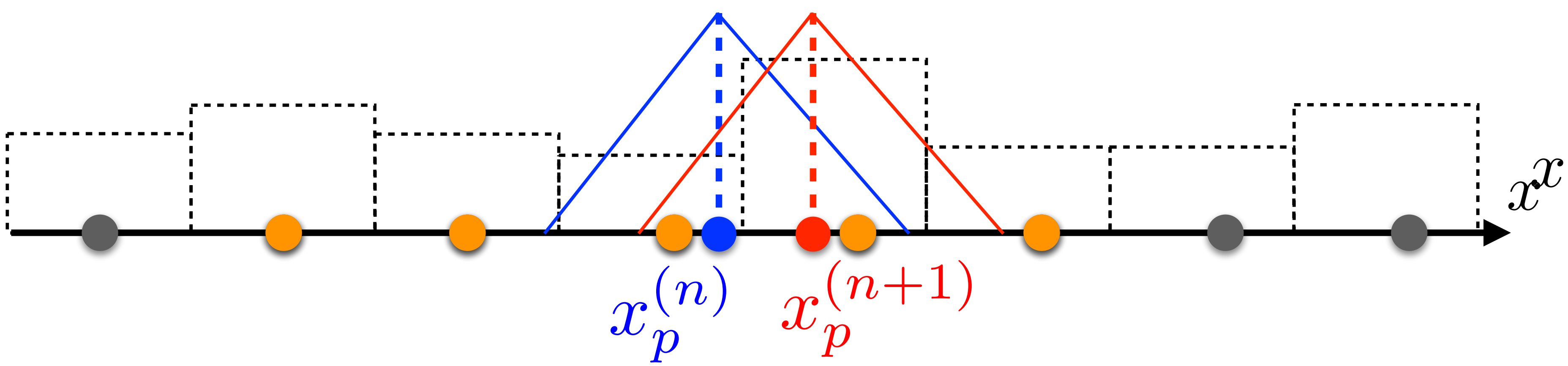

In 1D, current deposition is easily done directly from charge conservation:

$$\partial_x J_x = -\partial_t \rho$$

while other component are 'directly' projected onto the grid (see interpolation)

In 2D & 3D, Esirkepov's method allows to conserve charge (within machine presicion)

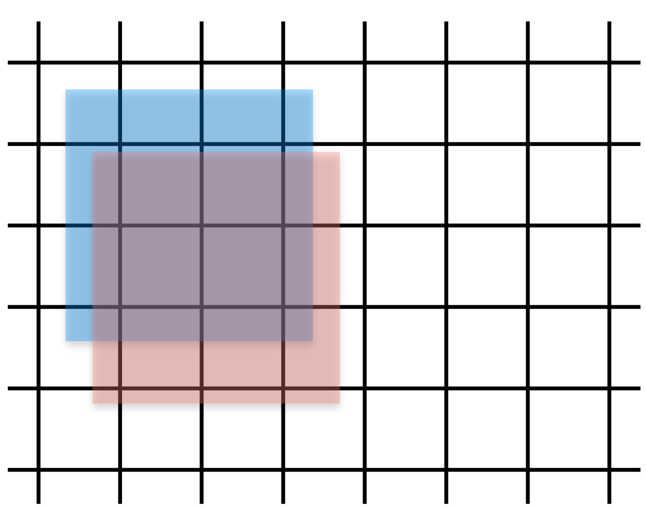

$$(J_{x,p})_{i+\frac{1}{2},j}^{(n+\frac{1}{2})} = (J_{x,p})_{i-\frac{1}{2},j}^{(n+\frac{1}{2})} + q_s\, w_p\, \frac{\Delta x}{\Delta t}\, (W_x)_{i+\frac{1}{2},j}^{(n+\frac{1}{2})}$$

$$(J_{y,p})_{i,j+\frac{1}{2}}^{(n+\frac{1}{2})} = (J_{y,p})_{i,j-\frac{1}{2}}^{(n+\frac{1}{2})} + q_s\, w_p\, \frac{\Delta y}{\Delta t}\, (W_y)_{j,i+\frac{1}{2}}^{(n+\frac{1}{2})}$$

Esirkepov, Comp. Phys. Comm. **135**, 144 (2001)

Courtesy of M. Grech

Step 4

The Finite-Difference Time-Domain (FDTD) method is a popular method for solving Maxwell's Equations

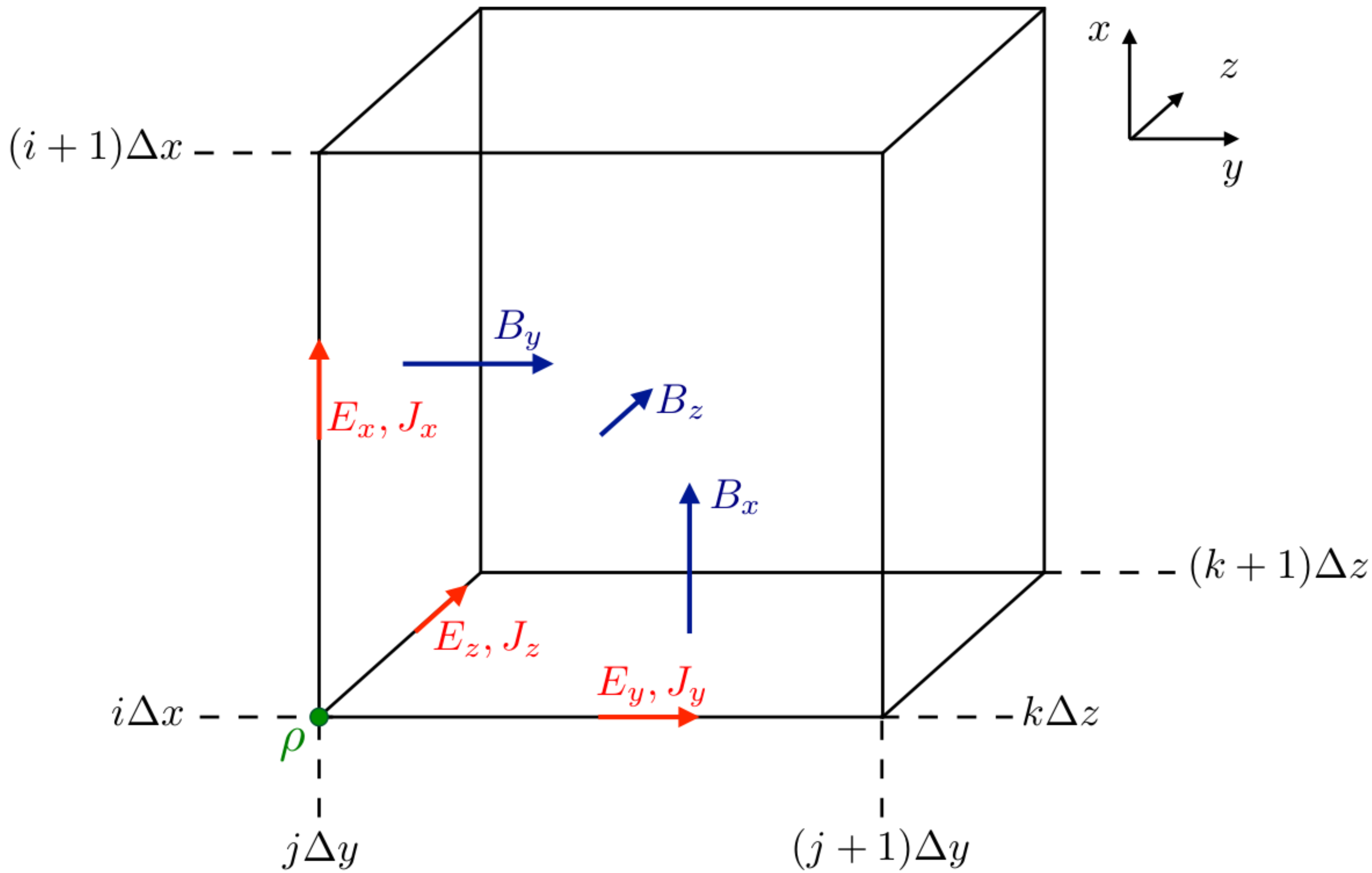

Courtesy of M. Grech

A. Taflove, *Computation electrodynamics: The finite-difference time-domain method*, 3rd Ed. (2005)

Step 4

Numerical analysis of the FDTD solvers gives you access to the numerical dispersion relation & CFL condition

After some algebra, one finds the *numerical dispersion relation*:

$$\frac{\sin^2(\omega\Delta t/2)}{\Delta t^2} = \sum_\mu \frac{\sin^2(k_\mu \Delta\mu/2)}{\Delta\mu^2}$$

There exists a stability condition: Courant-Friedrich-Lewy (CFL)

$$\Delta t < \sum_\mu \left(\Delta\mu^{-2}\right)^{-1/2} \xrightarrow[\Delta x = \Delta y]{\text{2D}} \Delta t < \Delta x/\sqrt{2}$$

The FDTD solver is subject to *numerical dispersion* as the numerical light wave velocity is found to depend on its wavenumber and orientation.

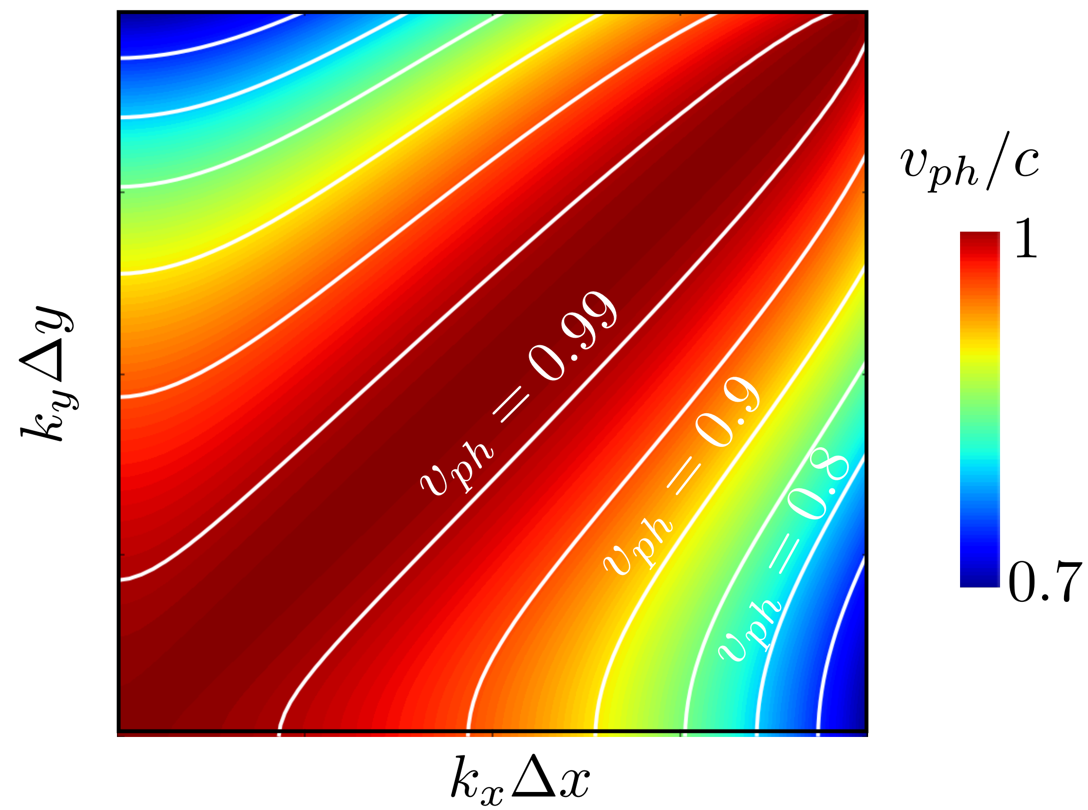

Nuter et al., Eur. Phys. J. D (2014); All papers by B. Godfrey, from the 70's up to now !!!

Step 4

Numerical analysis of the FDTD solvers gives you access to the numerical dispersion relation & CFL condition

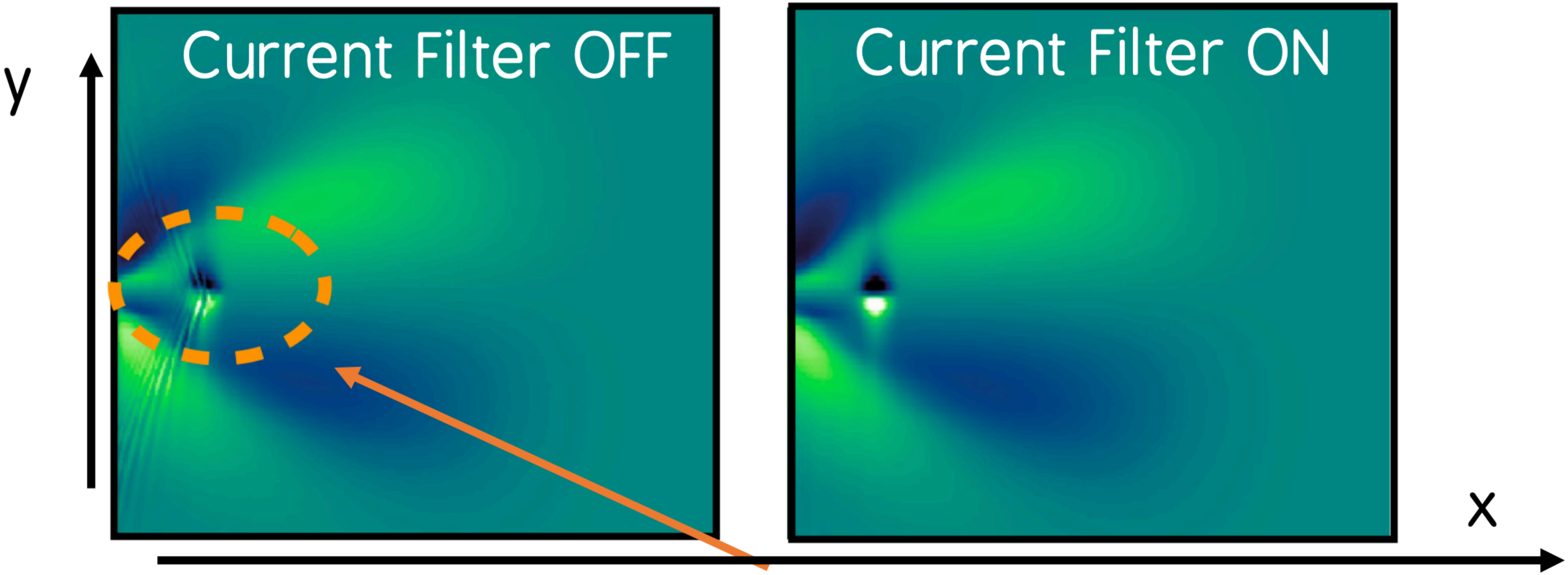

Filtering can reduce Numerical Cherenkov Radiation

Nuter et al., Eur. Phys. J. D (2014);   All papers by B. Godfrey, from the 70's up to now !!!

Courtesy of M. Grech

Alternative: Directional splitting (DS) method for PIC

$$\frac{1}{c}\frac{\partial \mathbf{E}}{\partial t} = \nabla \times \mathbf{B} - \frac{4\pi}{c}\mathbf{J} \qquad \frac{1}{c}\frac{\partial \mathbf{B}}{\partial t} = -\nabla \times \mathbf{E}$$

$$\partial_t E_x = -4\pi j_x \qquad \partial_t B_x = 0$$

$$\partial_t E_y = -c\partial_x B_z - 4\pi j_y \qquad \partial_t B_y = c\partial_x E_z$$

$$\partial_t E_z = c\partial_x B_y - 4\pi j_z \qquad \partial_t B_z = -c\partial_x E_y$$

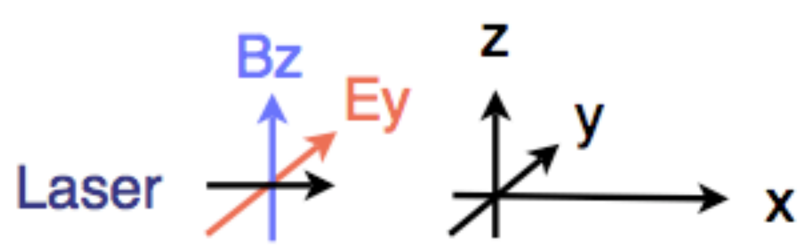

Alternative: Directional splitting (DS) method for PIC

$$\partial_t E_x = -4\pi j_x \qquad \text{.......... (1)}$$

$$\partial_t E_y = -c\partial_x B_z - 4\pi j_y \qquad \text{.......... (2)}$$

$$\partial_t B_z = -c\partial_x E_y \qquad \text{.......... (3)}$$

$$E_y^{\pm} \equiv E_y \pm B_z$$

(2)±(3) $$(\partial_t \pm c\,\partial_x)E_y^{\pm} = -4\pi j_y$$

when $c\Delta t = \Delta x$

$$E_y^{\pm}(x \pm \Delta x, t + \frac{\Delta t}{2}) = E_y^{\pm}(x, t - \frac{\Delta t}{2}) - 4\pi j_y(x \pm \frac{\Delta x}{2}, t)$$

Alternative: Directional splitting (DS) method for PIC

Maxwell equation

$$\frac{\partial \mathbf{B}}{\partial t} = -c\nabla \times \mathbf{E}$$

$$\frac{\partial \mathbf{E}}{\partial t} = c\nabla \times \mathbf{B} - 4\pi\mathbf{J}$$

$$\frac{\partial}{\partial t}\begin{pmatrix} E_x \\ E_y \\ B_z \end{pmatrix} + \begin{pmatrix} 0 & 0 & 0 \\ 0 & 0 & -c \\ 0 & -c & 0 \end{pmatrix}\frac{\partial}{\partial x}\begin{pmatrix} E_x \\ E_y \\ B_z \end{pmatrix} + \begin{pmatrix} 0 & 0 & c \\ 0 & 0 & 0 \\ c & 0 & 0 \end{pmatrix}\frac{\partial}{\partial y}\begin{pmatrix} E_x \\ E_y \\ B_z \end{pmatrix} = -\begin{pmatrix} J_x \\ J_y \\ 0 \end{pmatrix}$$

Step1: x-direction

$$E_y^{\pm} = B_z \pm E_y$$

$$\frac{\partial E_y^+}{\partial t} + c\frac{\partial E_y^+}{\partial x} = -\frac{1}{2}J_y$$

$$\frac{\partial E_y^-}{\partial t} - c\frac{\partial E_y^-}{\partial x} = +\frac{1}{2}J_y$$

$$\frac{\partial}{\partial t}\begin{pmatrix} E_x \\ E_y \\ B_z \end{pmatrix} + \begin{pmatrix} 0 & 0 & 0 \\ 0 & 0 & -c \\ 0 & -c & 0 \end{pmatrix}\frac{\partial}{\partial x}\begin{pmatrix} E_x \\ E_y \\ B_z \end{pmatrix} + \begin{pmatrix} 0 & 0 & c \\ 0 & 0 & 0 \\ c & 0 & 0 \end{pmatrix}\frac{\partial}{\partial y}\begin{pmatrix} E_x \\ E_y \\ B_z \end{pmatrix} = -\begin{pmatrix} J_x \\ J_y \\ 0 \end{pmatrix}$$

Step2: y-direction

$$E_x^{\pm} = B_z \mp E_x$$

$$\frac{\partial E_x^+}{\partial t} + c\frac{\partial E_x^+}{\partial y} = +\frac{1}{2}J_x$$

$$\frac{\partial E_x^-}{\partial t} - c\frac{\partial E_x^-}{\partial y} = -\frac{1}{2}J_x$$

$$\frac{\partial}{\partial t}\begin{pmatrix} E_x \\ E_y \\ B_z \end{pmatrix} + \begin{pmatrix} 0 & 0 & 0 \\ 0 & 0 & -c \\ 0 & -c & 0 \end{pmatrix}\frac{\partial}{\partial x}\begin{pmatrix} E_x \\ E_y \\ B_z \end{pmatrix} + \begin{pmatrix} 0 & 0 & c \\ 0 & 0 & 0 \\ c & 0 & 0 \end{pmatrix}\frac{\partial}{\partial y}\begin{pmatrix} E_x \\ E_y \\ B_z \end{pmatrix} = -\begin{pmatrix} J_x \\ J_y \\ 0 \end{pmatrix}$$

I. Numerical dispersion free Maxwell solver

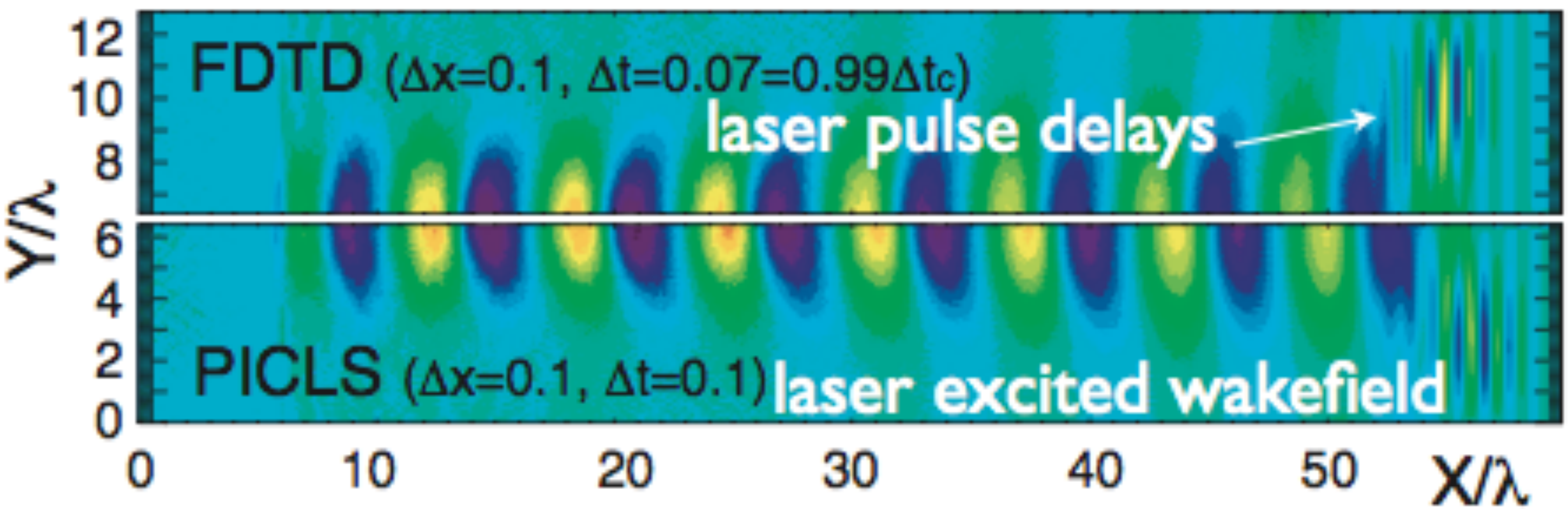

Waves delay due to the numerical diffusion in the standard scheme (FDTD). PICLS can simulate wave propagation correctly with less number of meshes (5 mesh is enough).

A quick summary
The PIC approach in a nutshell

Initialization	time step $n = 0$, time $t = 0$

Particle loading $\forall p$, define $(\mathbf{x}_p)^{n=0}$, $(\mathbf{u}_p)^{n=-\frac{1}{2}}$

Charge projection on grid $\left[\forall p, (\mathbf{x}_p)^{n=0}\right] \rightarrow \rho^{(n=0)}(\mathbf{x})$

Compute initial fields - solve Poisson on grid: $\left[\rho^{(n=0)}(\mathbf{x})\right] \rightarrow \mathbf{E}_{\text{stat}}^{(n=0)}(\mathbf{x})$

- add external fields: $\mathbf{E}^{(n=0)}(\mathbf{x}) = \mathbf{E}_{\text{stat}}^{(n=0)}(\mathbf{x}) + \mathbf{E}_{\text{ext}}^{(n=0)}(\mathbf{x})$

$$\mathbf{B}^{(n=\frac{1}{2})}(\mathbf{x}) = \mathbf{B}_{\text{ext}}^{(n=\frac{1}{2})}(\mathbf{x})$$

PIC loop: from time step n to $n+1$, time $t = (n+1)\,\Delta t$

Restart charge & current densities
Save magnetic fields value (used to center magnetic fields)

Interpolate fields at particle positions $\forall p$, $[\mathbf{x}_p, \mathbf{E}^{(n)}(\mathbf{x}), \mathbf{B}^{(n)}(\mathbf{x})] \rightarrow \mathbf{E}_p^{(n)}, \mathbf{B}_p^{(n)}$

Push particles - compute new velocity $\forall p$, $\mathbf{p}_p^{(n-\frac{1}{2})} \left[\mathbf{E}_p^{(n)}, \mathbf{B}_p^{(n)}\right] \mathbf{p}_p^{(n+\frac{1}{2})}$

- compute new position $\forall p$, $\mathbf{x}_p^{(n)} \left[\mathbf{p}_p^{(n+\frac{1}{2})}\right] \mathbf{x}_p^{(n+1)}$

Project current onto the grid using a charge-conserving scheme

$$\left[\forall p \;\; \mathbf{x}_p^{(n)}, \mathbf{x}_p^{(n+1)}, \mathbf{p}_p^{(n+\frac{1}{2})}\right] \rightarrow \mathbf{J}^{(n+\frac{1}{2})}(\mathbf{x})$$

Solve Maxwell's equations

- solve Maxwell-Faraday: $\mathbf{E}^{(n)}(\mathbf{x}) \left[\mathbf{J}^{(n+\frac{1}{2})}(\mathbf{x})\right] \mathbf{E}^{(n+1)}(\mathbf{x})$
- solve Maxwell-Ampère: $\mathbf{B}^{(n+\frac{1}{2})}(\mathbf{x}) \left[\mathbf{E}^{(n+1)}(\mathbf{x})\right] \mathbf{B}^{(n+\frac{3}{2})}(\mathbf{x})$
- center magnetic fields: $\mathbf{B}^{(n+1)}(\mathbf{x}) = \frac{1}{2}\left(\mathbf{B}^{(n+\frac{1}{2})}(\mathbf{x}) + \mathbf{B}^{(n+\frac{3}{2})}(\mathbf{x})\right)$

Courtesy of M. Grech

There are still a few things to know before running your first PIC simulation

- **noise is inherent to PIC code**
  electromagnetic fluctuations inherent to a thermal plasma
  the level of noise is however much exaggerated in PIC codes

- **some numerical instabilities have to be taken care off carefully**
  - numerical heating usually requires $\Delta x \lesssim \lambda_{De}$
  - numerical-Cherenkov can also plague simulation with relativistically drifting particles

- **PIC codes are usually very robust, beware of your results!**
  A PIC code will most likely not crash, even if your simulation is complete non-sense!

- **I did not discuss boundary conditions nor ghost-cells**

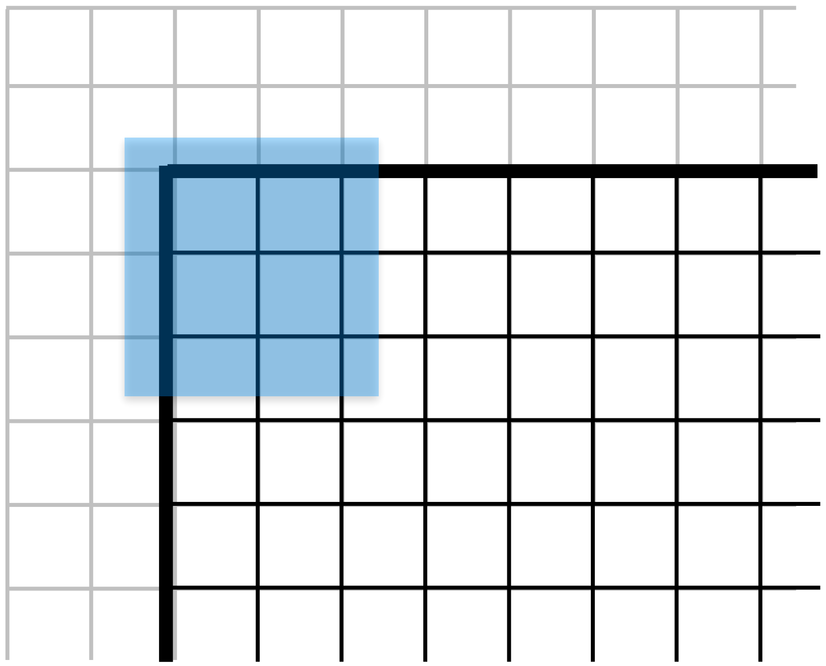

Courtesy of M. Grech

Parallelization and supercomputers

Super-computers are mandatory for large-scale PIC simulation

Large scale PIC simulation of
magnetic reconnection at the earth magnetopause

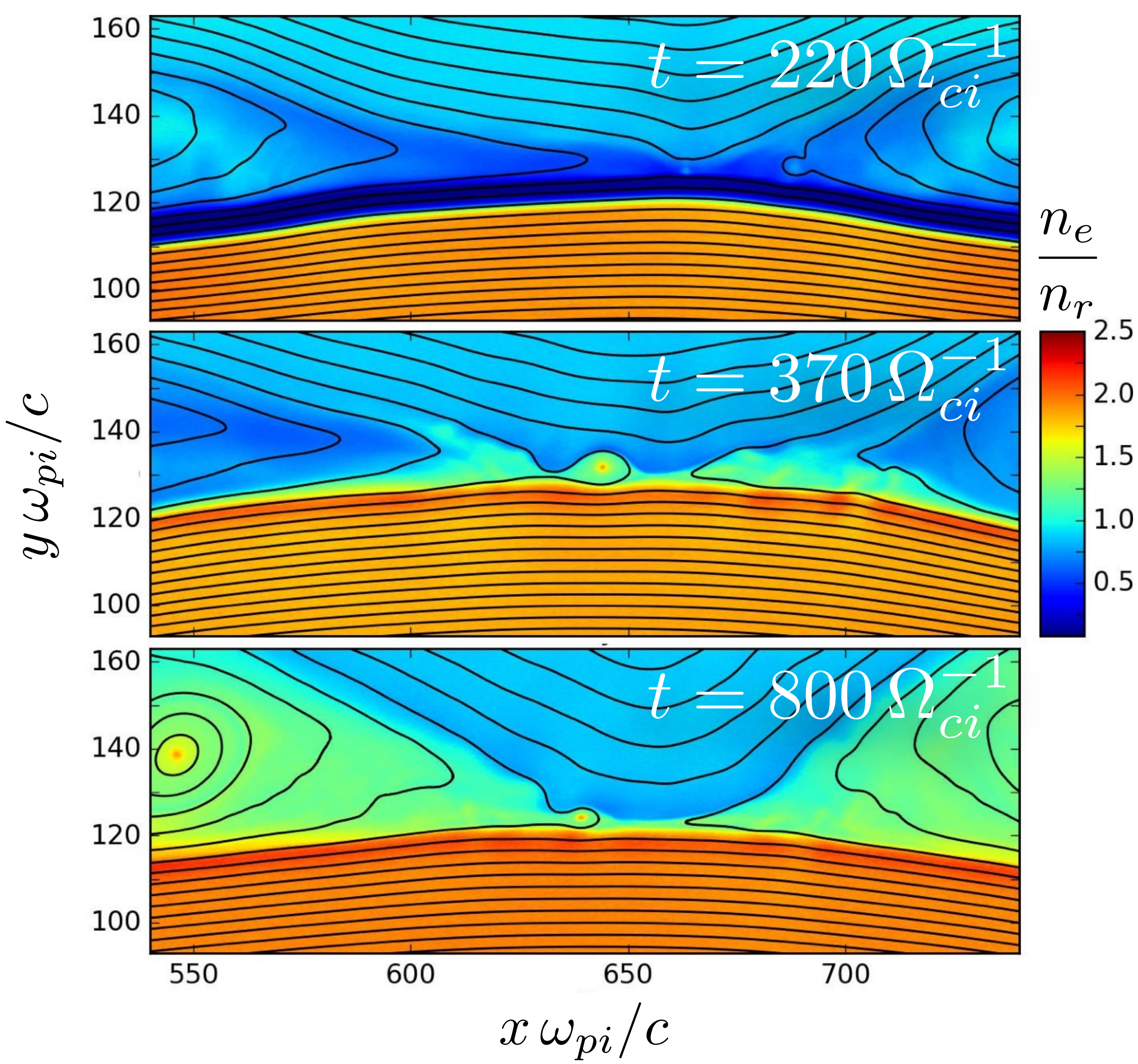

Simulation box: $1280\,\frac{c}{\omega_{pi}} \times 256\,\frac{c}{\omega_{pi}}$

25600×10240 PIC cells

run up to $t = 800\,\Omega_{ci}^{-1}$

$N_t \sim 9.5 \times 10^5$ timesteps

for a total of 22×10^9 quasi-particles.

Required simulation time:
14 000 000 hours ~ 1600 years!!!

Solution:
share the work on 16384 CPUs !!!

Courtesy of M. Grech

Super-computers are more & more performant

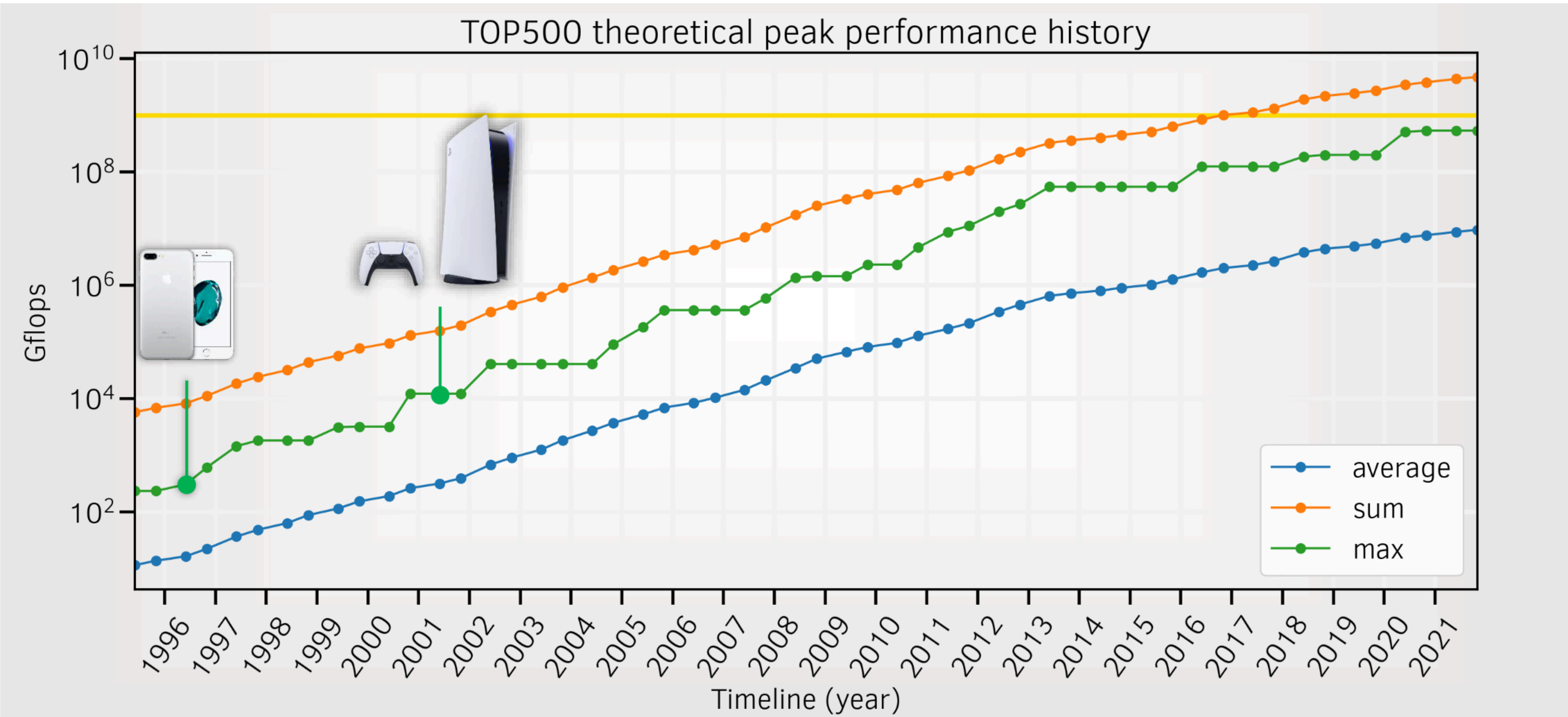

Courtesy of M. Grech

Super-computers are becoming more & more complex

Summit super-computer

- USA
- IBM CPUs + NVIDIA V100 GPUs
- 149 Pflops
- 15 Gflops/Watt

Fugaku super-computer

- Japan
- ARM CPUs
- 442 Pflops
- 15 Gflops/Watt

Sunway TaihuLight super-computer

- China
- RISC CPUs
- 93 Pflops
- 6.2 Gflops / Watt

Juwels super-computer

- Germany
- AMD CPUs + A100 NVIDIA GPUs
- 71 Pflops
- 42 Gflops/Watt

Courtesy of M. Grech

Super-computers are more & more complex

Tianhe-2 (2014)	Sunway TaihuLight (2018)	1 Exaflop machine (2022)
37 Pfloaps	125 Pfloaps	1000 Pfloaps
17 MW	15 MW	120 MW

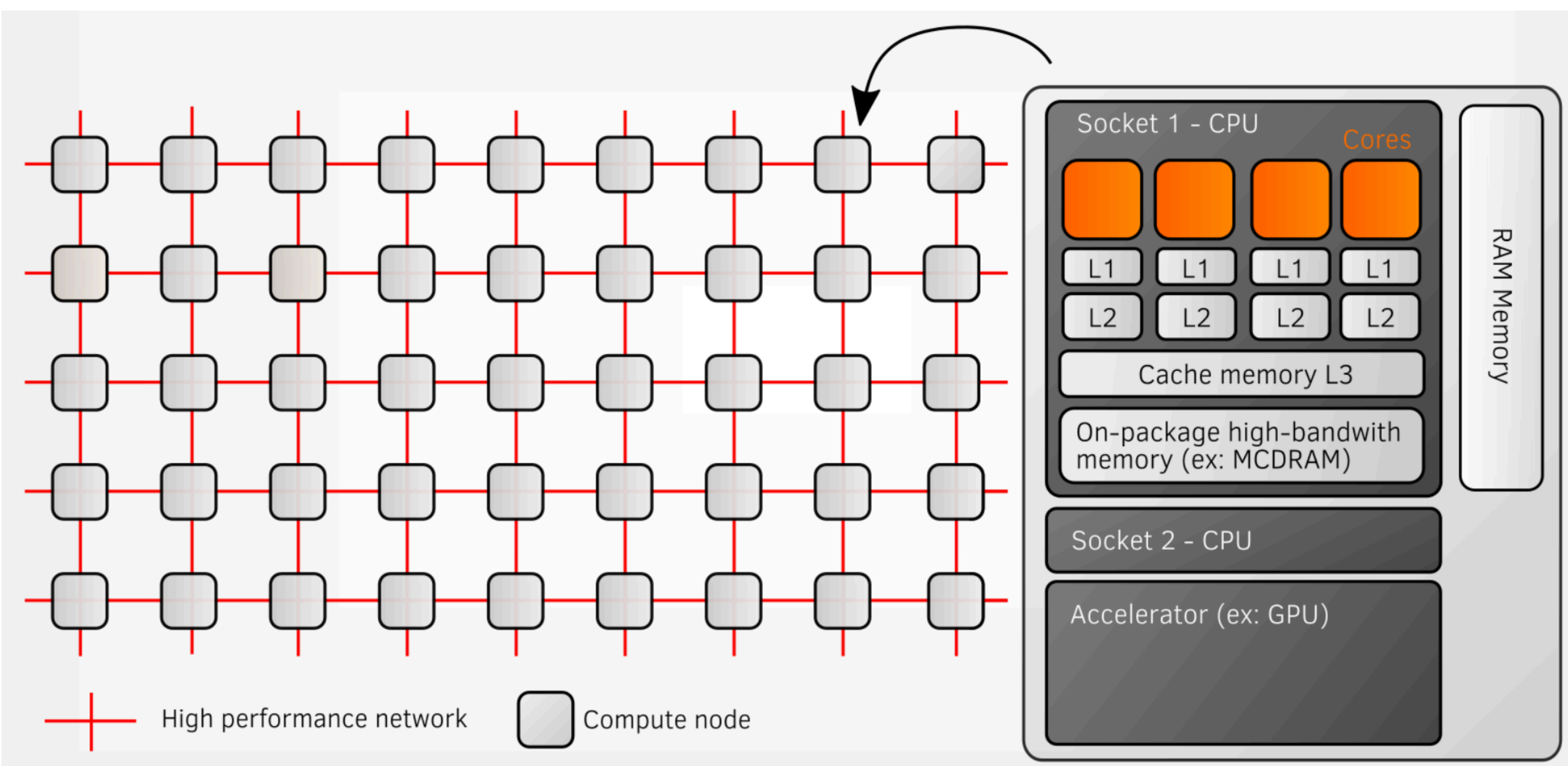

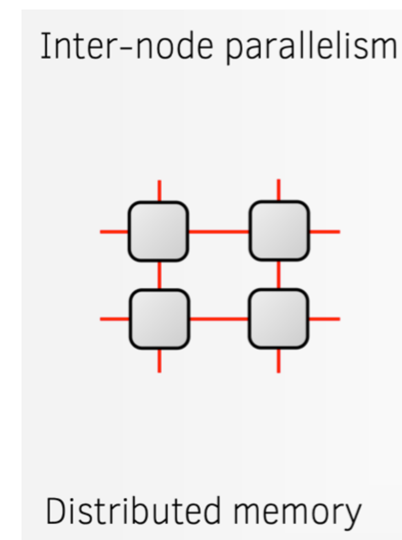

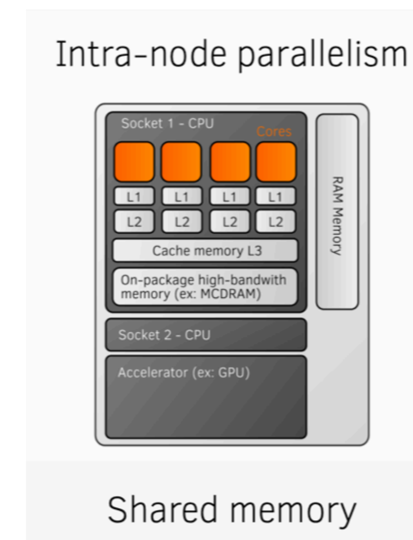

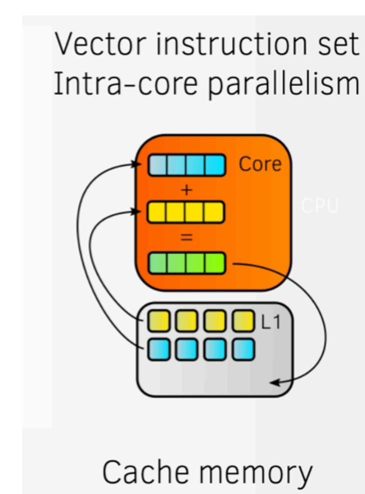

(Massive) Parallelism • Vectorization • Memory management • I/O management

Courtesy of M. Grech

PIC codes are well adapted to massive parallelism

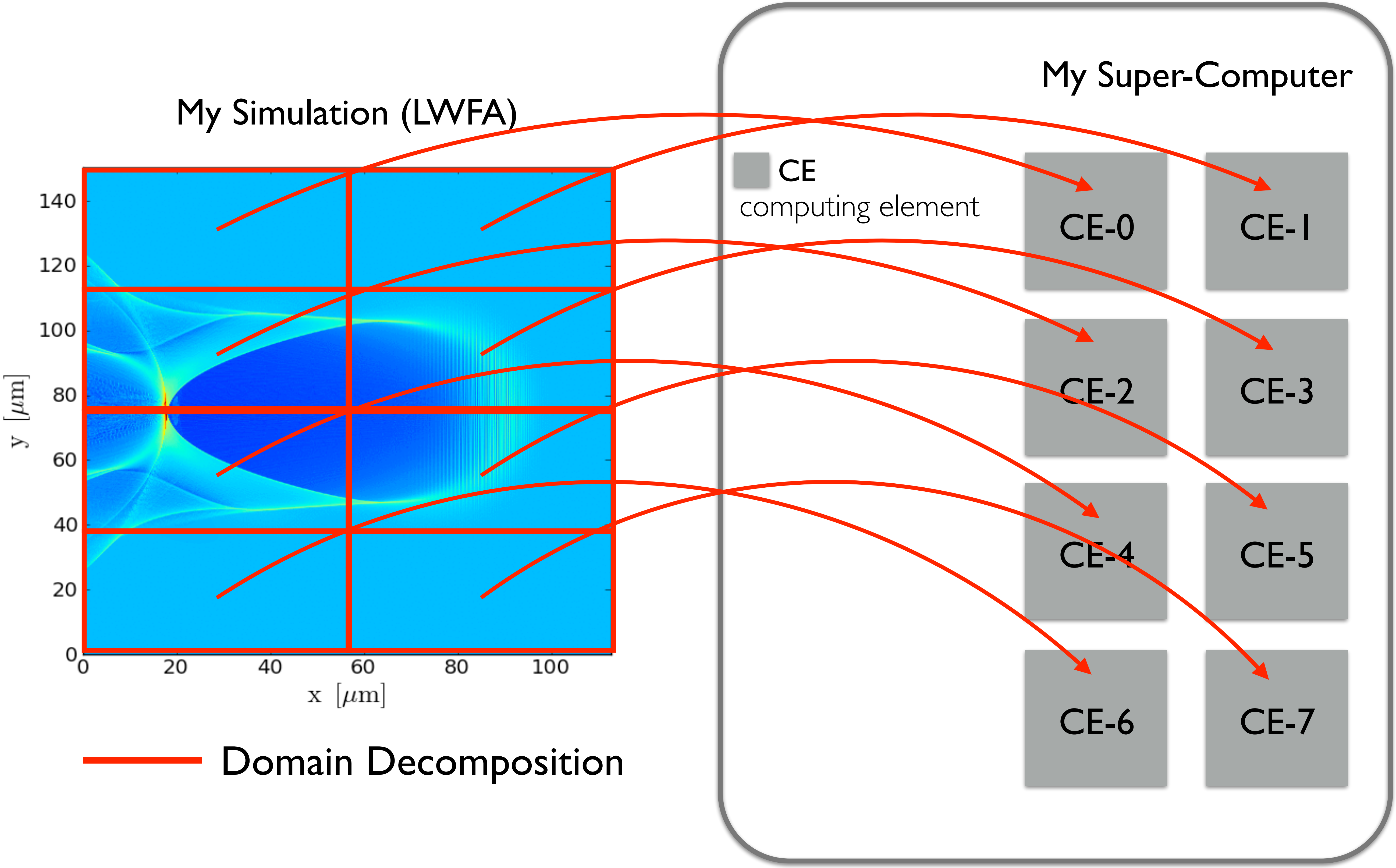

Courtesy of M. Grech

PIC codes are well adapted to massive parallelism

My Simulation (LWFA)

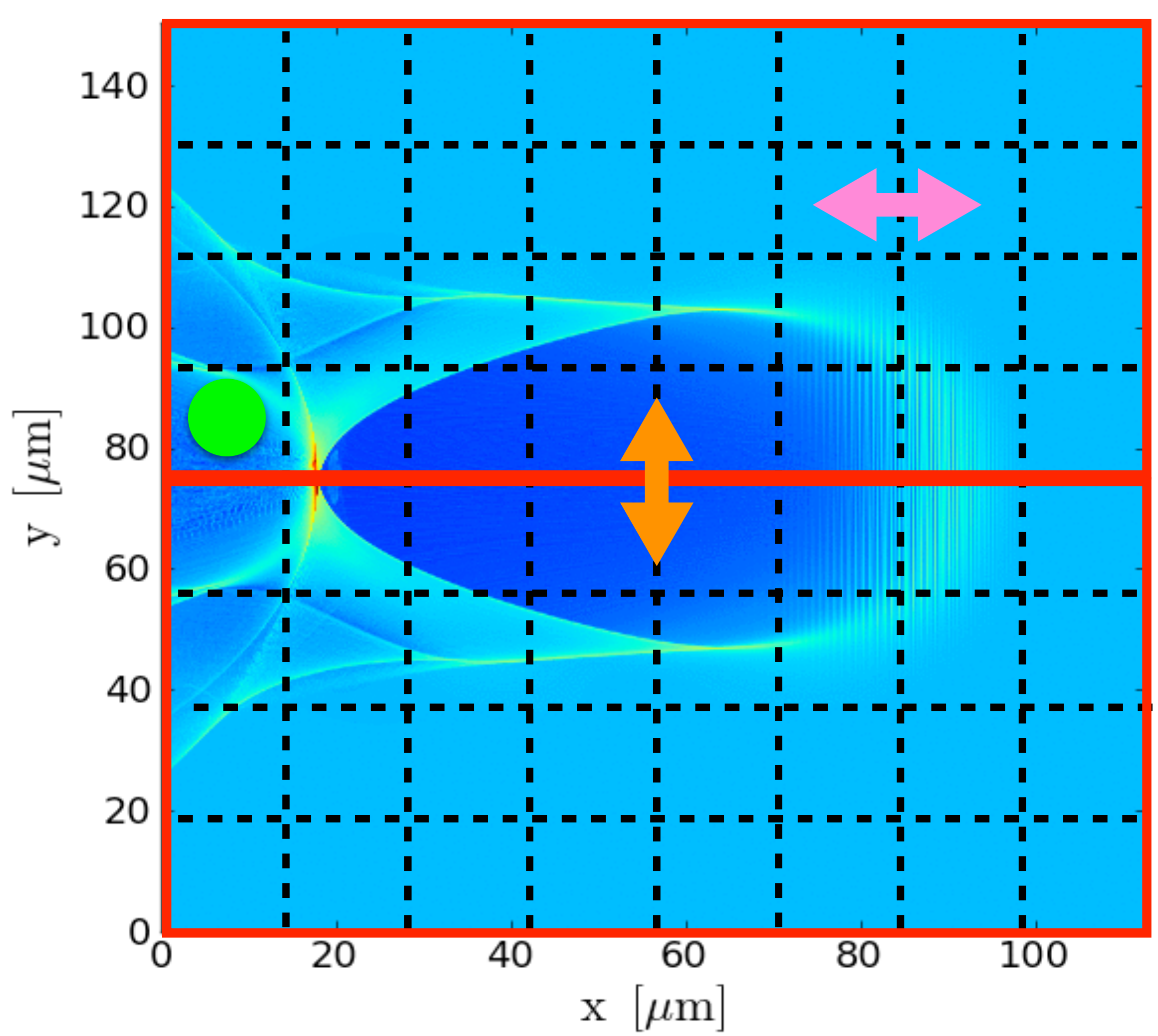

Domain Decomposition

Patch Decomposition

Courtesy of M. Grech

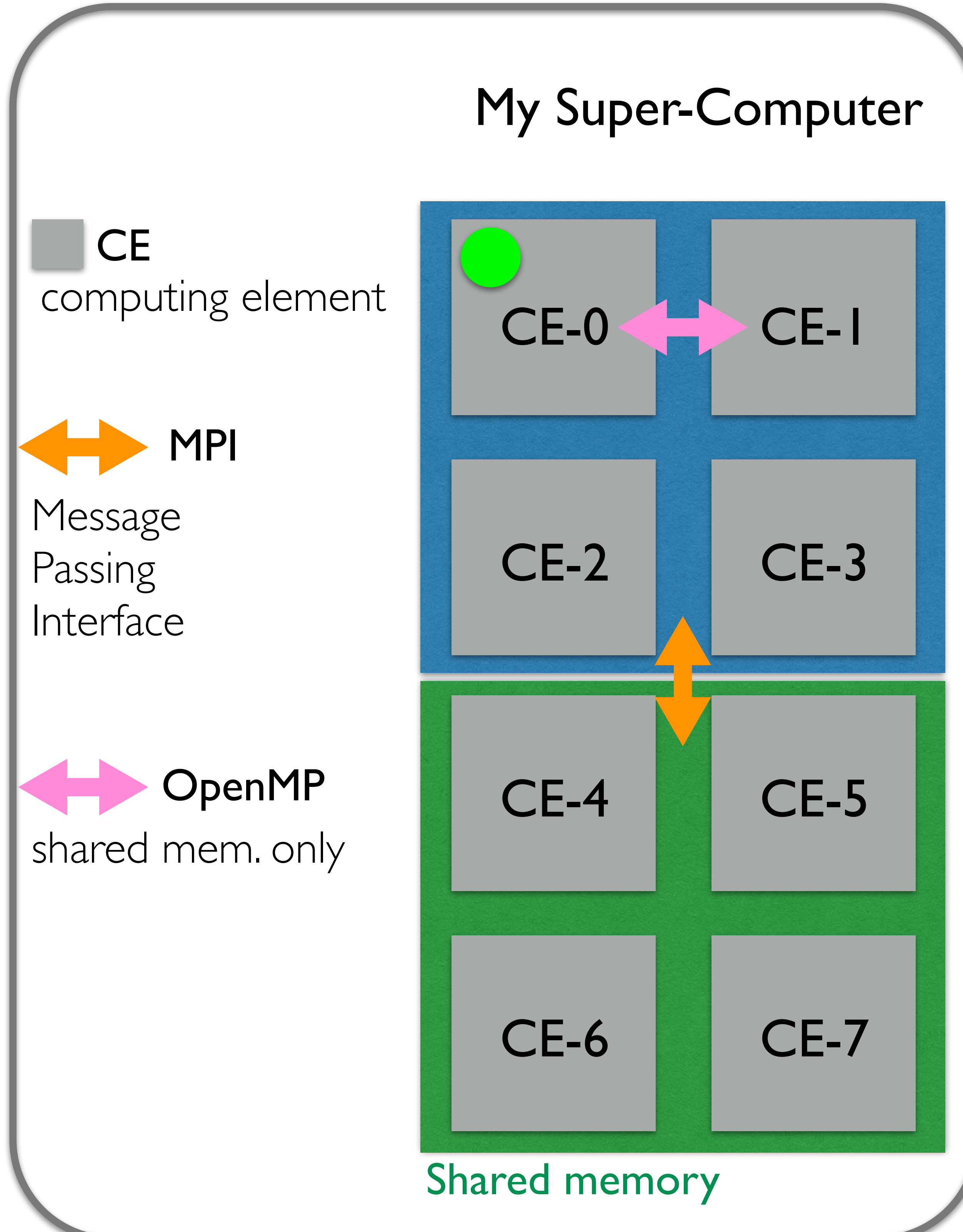

PIC codes are well adapted to massive parallelism

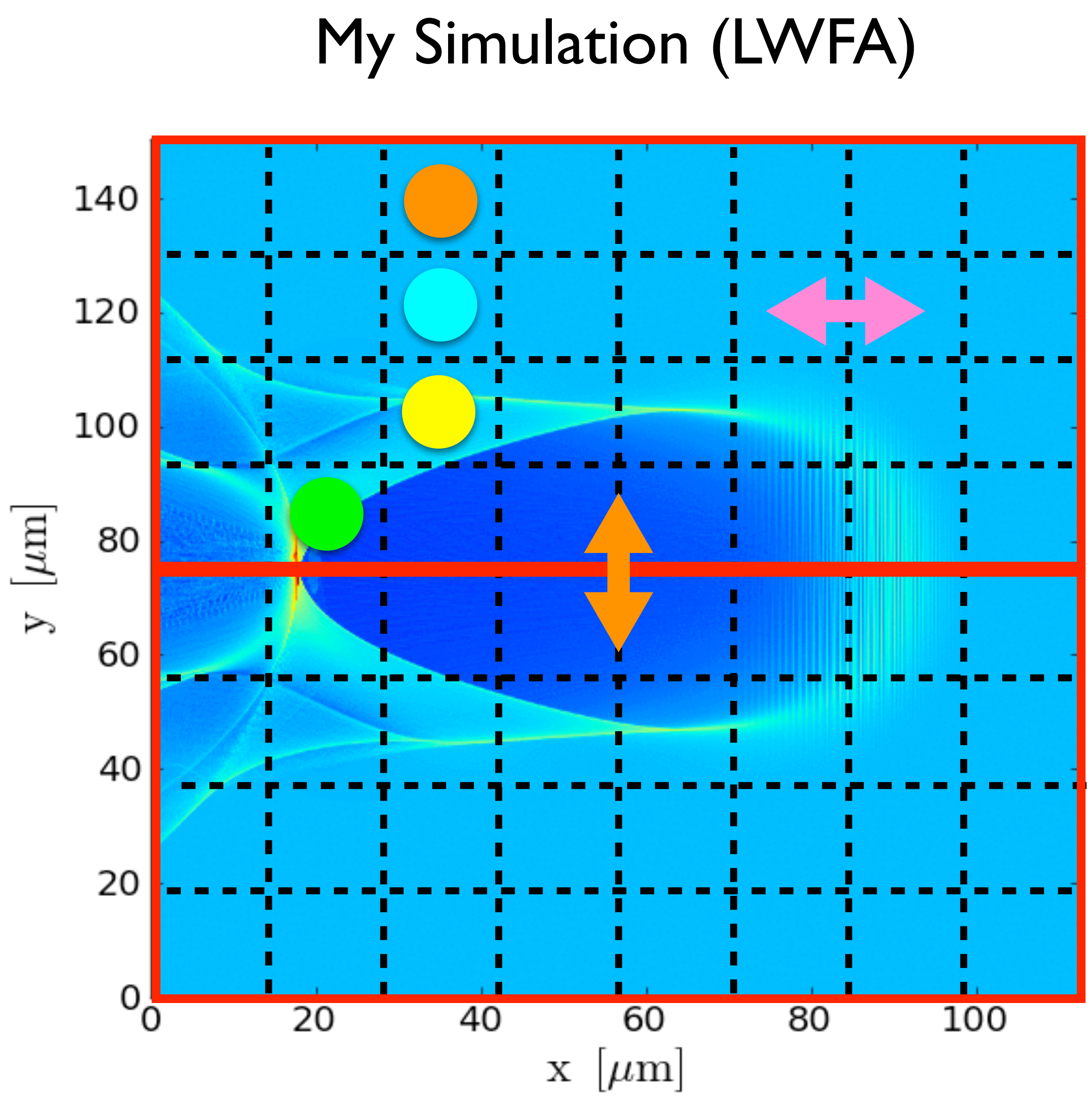

Domain Decomposition

Patch Decomposition

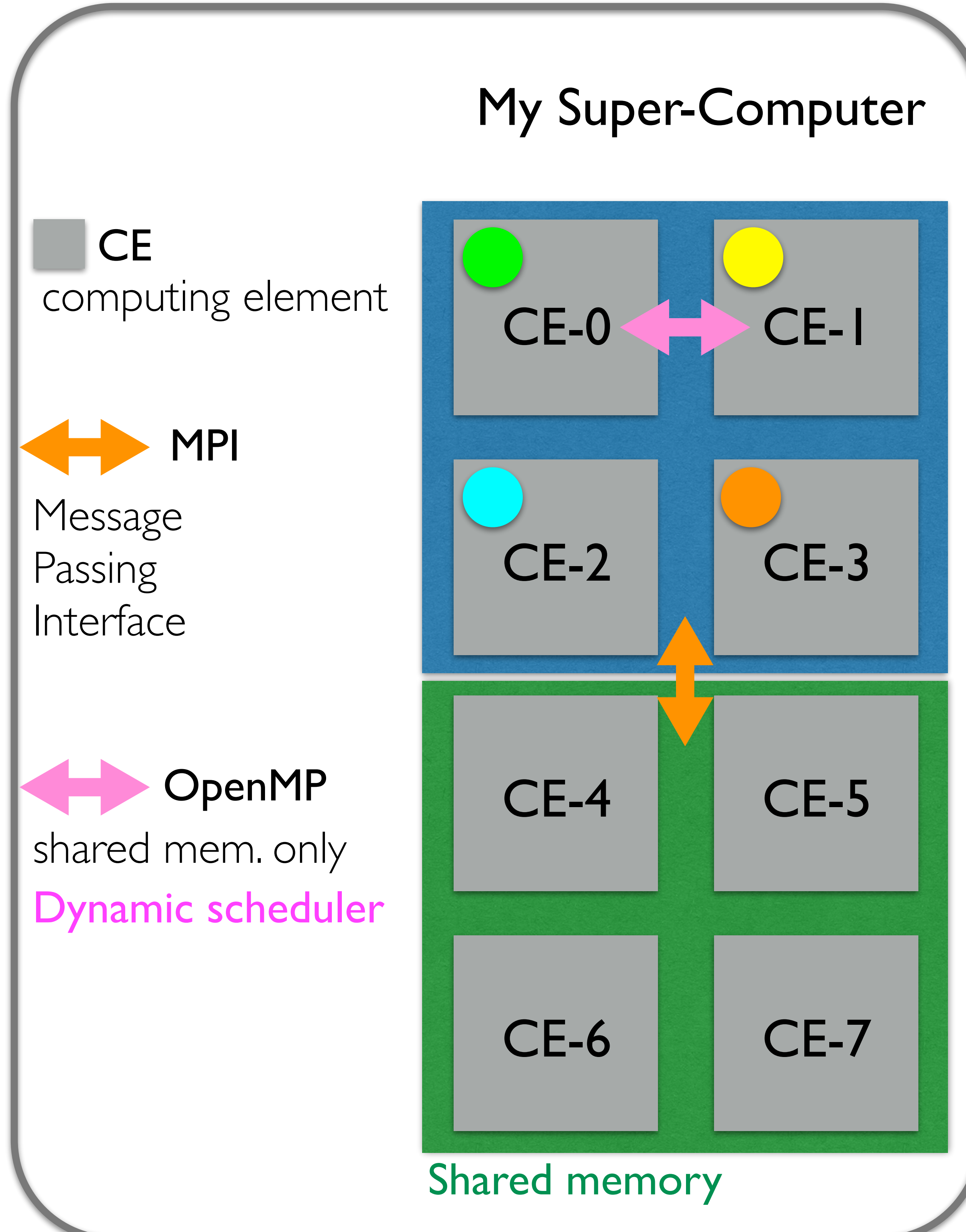

Hybrid parallelization significantly improves performance

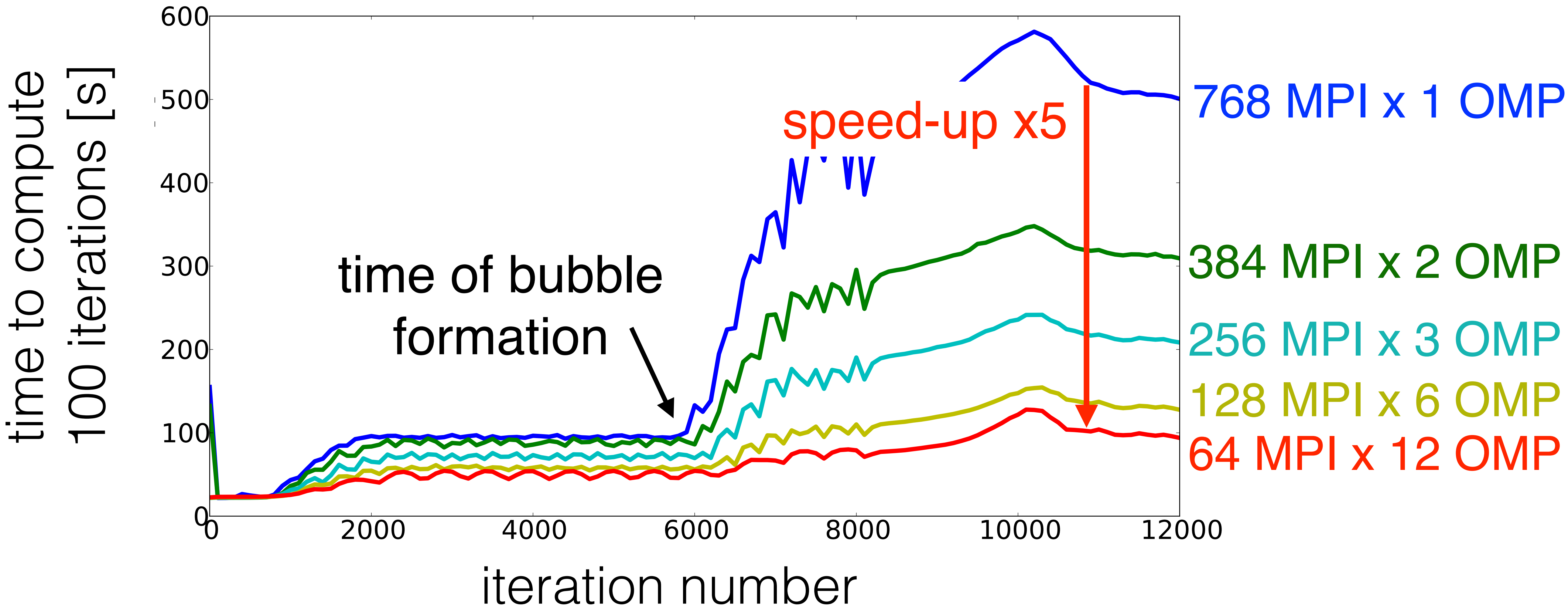

Courtesy of M. Grech

How to launch a Particle in Cell simulation

PICLS 1D parameters (1)

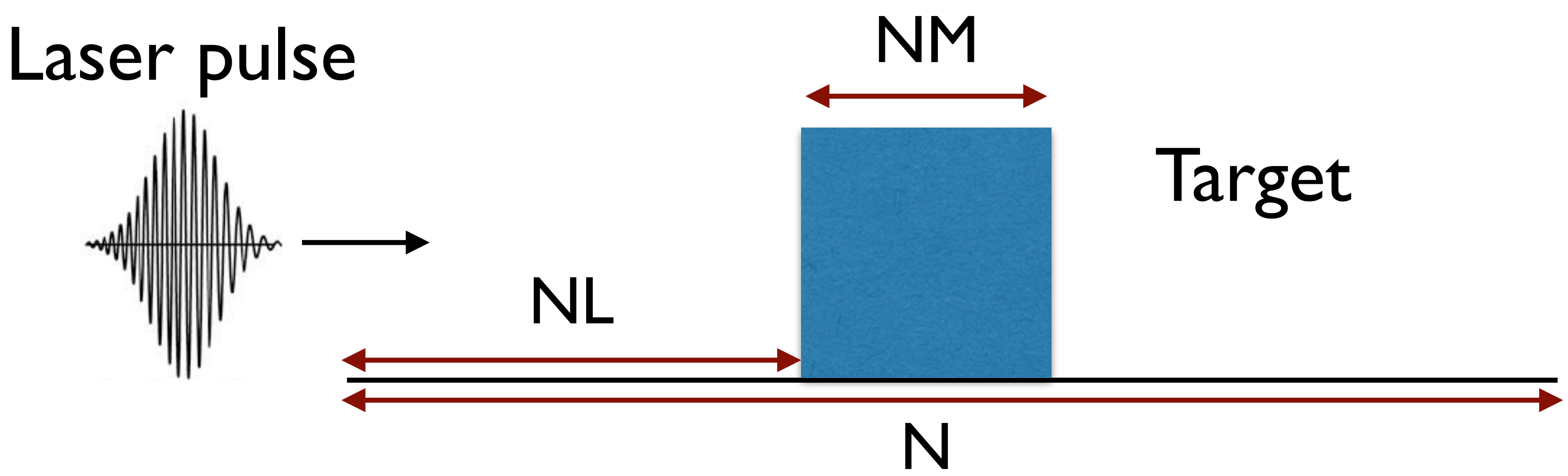

n_time : number of time steps

N : total number of cells

NM : number of plasma cells

NL : number of vaccum cells in front of the plasma

igeom : density profile number (99=square profile, 194=double target with a separation of 40% of the total plasma length and with preplasma)

an0 : maximum density in critical densities

res : number of cells per wavelength and time step per laser period

PICLS 1D parameters (2)

int_snap : number of time steps between two diagnostics

N_d : spatial diagnostics are mesured every N_d cells

N_dp : particle diagnostics are measured every N_dp particles

No_ion : number of ion species

p_mass_i : ion mass in electron mass

q_i : ion charge in - electron charge

T_i : ion temperature in keV

Nx_dlt_i : number of ions per cell

No_eon : number of electron species

p_mass_e : electron mass in electron mass

q_e : electron charge in - electron charge

T_e : electron temperature in keV

Nx_dlt_e : number of electrons per cell

PICLS 1D parameters (3)

Ey0 : Ey normalized amplitude = 0.85*sqrt((I/10^18 W/cm^2)*(lambda/1 micron))

Ez0 : Ez normalized amplitude = 0.85*sqrt((I/10^18 W/cm^2)*(lambda/1 micron))

nshp1 : front pulse profile

nshp2 : rear pulse profile

1: gaussian, 2: linear, 3: sin, other: constant

tau1 : number of laser periods composing the first half of the laser

tau2 : number of laser periods composing the second half of the laser

col_opt : option to treat collisions

p1_opt : collisions between particles of the same specie

p2_opt : collisions between particles of different species

Sample PIC simulation in 1D

Plasma consists of a group of charged particles!

Maxwell equations (grid)

$$\frac{\partial \mathbf{B}}{\partial t} = -c\nabla \times \mathbf{E}$$

$$\frac{\partial \mathbf{E}}{\partial t} = c\nabla \times \mathbf{B} - 4\pi \mathbf{J}$$

Kinetic equations (particles)

$$\frac{d\mathbf{P}_i}{dt} = q_i\left(\mathbf{E} + \frac{\mathbf{P}_i}{m_i c\gamma_i} \times \mathbf{B}\right)$$

$$\frac{d\mathbf{x}_i}{dt} = \frac{\mathbf{p}_i}{\gamma_i m_i}$$

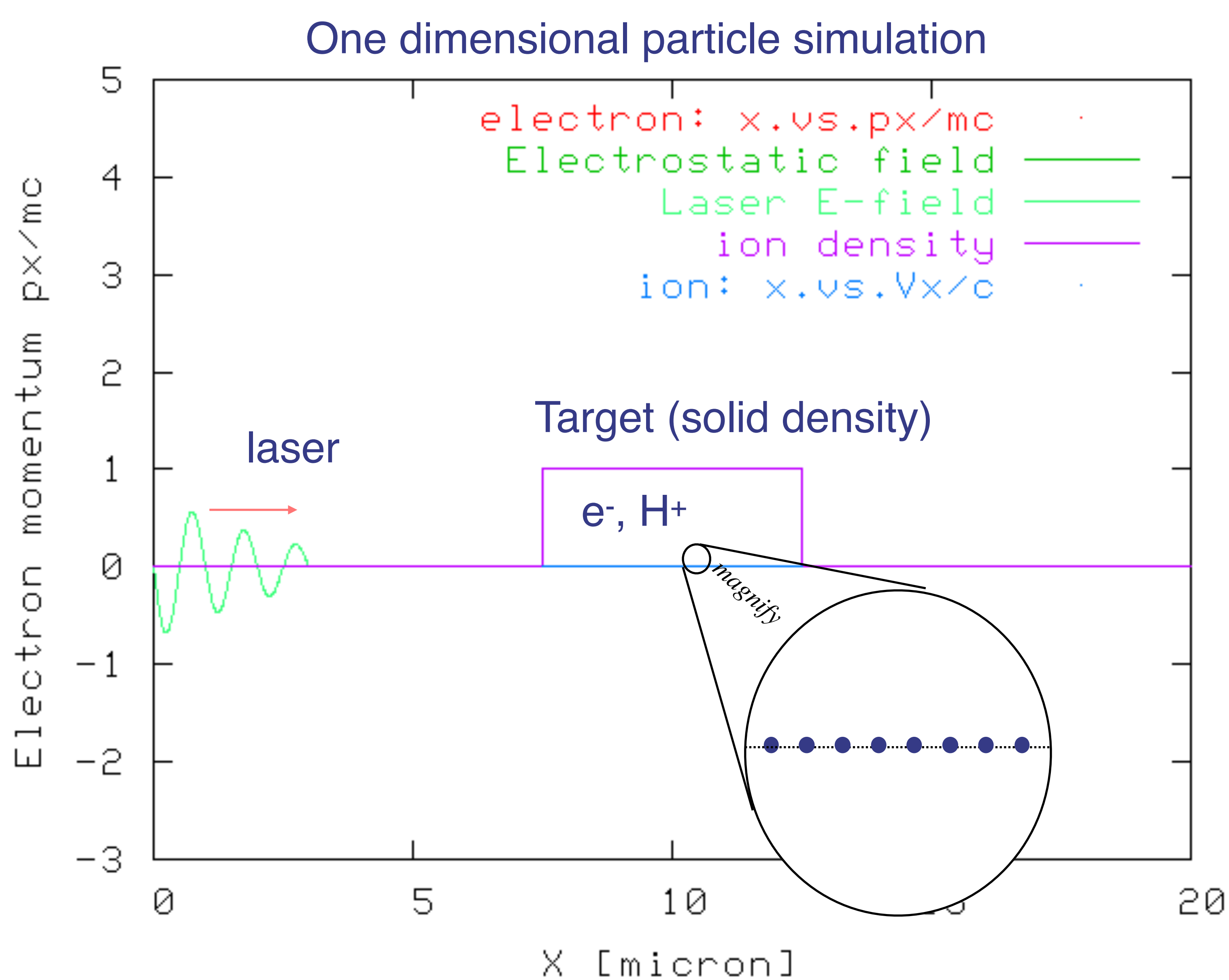

sample simulation (1d)

laser: $I=10^{19}$W/cm^2

target: fully ionized hydrogen plasma (solid density)

Number of simulation particle: 25,000

Ions are accelerated by gigabar pressure and TeV/m electrostatic field

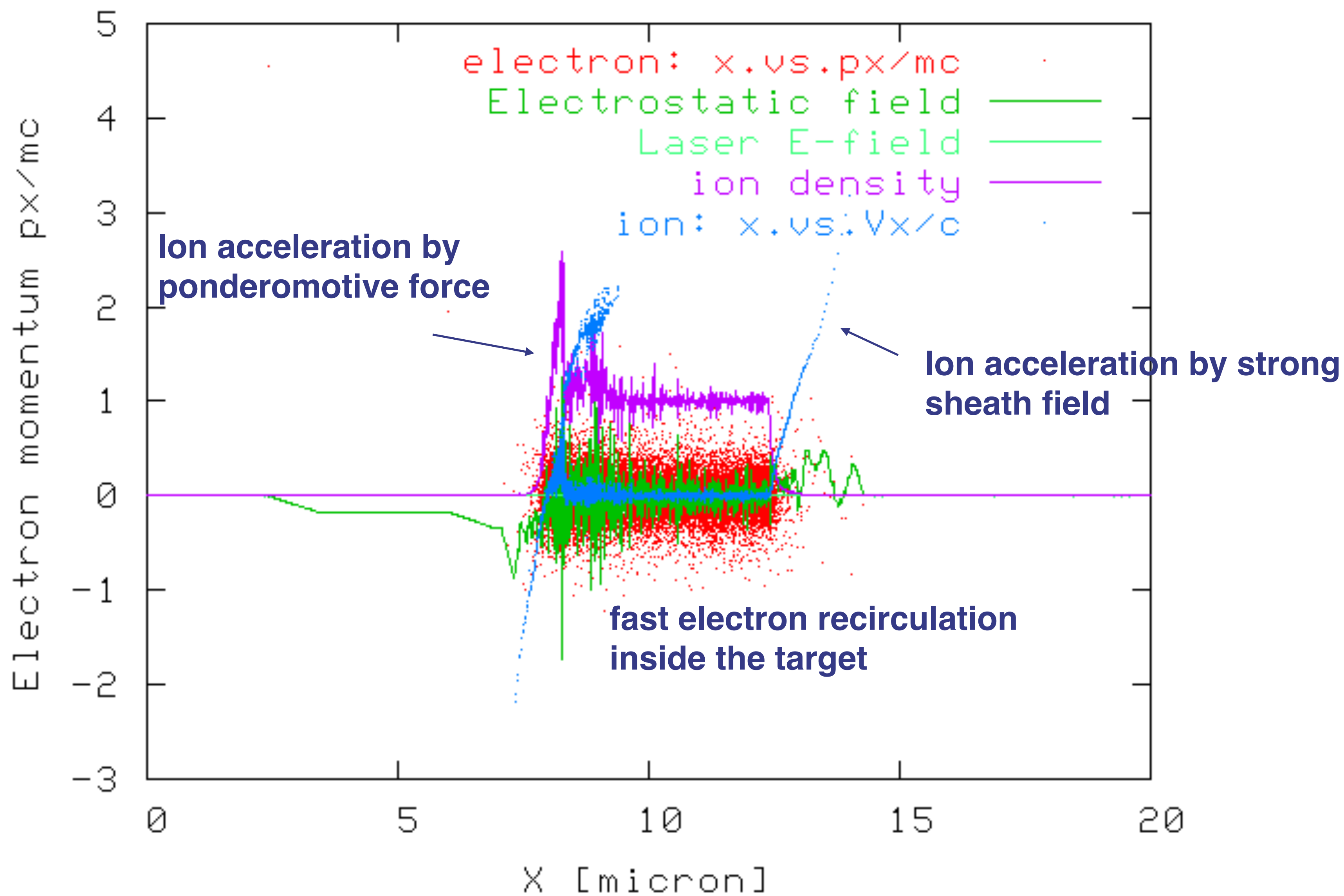

PIC simulation includes lots of physics self-consistently.

1D laser wakefield example

Laser: $I=1.38\times10^{18}$ W/cm^2, 10 fs pulse duration, gaussian pulse.

Target: 0.02533 n_c, constant density, 70 µm long.

Simulation parameters: 10 cells per wavelength, 330 fs total simulation time and one diagnostic every 16.5 fs.

Variation with intensity (after 198 fs)

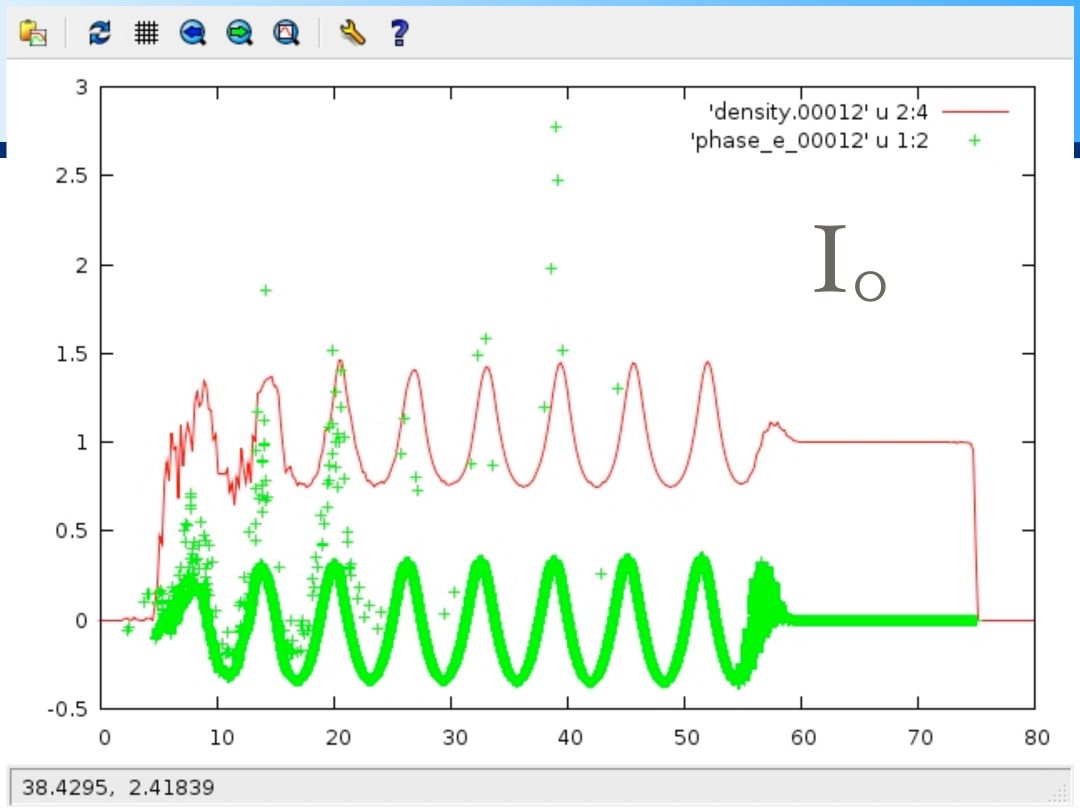

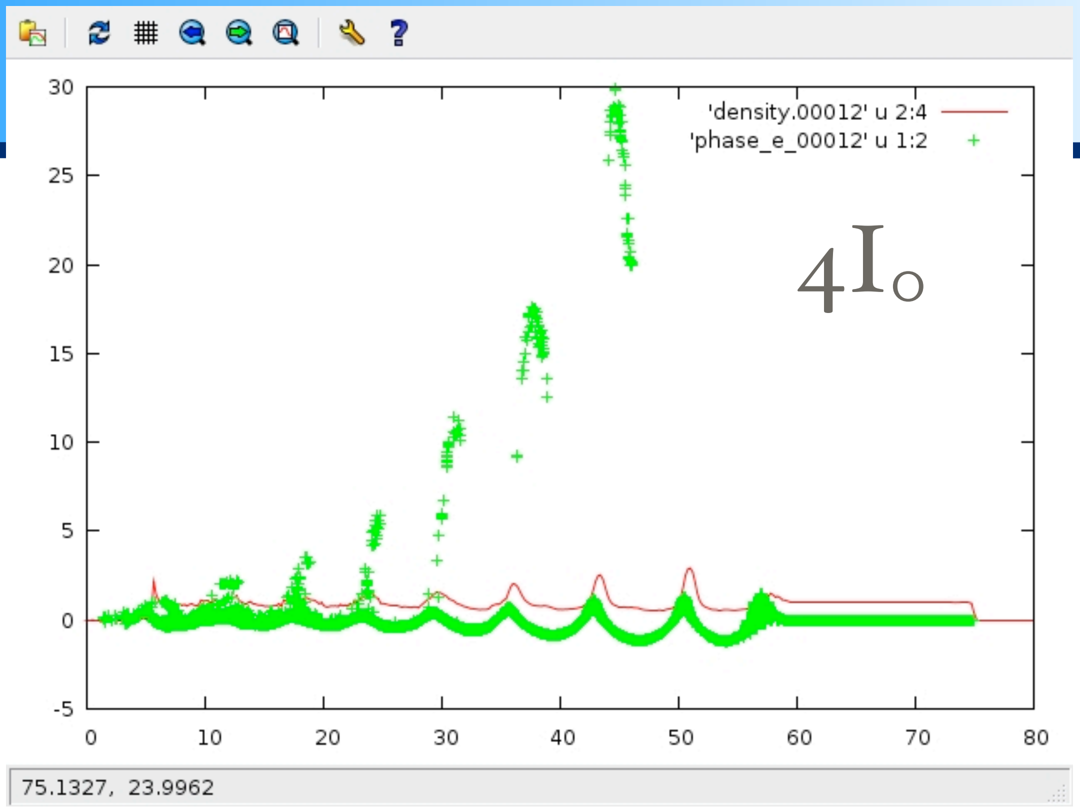

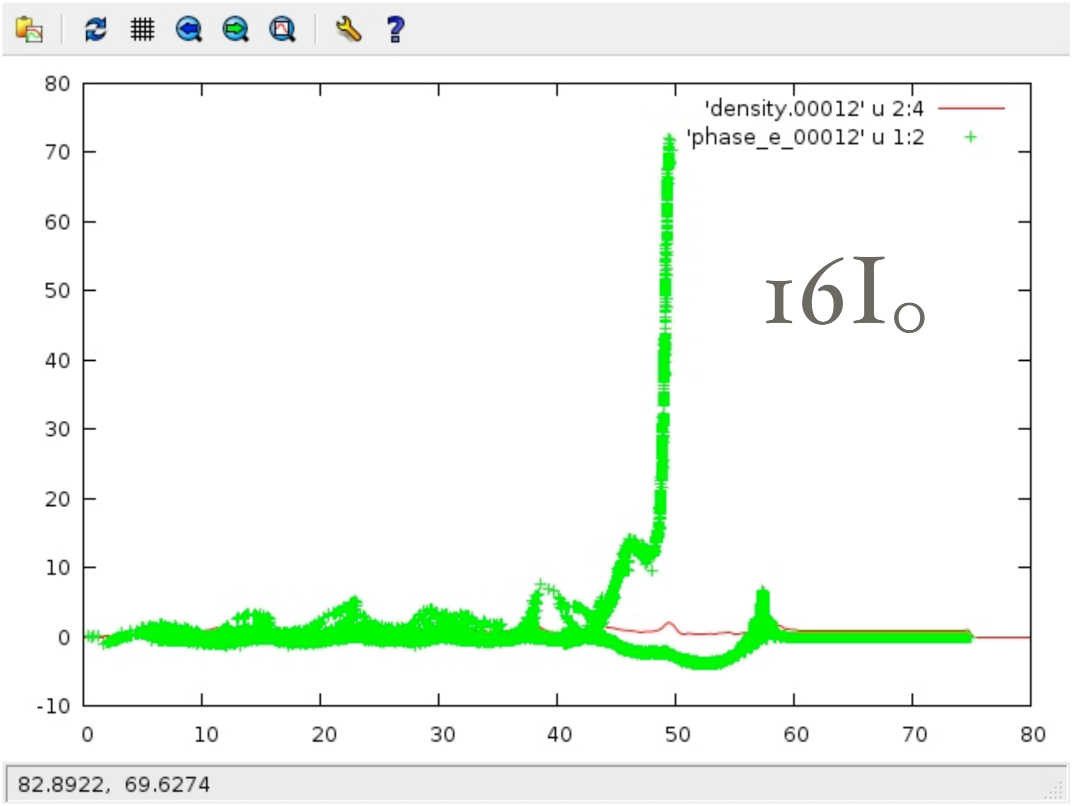

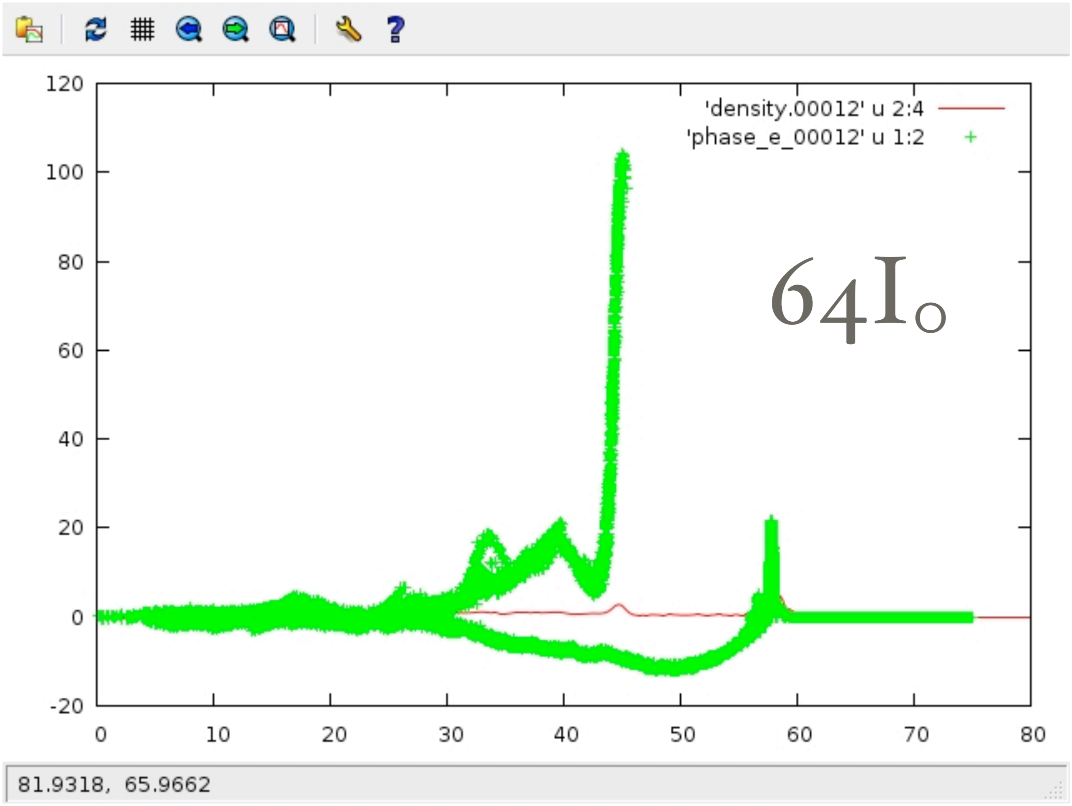

Variation with laser pulse duration (after 198 fs)

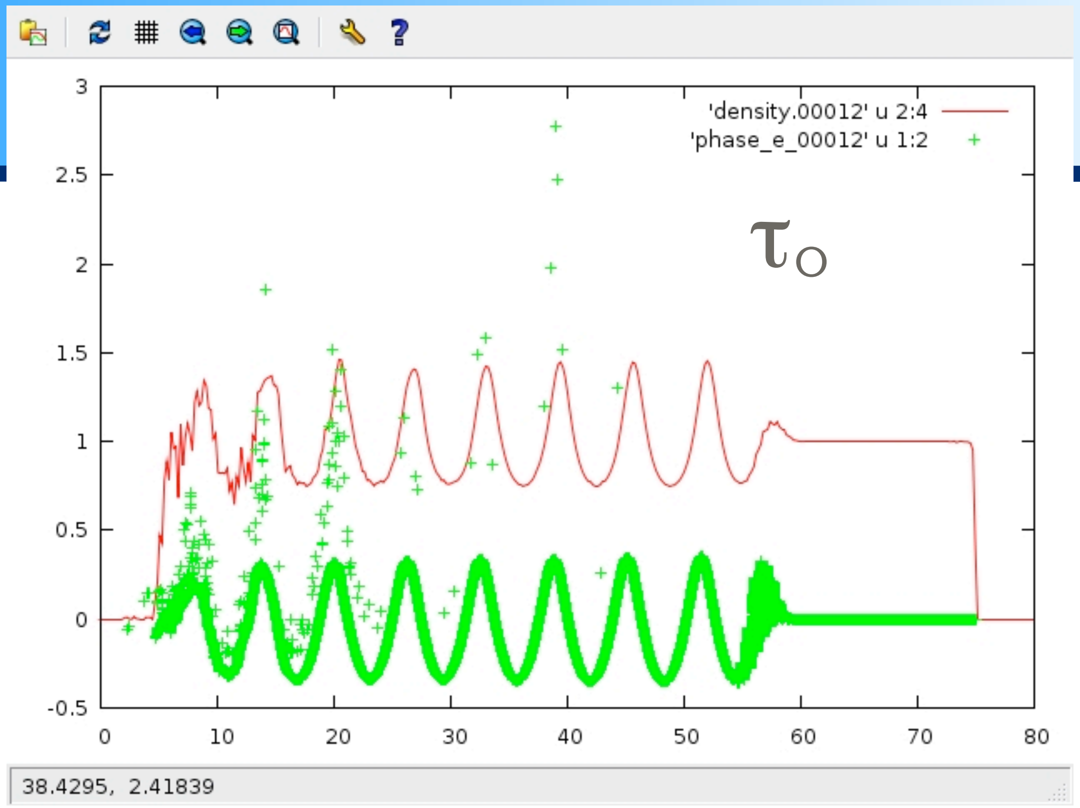

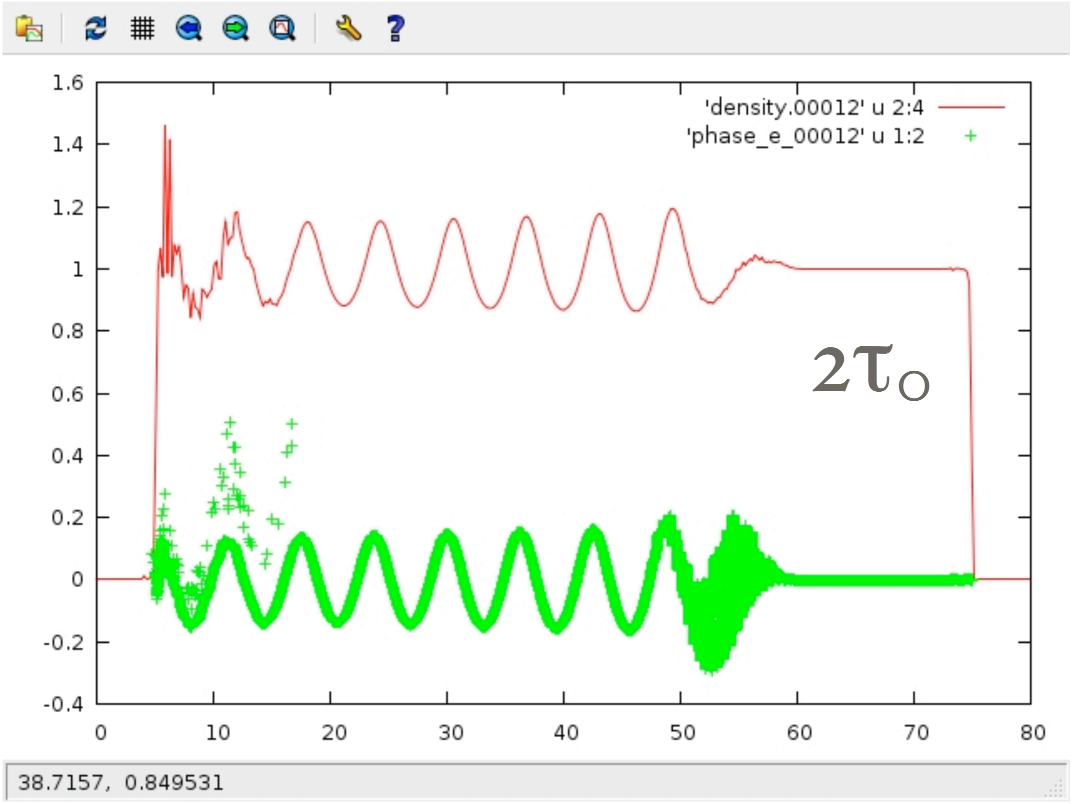

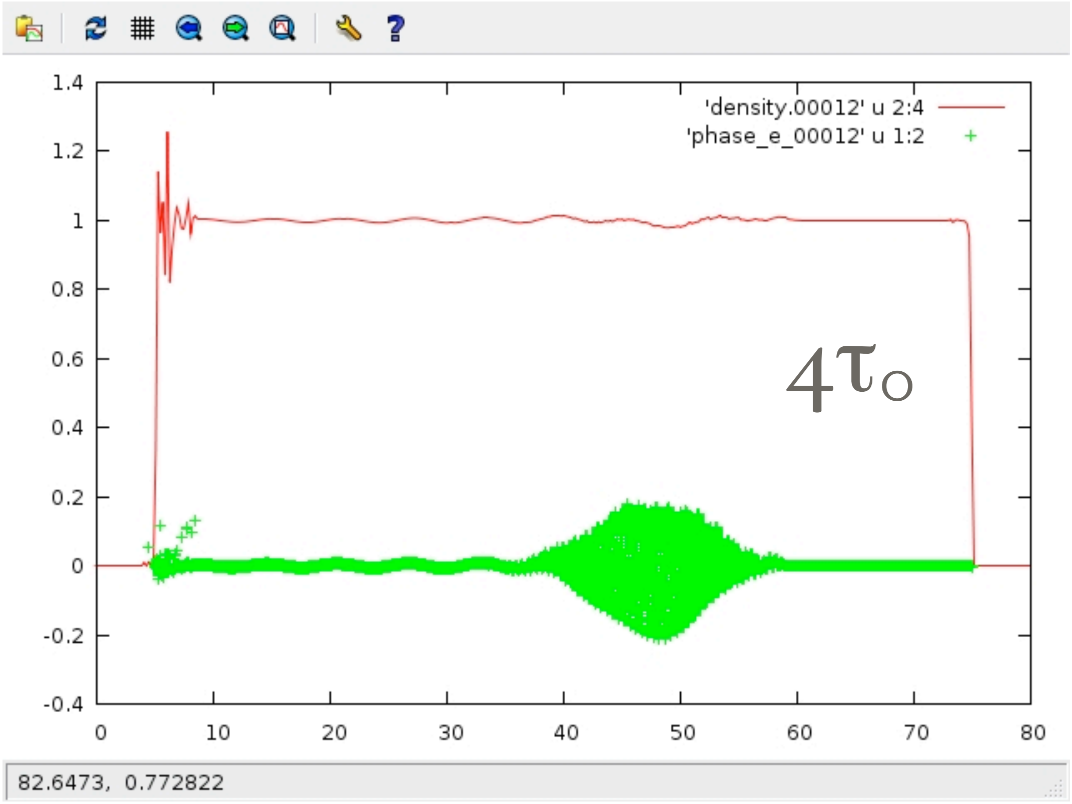

Variation with the target plasma density (after 198 fs)

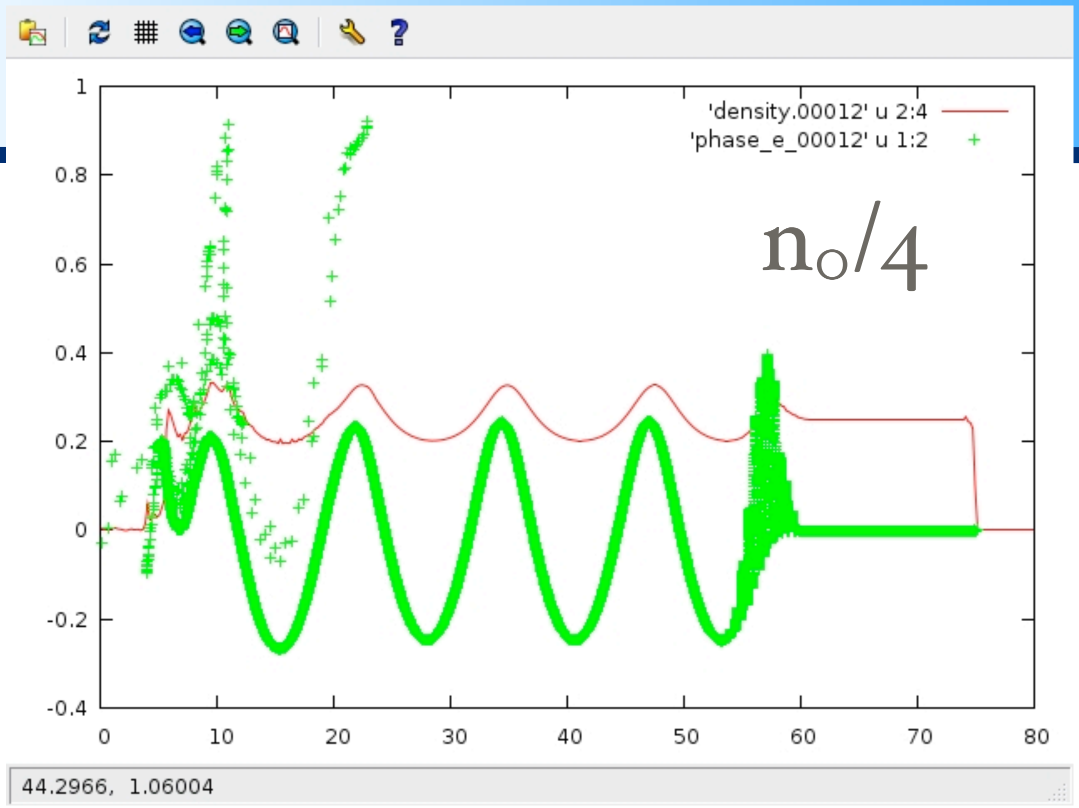

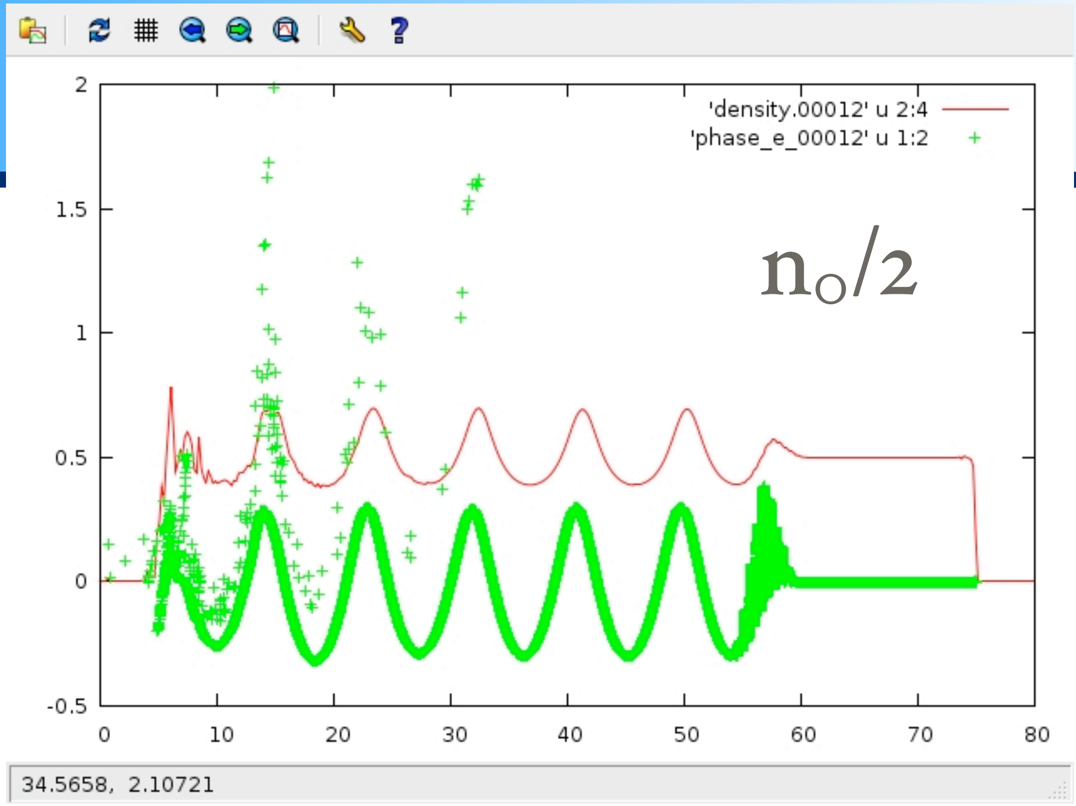

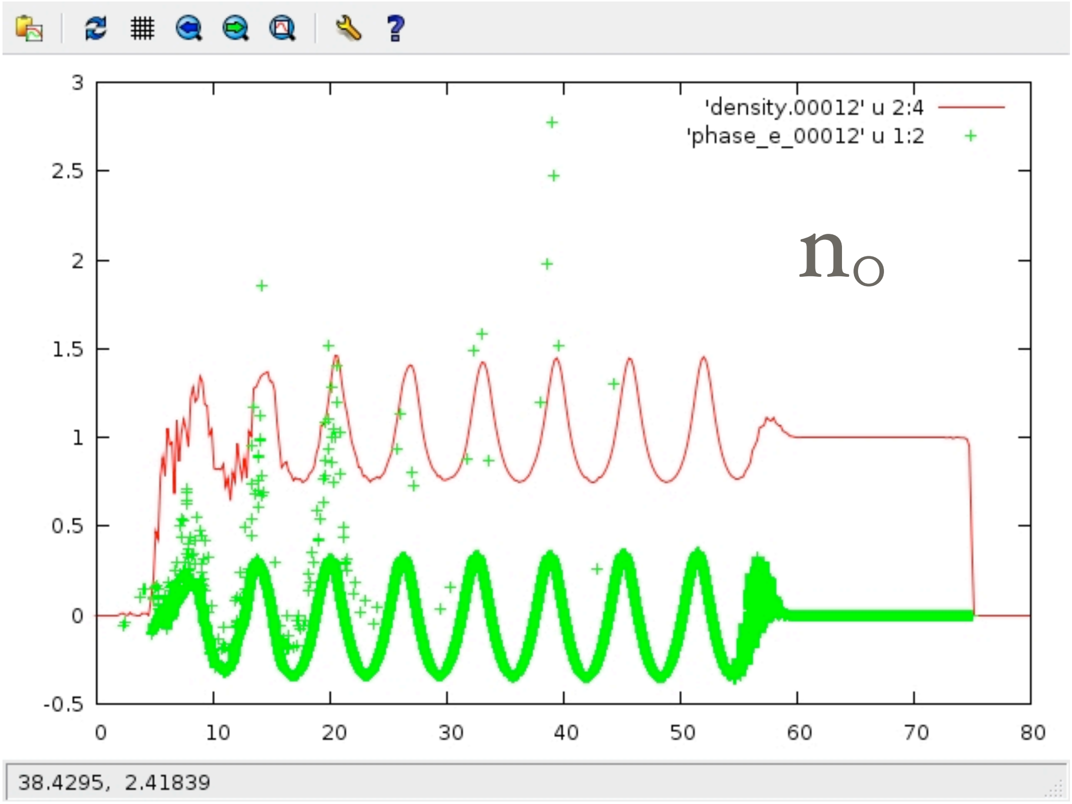

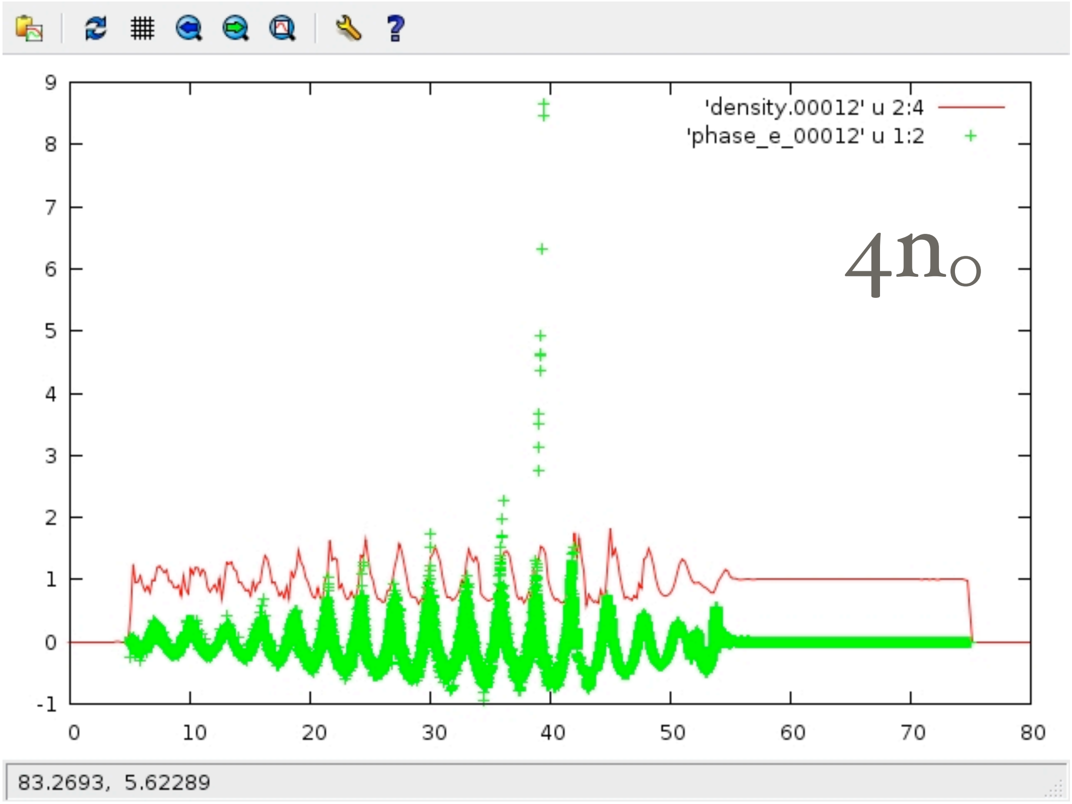

Additional physical modules

Structure of relativistic electromagnetic PIC code PICLS for HEDP

PICLS

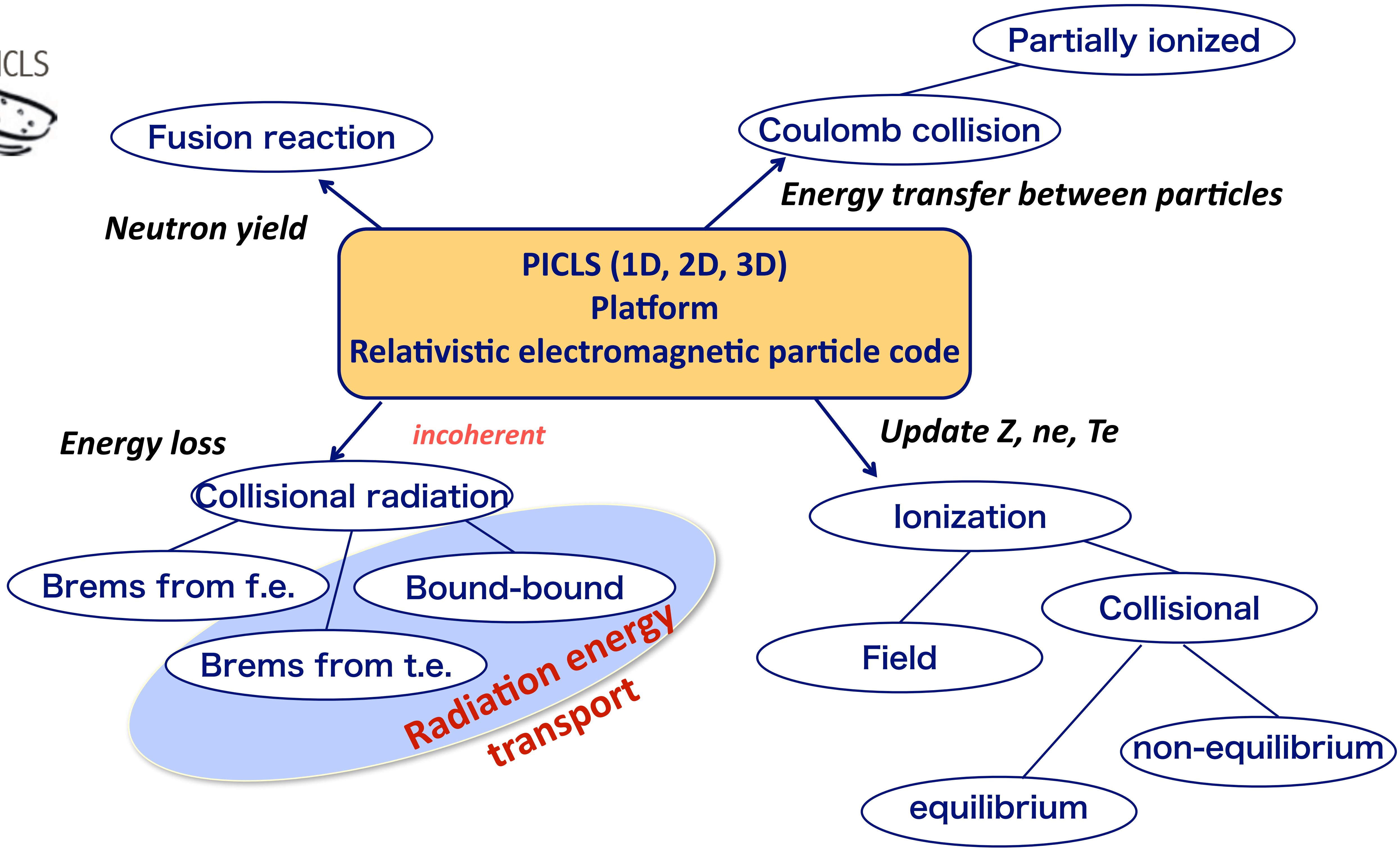

[1] Y. Sentoku, and A. J. Kemp J. Comput. Phys. 227, 6846 (2008)
[2] Y. Sentoku, E. d'Humières et al., PRL 107, 135001 (2011)
[3] R. Mishra, P. Leblanc, Y. Sentoku et al. Phys. Plasmas 20, 072704 (2013)

Visualization using IDL or Python

PARTICLE-IN-CELL CODE TIME STEP

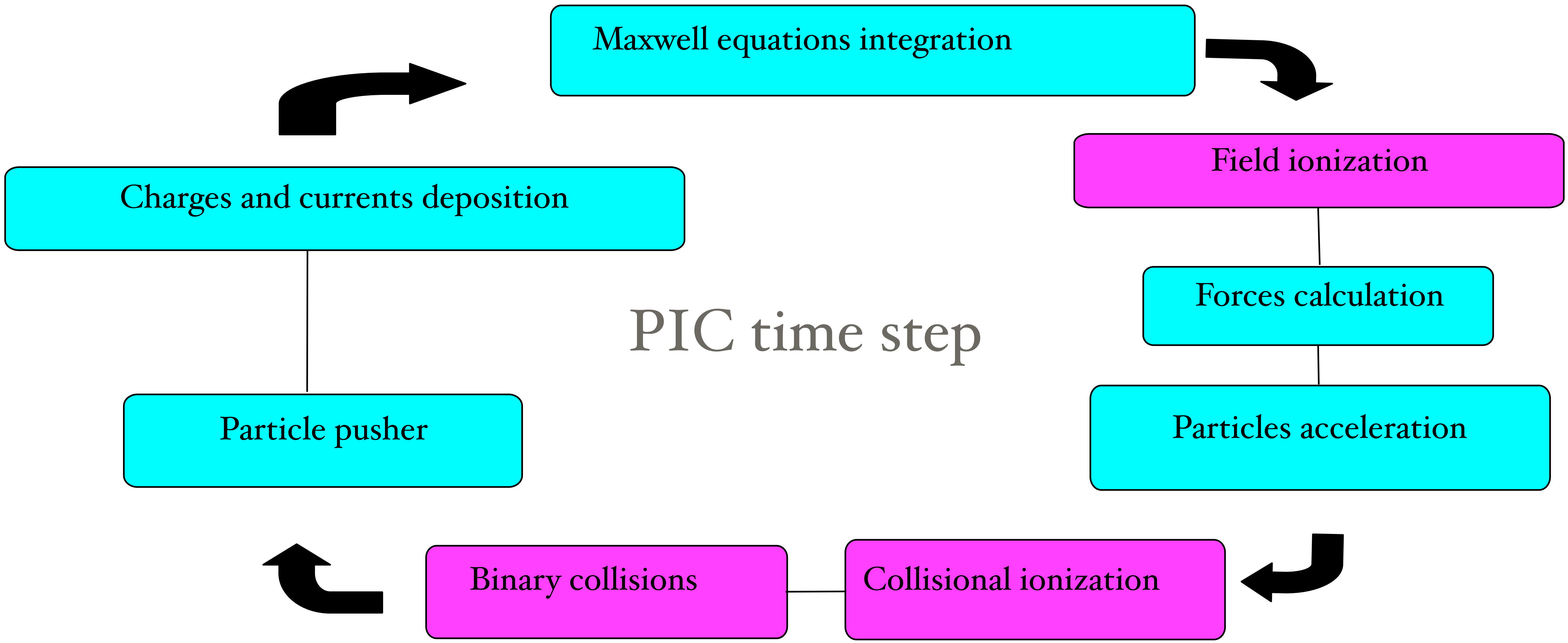

The physics cannot be scaled anymore (ω_r needs to be fixed)

Collisions can be introduced using an *ad-hoc* Monte-Carlo module

Collisions are computed inside the cell

To avoid the N-body problem, quasi-particles in the cell are randomly "paired"

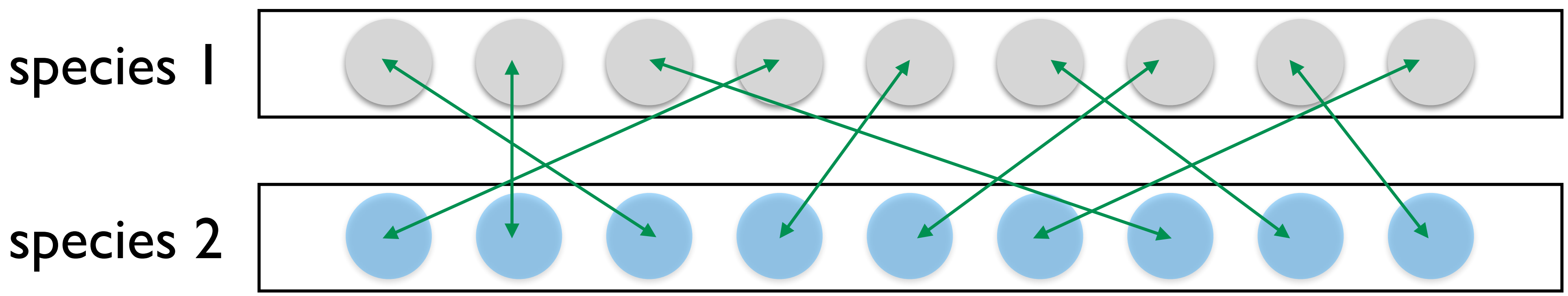

A single particle goes through many ($N \gg 1$) collisions at small angle θ which translates in a total deflection angle χ (not necessarily small)

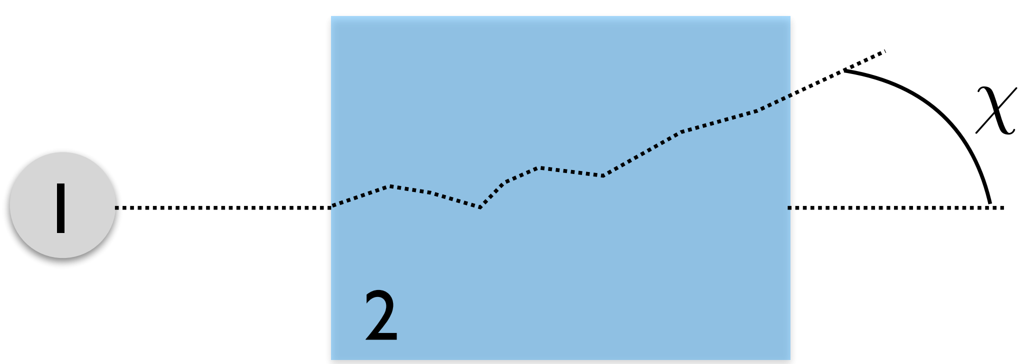

for each pair (Monte-Carlo)
- compute the collision rate
- compute the deflection angle
- deflect one or both particles

Nanbu, Phys. Rev. E **55**, 4642 (1997); J. Comp. Phys. **145**, 639 (1998)
F. Pérez et al., Phys. Plasmas **19**, 083104 (2012)
Y. Sentoku and A. Kemp, Journal Comp. Phys. 227, 6846 (2008)

PIC codes are then able to treat purely collisional processes

Thermalization
(hydrogen plasma)

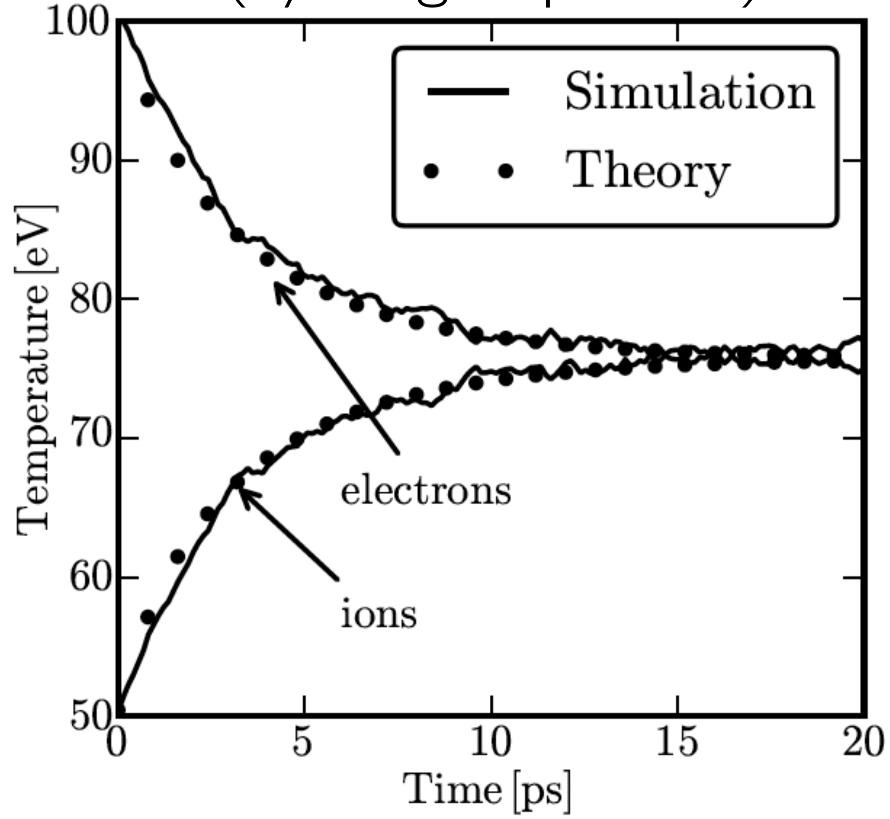

Isotropization
(electron plasma)

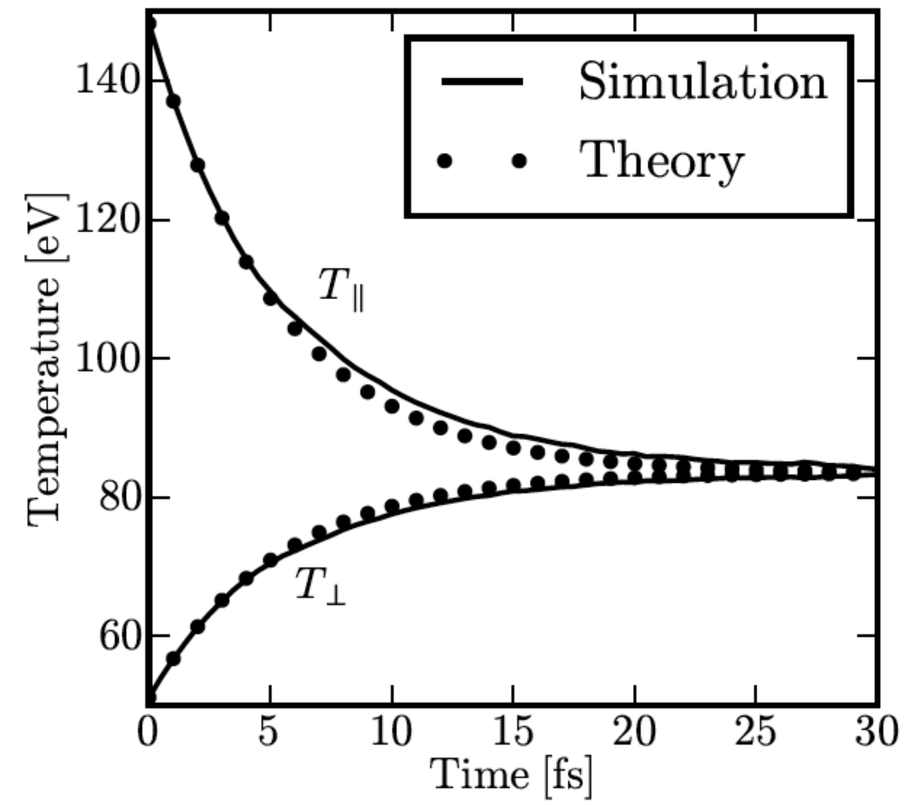

Collisions are important for:

- hot electron transport in dense plasmas
- resistive heating by strong current
- heat transport in HED & fusion plasmas

J. Derouillat et al., *SMILEI: a collaborative, open-source, multi-purpose PIC code for plasma simulation,* Comp. Phys. Comm. **222**, 351 (2018)

Electron Energy Density

- Laser Intensity: 10^{19}W/cm^2
- 1ps Gaussian Pulse
- Target: solid
  aluminum (initial Z=3)
  CH plastic (initial Z=0)

PICLS, Y. Sentoku

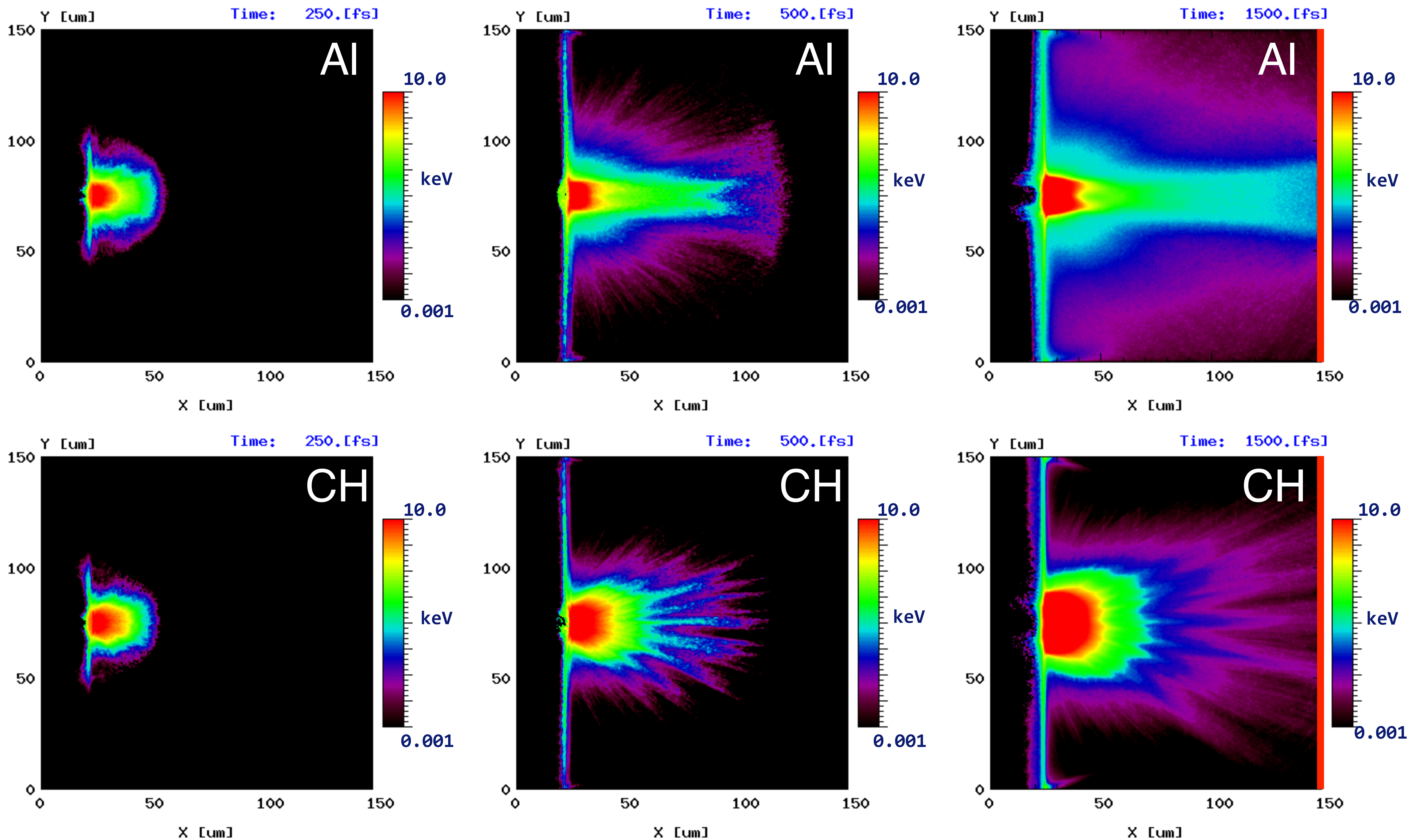

Resistive Magnetic Fields

PICLS, Y. Sentoku

t=500fs

Resistive magnetic fields

Resistivity

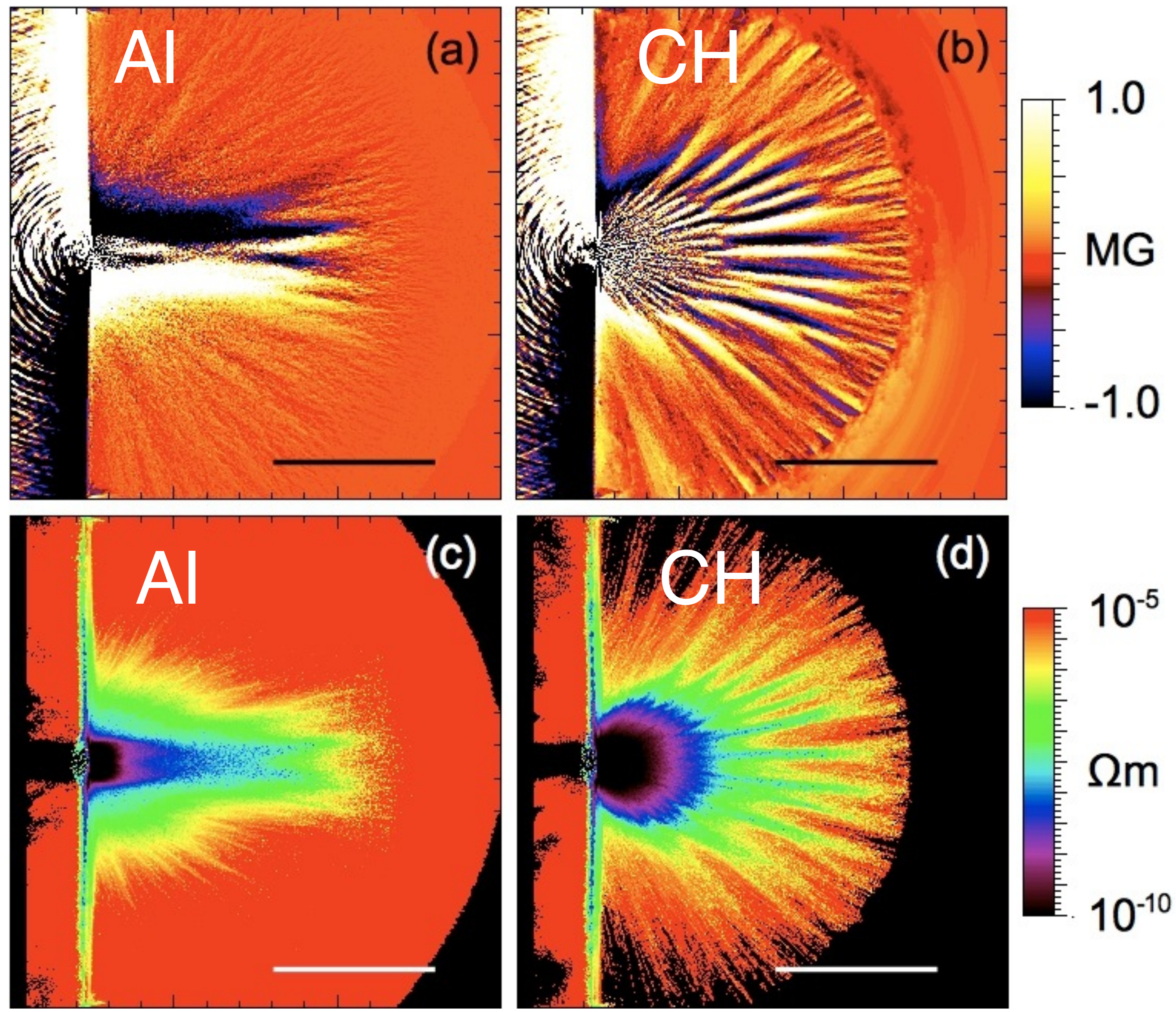

The mega-gauss magnetic fields pattern are consistent with the resistivity topology, which confirms the strong magnetic fields originate from the resistive gradient.

Similarly field and collisional ionization can be treated using a Monte-Carlo approach

Field ionization is important for laser wakefield acceleration

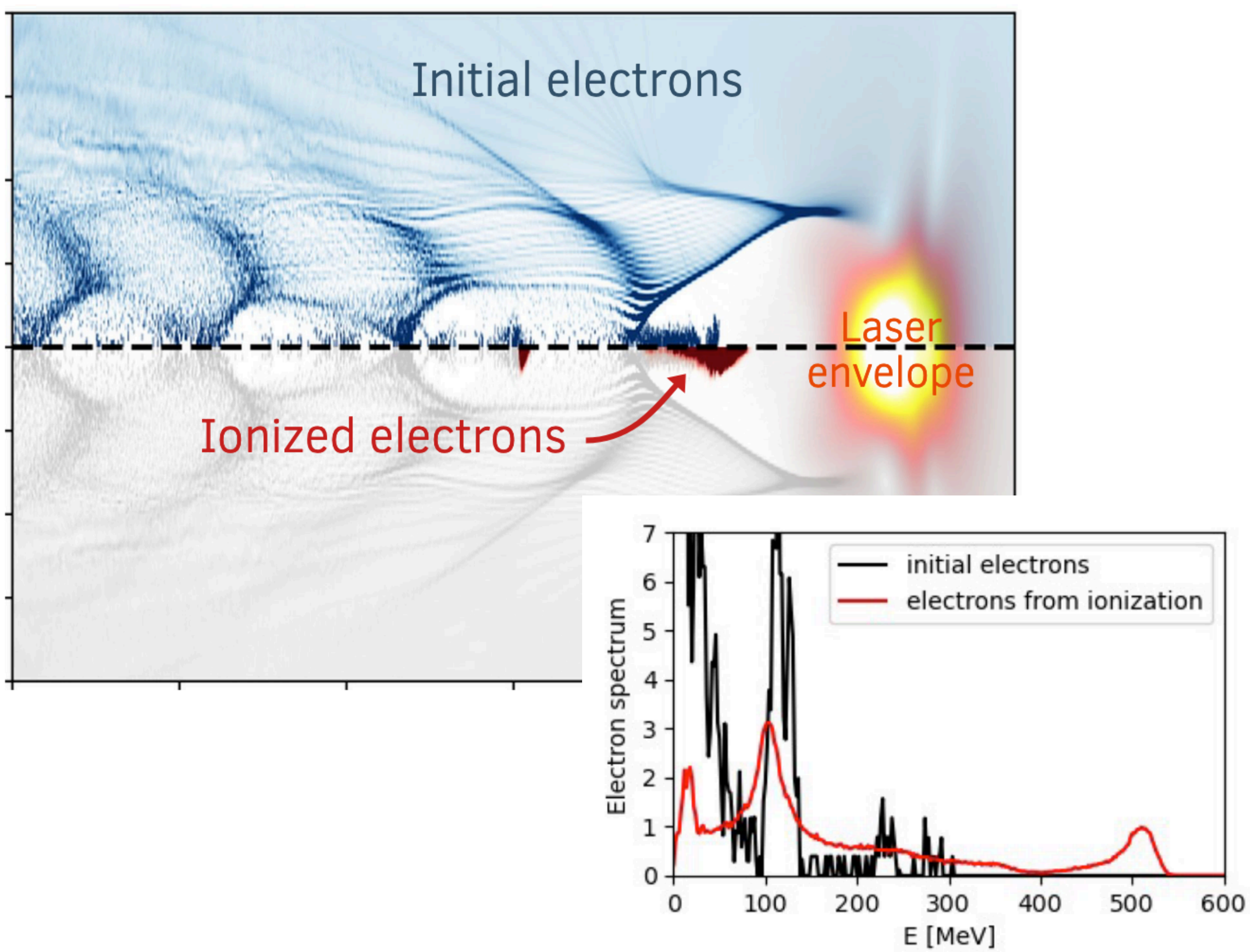

Stopping power of a cold aluminium plasma of density 10^{21} cm^{-3}

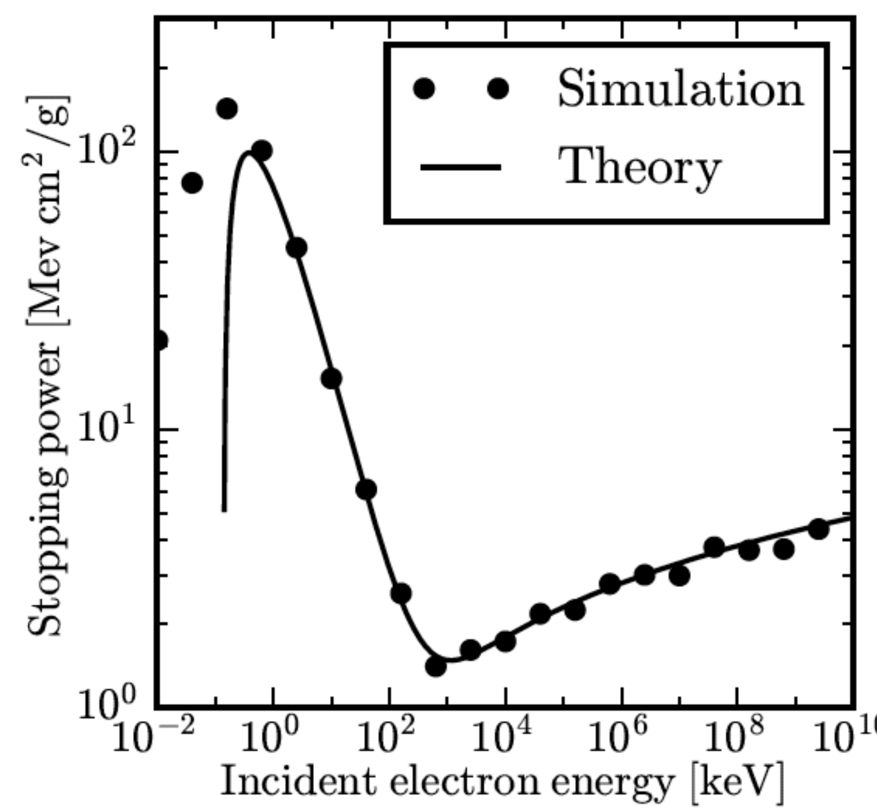

R. Nuter *et al.*, Phys. Plasmas **18**, 033107 (2011); F. Pérez et al., Phys. Plasmas **19**, 083104 (2012)

Laser-produced plasmas have large density and optical scales

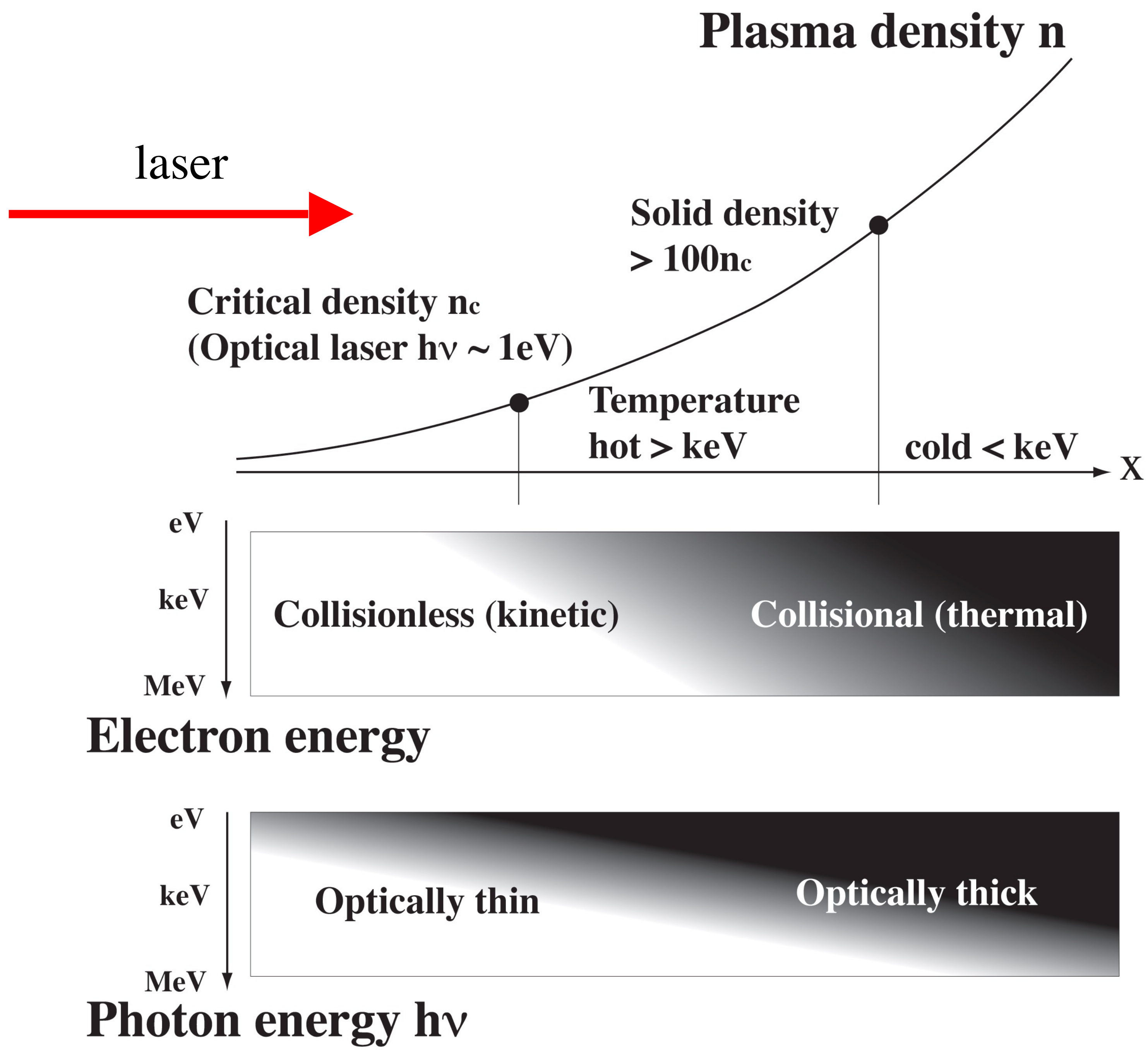

We cannot simplify the radiation processes by assuming an optically thin or optically thick plasma. We must directly solve the radiation transport equation.

coupling RT model to PIC code

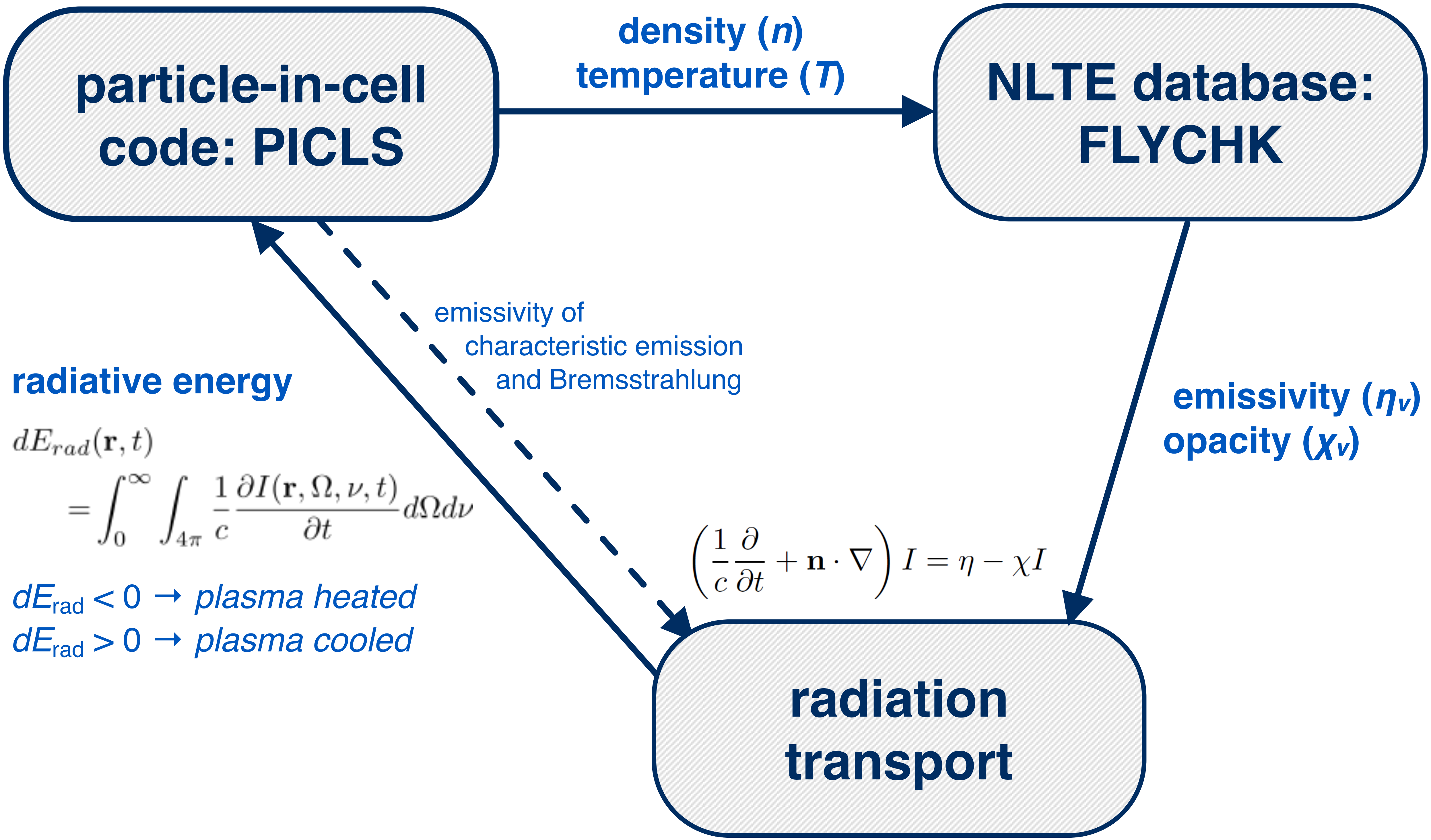

R. Royle et al. Phys. Rev. E 95, 063203 (2017)

Radiation transport model for intense laser-produced plasmas

Radiative transfer equation

$$\left(\frac{1}{c}\frac{\partial}{\partial t} + \mathbf{n}\cdot\nabla\right) I = \eta - \chi I$$

$\left\{\begin{array}{l} I(\mathbf{r},\Omega,h\nu,t) : \text{intensity of radiation} \\ \eta(\mathbf{r},h\nu,t) : \text{emissivity} \\ \chi(\mathbf{r},h\nu,t) : \text{opacity} \end{array}\right.$

(a) Multi-group method for photon energies

Radiation energy is divided into groups of finite energy width. The transport equation is integrated over the energy width for each group, then solved to obtain the radiation intensity for each group, I_g.

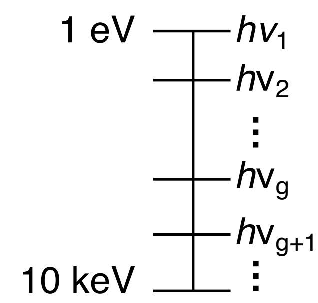

$$I_g(r,\Omega,t) = \int_{h\nu_{g+1}}^{h\nu_g} I(r,\Omega,h\nu,t)\,dh\nu$$

$$\eta_g(r,\Omega,t) = \int_{h\nu_{g+1}}^{h\nu_g} \eta(r,\Omega,h\nu,t)\,dh\nu$$

$$\tilde{\chi}_{a\,g}(r,t) = \int_{h\nu_{g+1}}^{h\nu_g} \tilde{\chi}_a(r,h\nu,t)\,dh\nu$$

(b) S_N method for direction

For the angular variables (polar angle θ and azimuthal angle ω), we apply the discrete ordinate method. The transport equation is solved for each discrete direction (m,n) to obtain the radiation intensity in that direction, $I_{m,n}$

Lee, C.E., Los Alamos Scientific Laboratory Report LA-2595, 1962

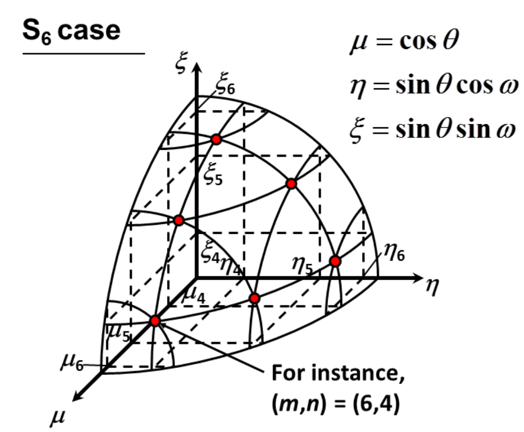

This method allows us to simulate anisotropic emission!

(c) CIP (Constrained Interpolation Profile) scheme for advection

CIP scheme having 3rd order spatial accuracy is applied for advection term. Because of explicit method, this scheme is suitable for MPI.

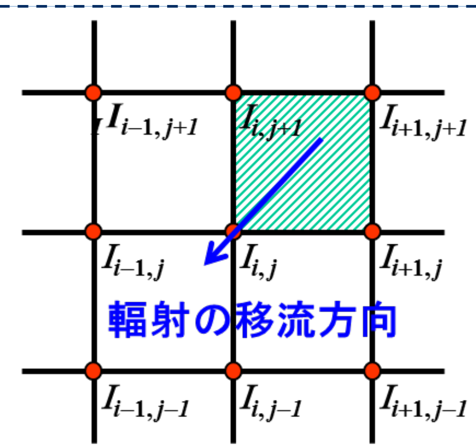

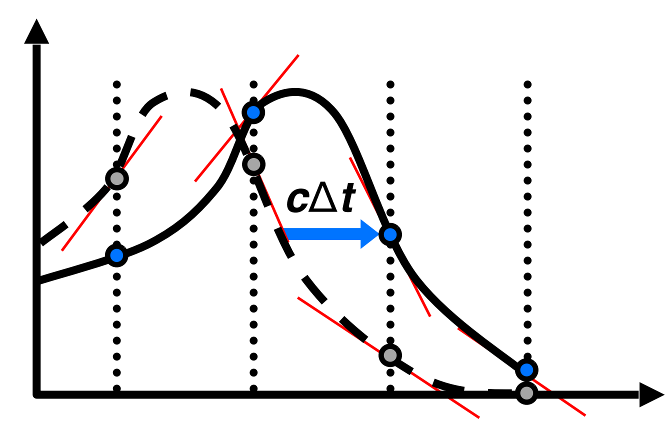

T. Yabe, et al., CPC **66** (1991) 233.; F. Xiao et al., CPC **93** (1996) 1; F. Xiao et al., CPC **94** (1996) 103.

(1) Direct comparison of X-rays with experiment, including characteristic (K_α) emissions

2 µm thin copper foil

Electron energy density

Kα energy density (8.04 keV)

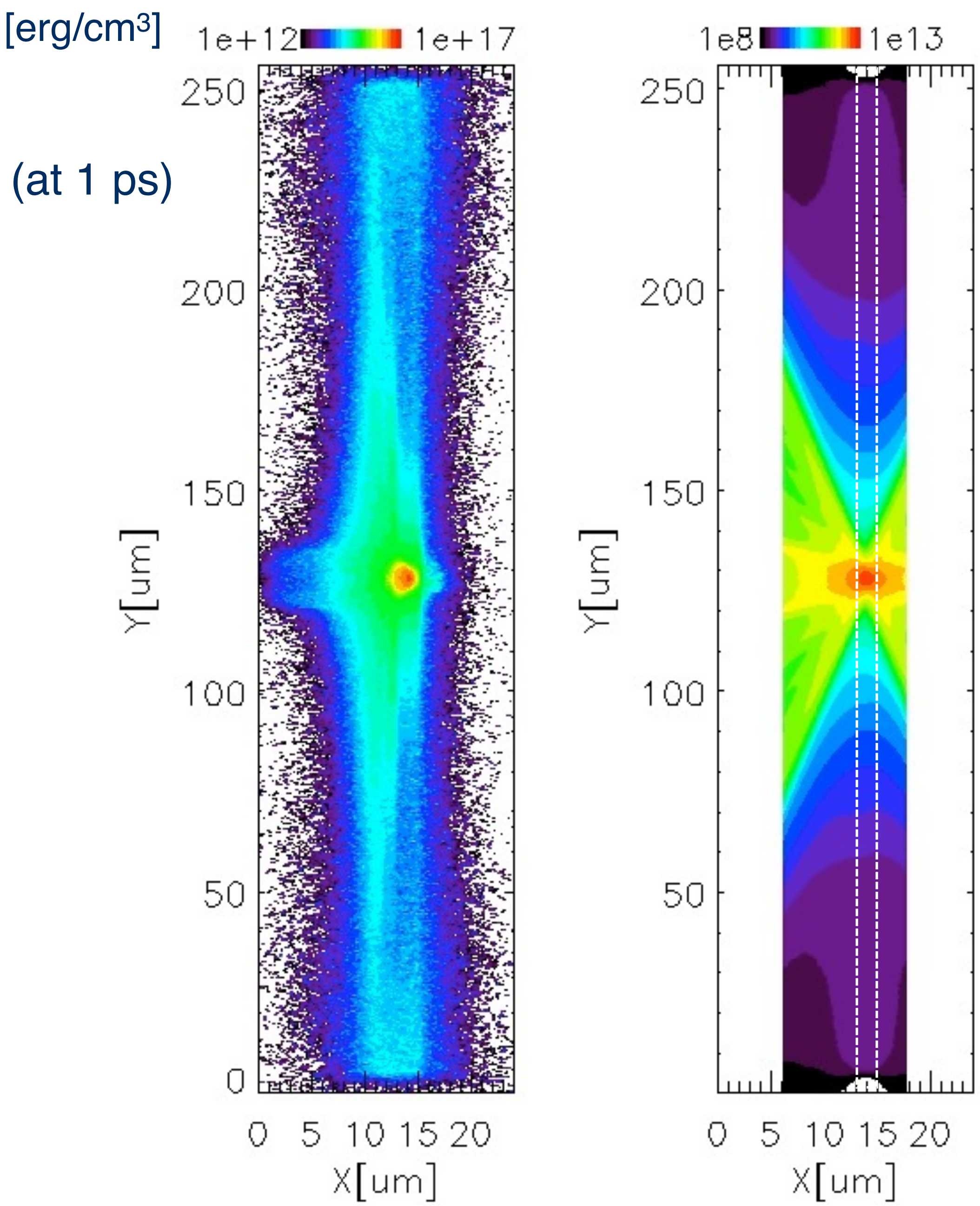

I=2x10^19 W/cm², 350fs pulse, 8µm spot

Courtesy of Y. Sentoku

Time integrated distribution on back surface

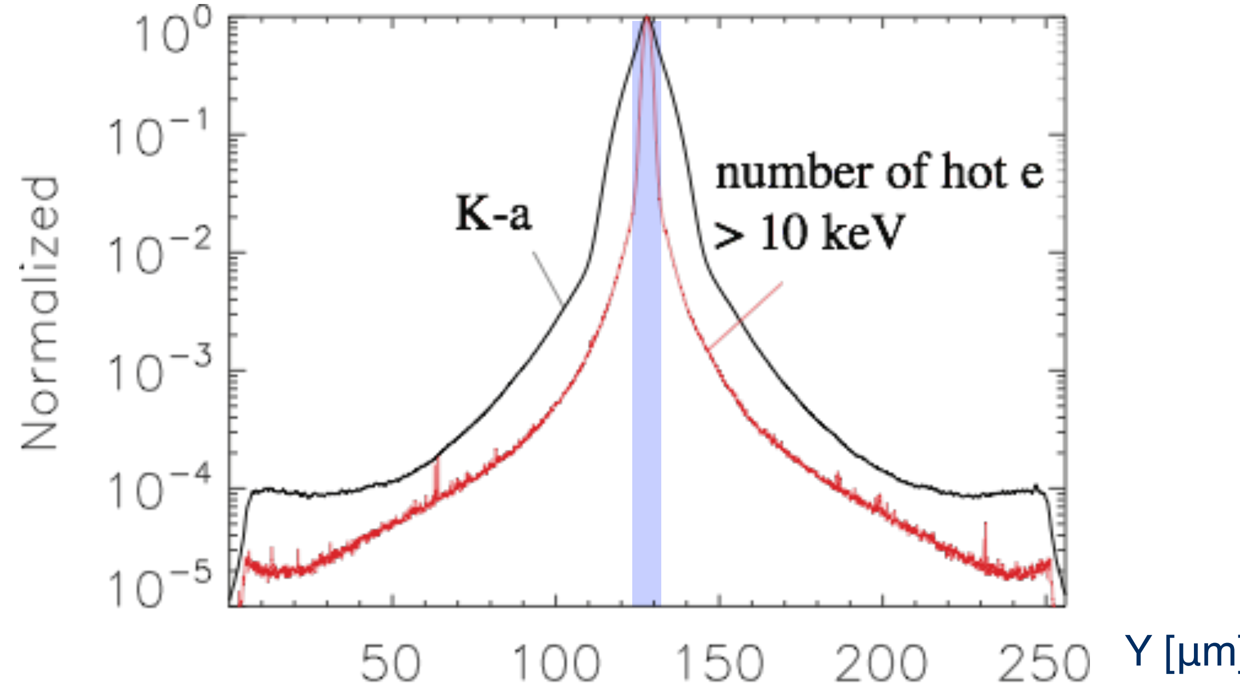

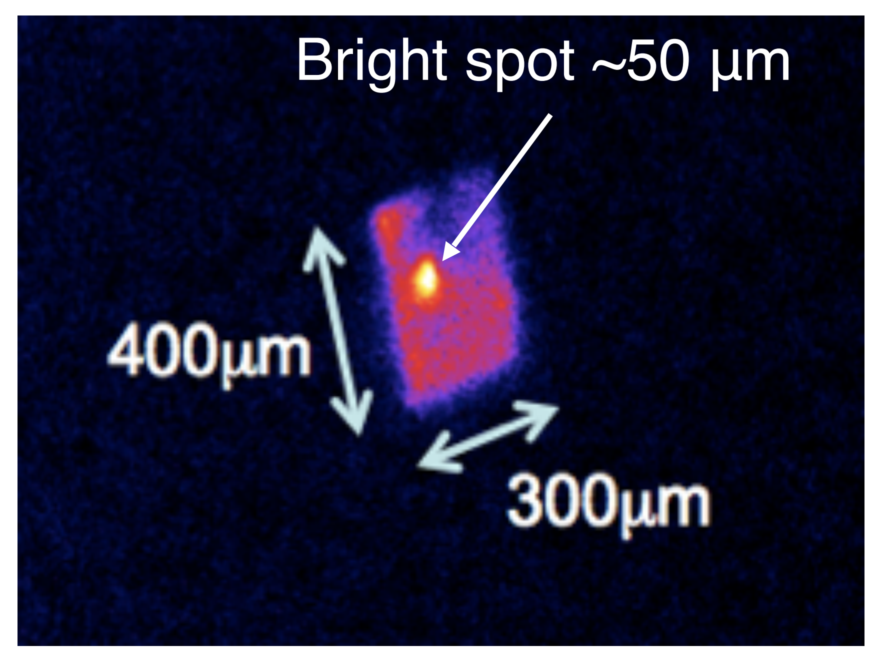

Figure: 2D monochromatic X-ray image of K_α (8 keV) of a 2 µm thick copper foil heated by the 100 TW Leopard laser (Hiroshi Sawada, UNR)

(2) Intense X-ray laser-matter interaction: kinetics of photoionized plasmas

Photoionization has been implemented to study the XFEL-matter interaction.

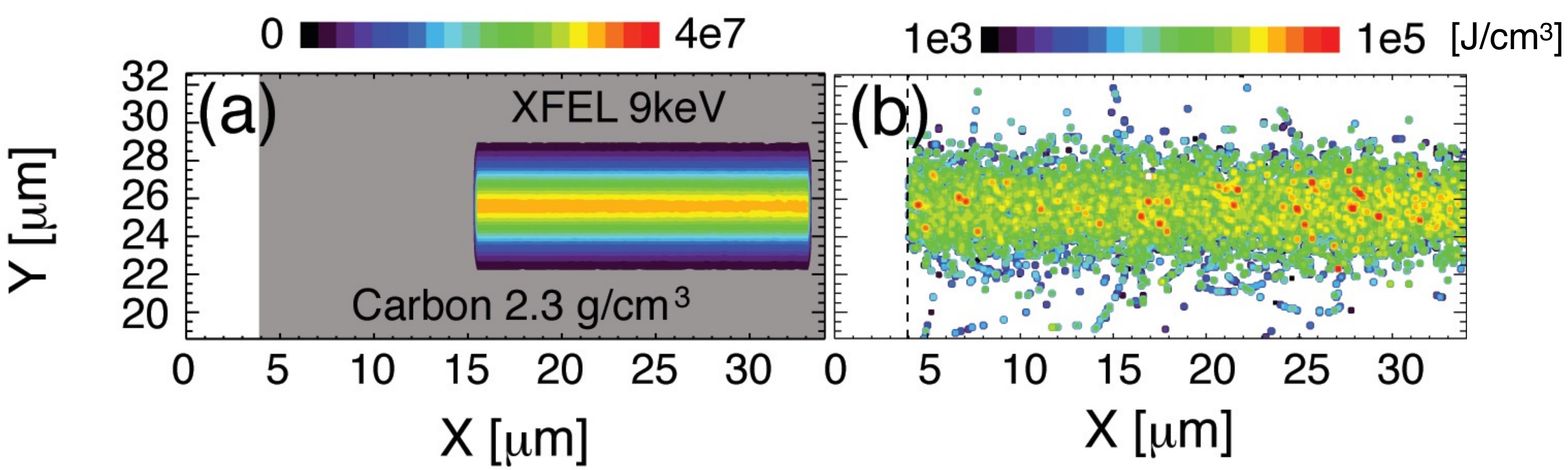

XFEL energy density at 100 fs. XFEL (9 keV) penetrates into solid graphite.

Electron energy density at 200 fs. A hot plasma column is formed behind the XFEL pulse.

Courtesy of Y. Sentoku

(3) γ-ray production in extremely intense LPI

10 μm copper target

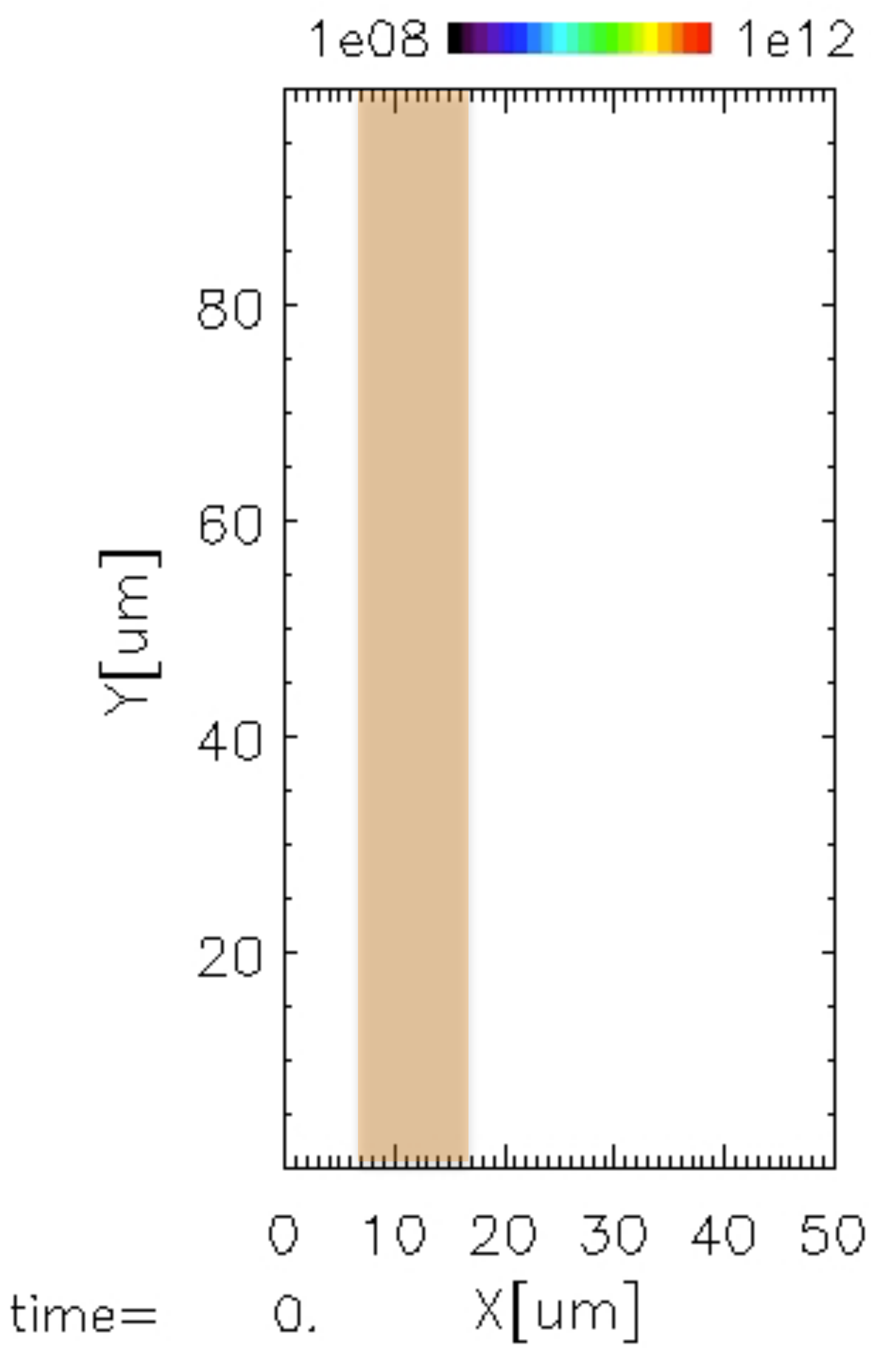

I = 10^{20} W/cm^2, 30 fs pulse, 5 μm spot

- γ-ray emissions are implemented in the radiation transport.
- Models of relativistic Bremsstrahlung and radiative damping will be introduced.
- Using the spatiotemporal information of γ-rays we can study the critical details of positron creation, nuclear reaction (γn), etc.

Courtesy of Y. Sentoku

Adding Quantum Electrodynamics (QED) effect is also very interesting for forthcoming multi-petawatt facilities

High-Energy Photon Production

Nonlinear Thomson and Compton scattering

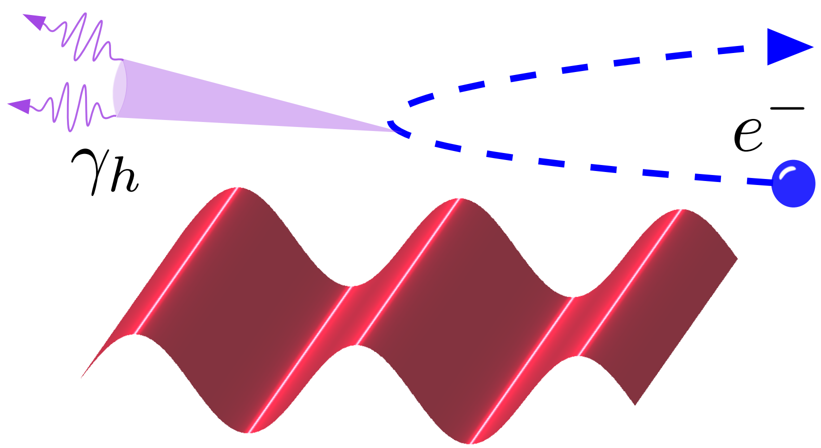

$$e^- + n\,\gamma_L \rightarrow e^- + \gamma_h$$

Bremsstrahlung

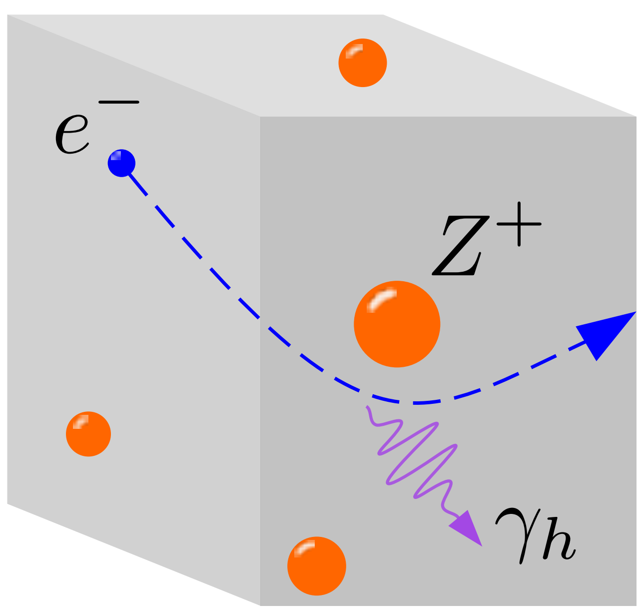

Electron-Positron Pair Production

Multi-Photon Breit-Wheeler Process

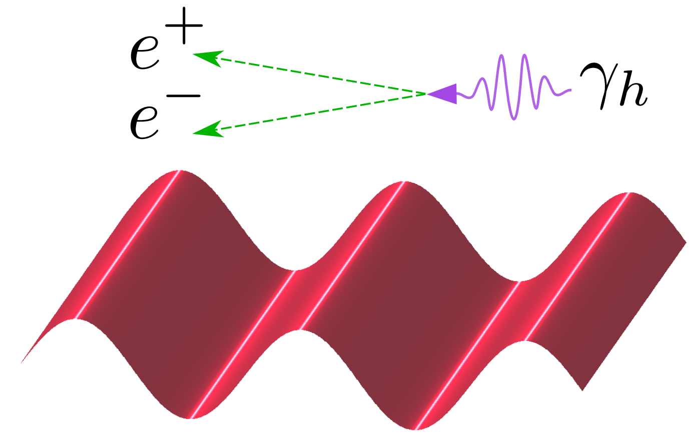

$$\gamma_h + n\,\gamma_L \rightarrow e^- + e^+$$

Pair production in strong Coulomb field

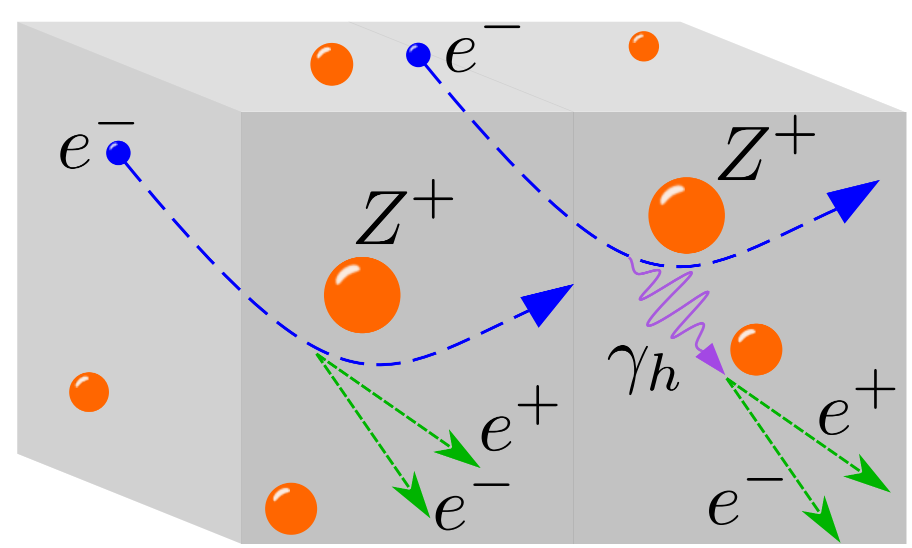

Courtesy of M. Grech

The Particle-In-Cell (PIC) Method

capture collective effects by solving the Vlasov-Maxwell Eqs.

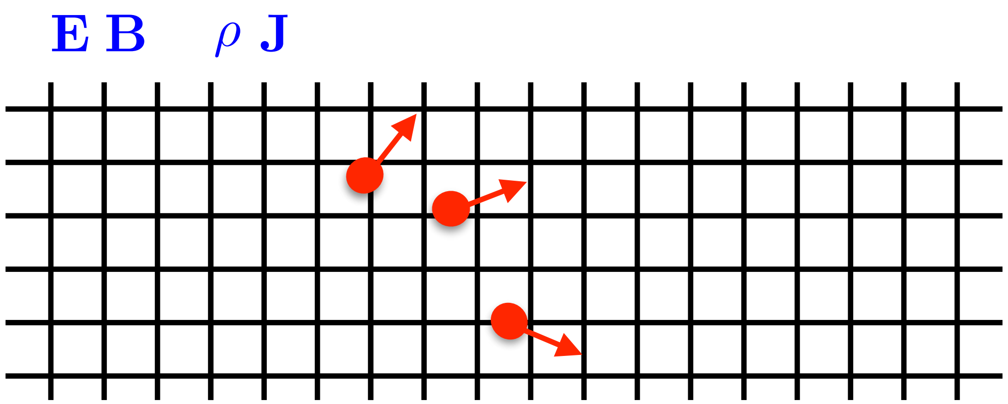

- Vlasov Eq. is solved using so-called macro-particles

$$f_s(t,\mathbf{x},\mathbf{p}) = \sum_N w^N\, S(\mathbf{x}-\mathbf{x}^N(t))\,\delta(\mathbf{p}-\mathbf{p}^N(t))$$

Interpolation

$$\forall N\ [\mathbf{E},\mathbf{B}] \rightarrow [\mathbf{E}^N,\mathbf{B}^N]$$

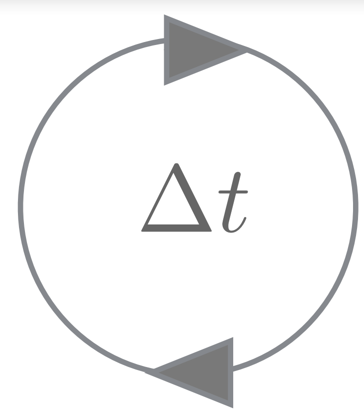

Projection

$$\forall N\ [\mathbf{x}^N,\mathbf{p}^N] \rightarrow [\rho,\mathbf{J}]$$

Maxwell Solver

$$\partial_t \mathbf{E} = -\mathbf{J} + \nabla\times\mathbf{B}$$
$$\partial_t \mathbf{B} = -\nabla\times\mathbf{E}$$

Modified Electron Pusher

$$\chi_e = \left|\frac{F^{\mu\nu}}{E_S}\frac{p^\nu}{m_e c}\right|$$

$\chi_e < 10^{-5}$ classical relativistic push.

$\chi_e < \chi_e^{th}$ radiation reaction force

$\chi_e > \chi_e^{th}$ Monte-Carlo method

Photon Pusher

for > 1.022 MeV photons:

$$\epsilon_\gamma > 2\,m_e c^2$$

$$\chi_\gamma = \left|\frac{F^{\mu\nu}}{E_S}\frac{\hbar k^\nu}{m_e c}\right|$$

multiphoton Breit-Wheeler process

Implemented in the PIC code CALDER

Lobet et al., arXiv:1311.1107 (2013)

Fusion modules

- DD fusion (PICLS, SMILEI)
- pB fusion (SMILEI, WARP-X)

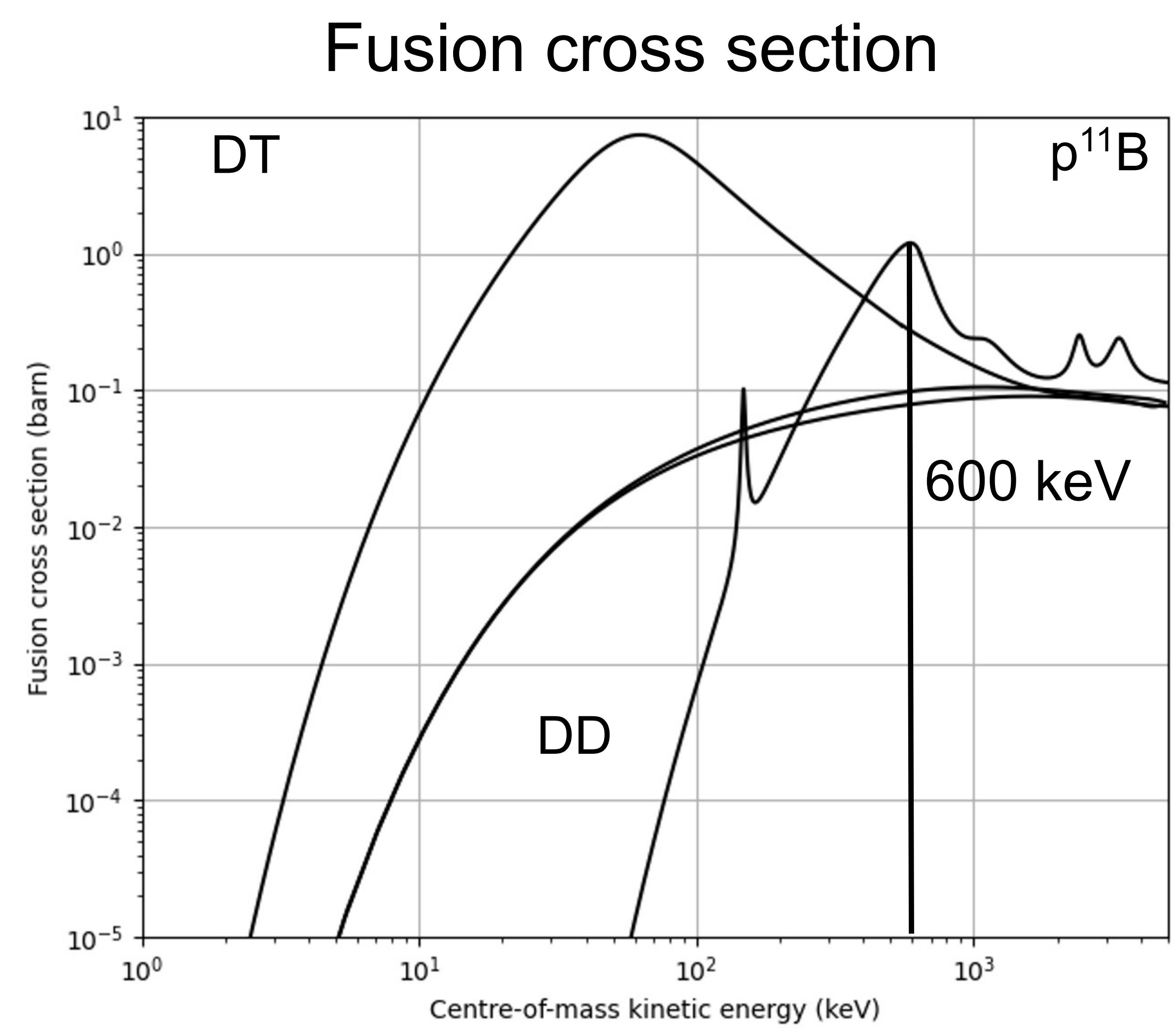

$$\mathrm{D} + \mathrm{T} \rightarrow \alpha\,(3.5\mathrm{MeV}) + \mathrm{n}\,(14.1\mathrm{MeV}) \qquad \mathrm{Q_{DT}} = 17.6\,\mathrm{MeV}$$

$$\mathrm{D} + \mathrm{D} \rightarrow \mathrm{T}\,(1.01\,\mathrm{MeV}) + \mathrm{p}\,(3.03\,\mathrm{MeV})$$
$$\mathrm{D} + \mathrm{D} \rightarrow {}^{3}\mathrm{H_e}\,(0.82\,\mathrm{MeV}) + \mathrm{n}\,(2.45\,\mathrm{MeV})$$

Aneutronic fusion

$$\mathrm{p} + {}^{11}\mathrm{B} \rightarrow 3\alpha\,(8.6\,\mathrm{MeV}) \qquad \mathrm{Q_{pB}} = 8.6\,\mathrm{MeV}$$

Examples of PIC simulations of high intensity LPI

Electromagnetic PIC codes are central for a wide range of plasma-physics-related studies

Laser - Plasma Interaction

Electron laser wakefield acceleration

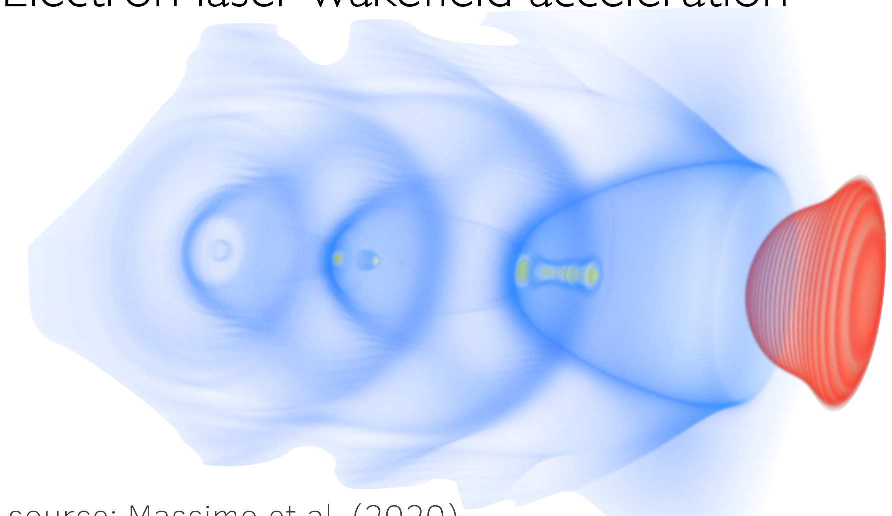

source: Massimo et al. (2020)

Ultra-high intensity laser-solid interaction

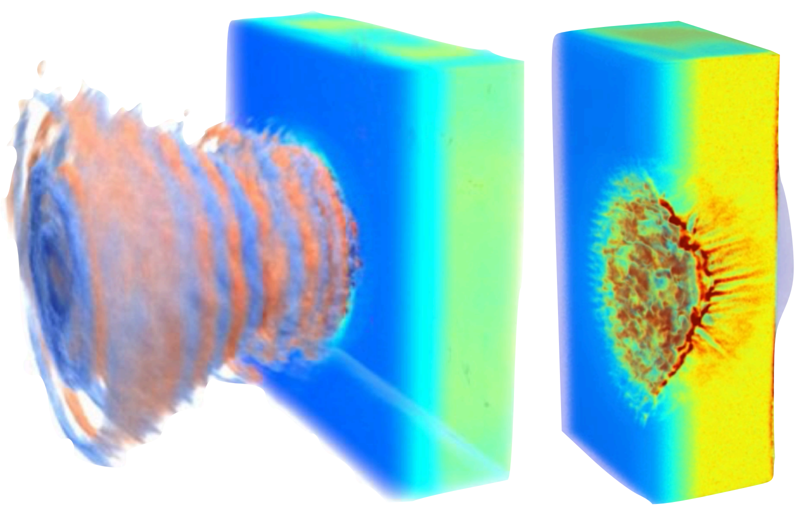

source: Smilei dev-team (2018)

Space and Astrophysical Plasmas

Magnetic reconnection at the Earth magnetopause

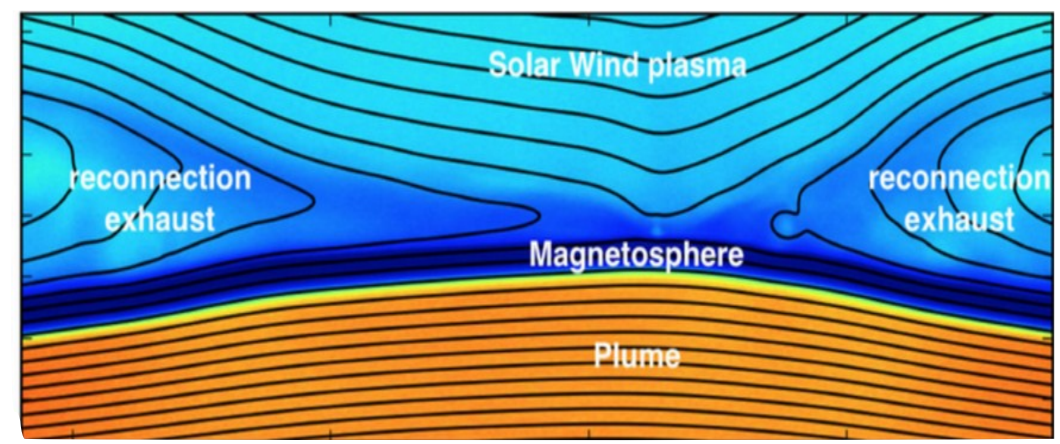

source: Dargent et al. (2017)

Weibel-mediated collisionless shock

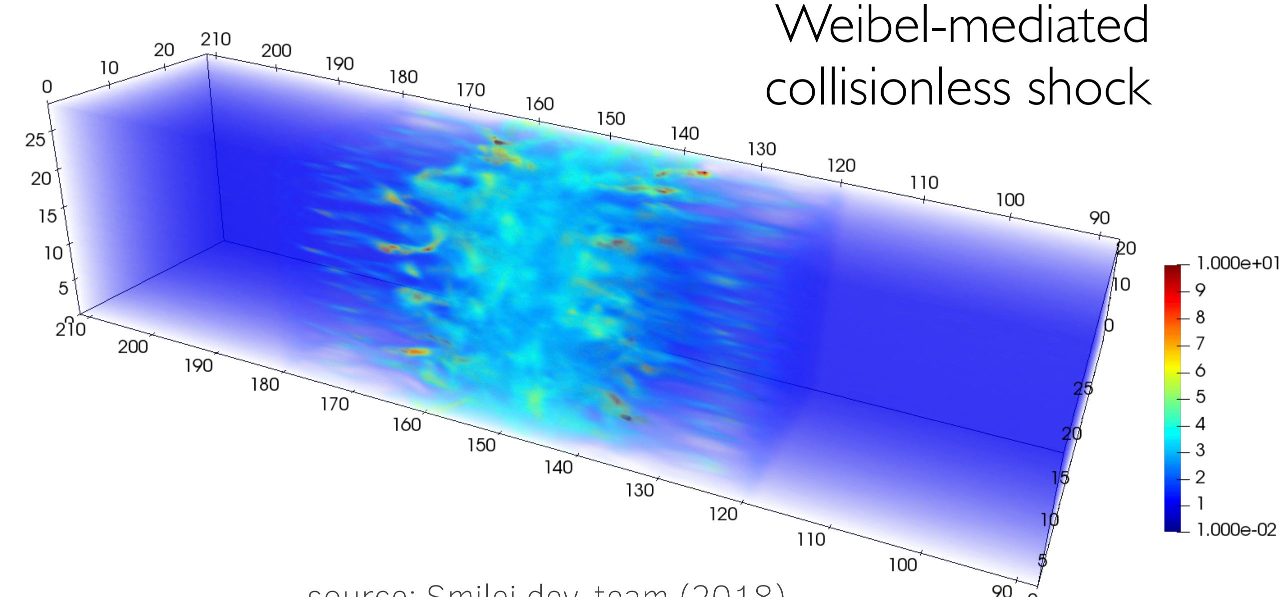

source: Smilei dev-team (2018)

Other examples

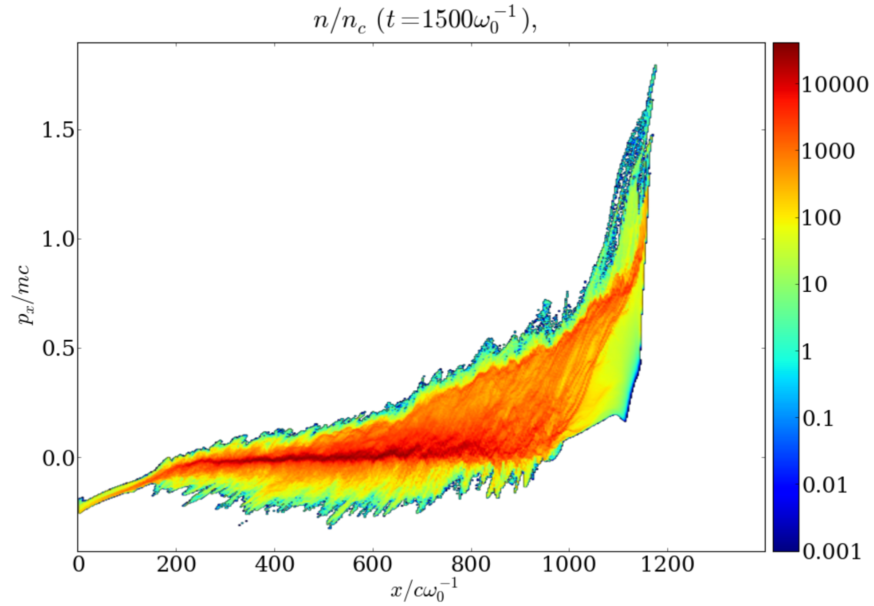

Relativistic laser accelerated ion beams

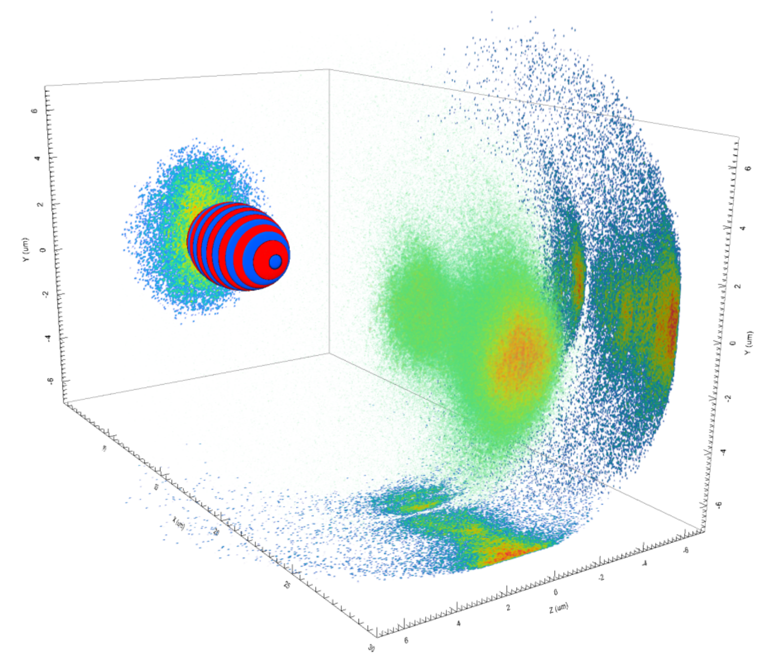

e-e+ pair plasmas

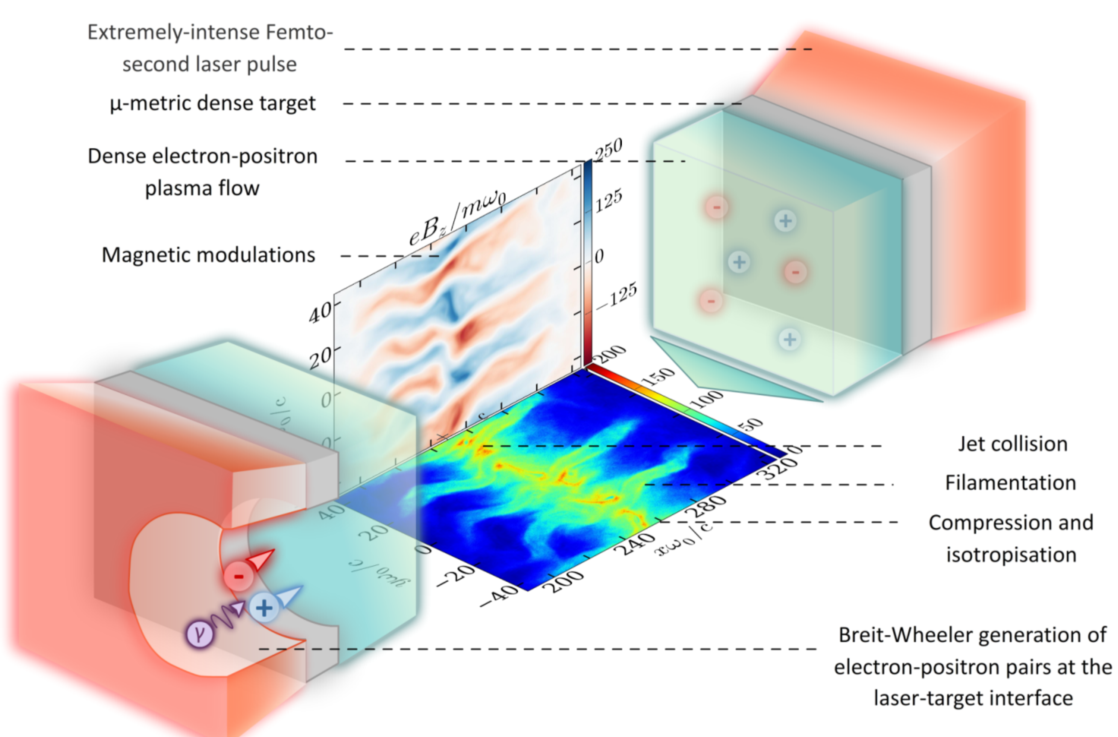

e-e+ pair plasmas collisions

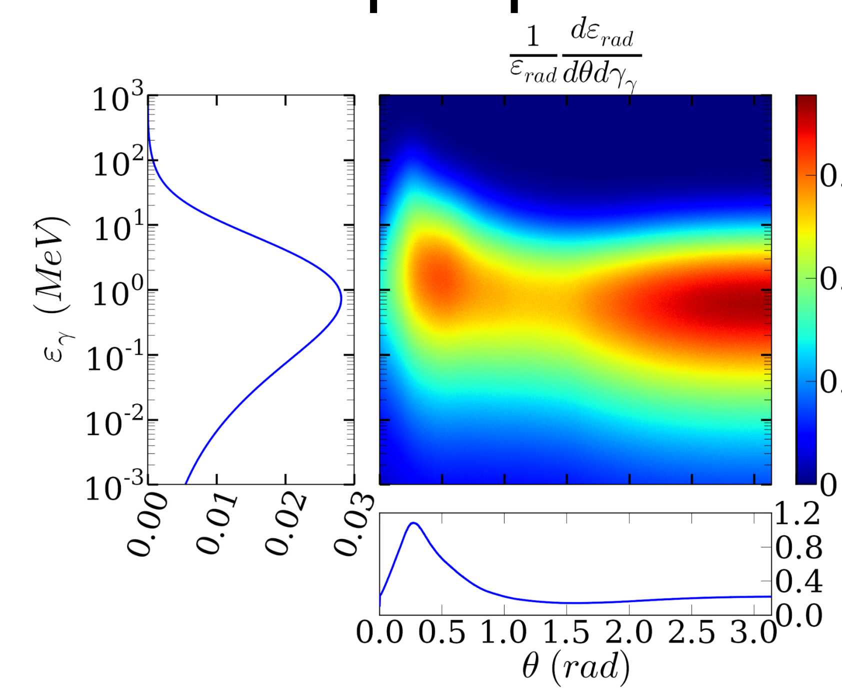

Intense γ beams to study the pure BW process

PIC codes are an excellent tool to support theoretical modelling

Even 1D simulation can bring a deep insight into the physics at play

Relativistically-Induced Transparency

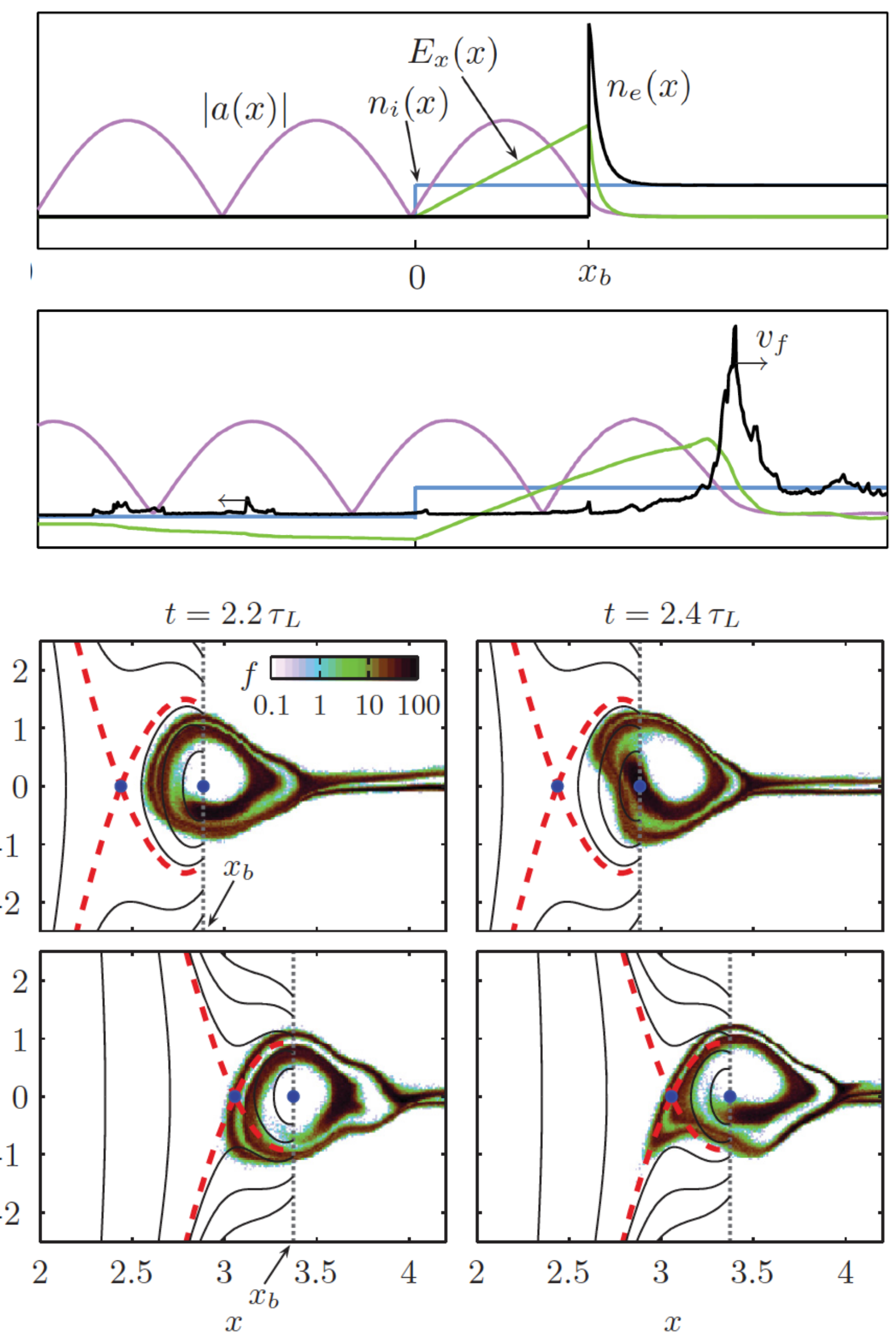

E. Siminos *et al.*, Phys. Rev. E **86**, 056404 (2012)

Weibel instability in the presence of an external magnetic field

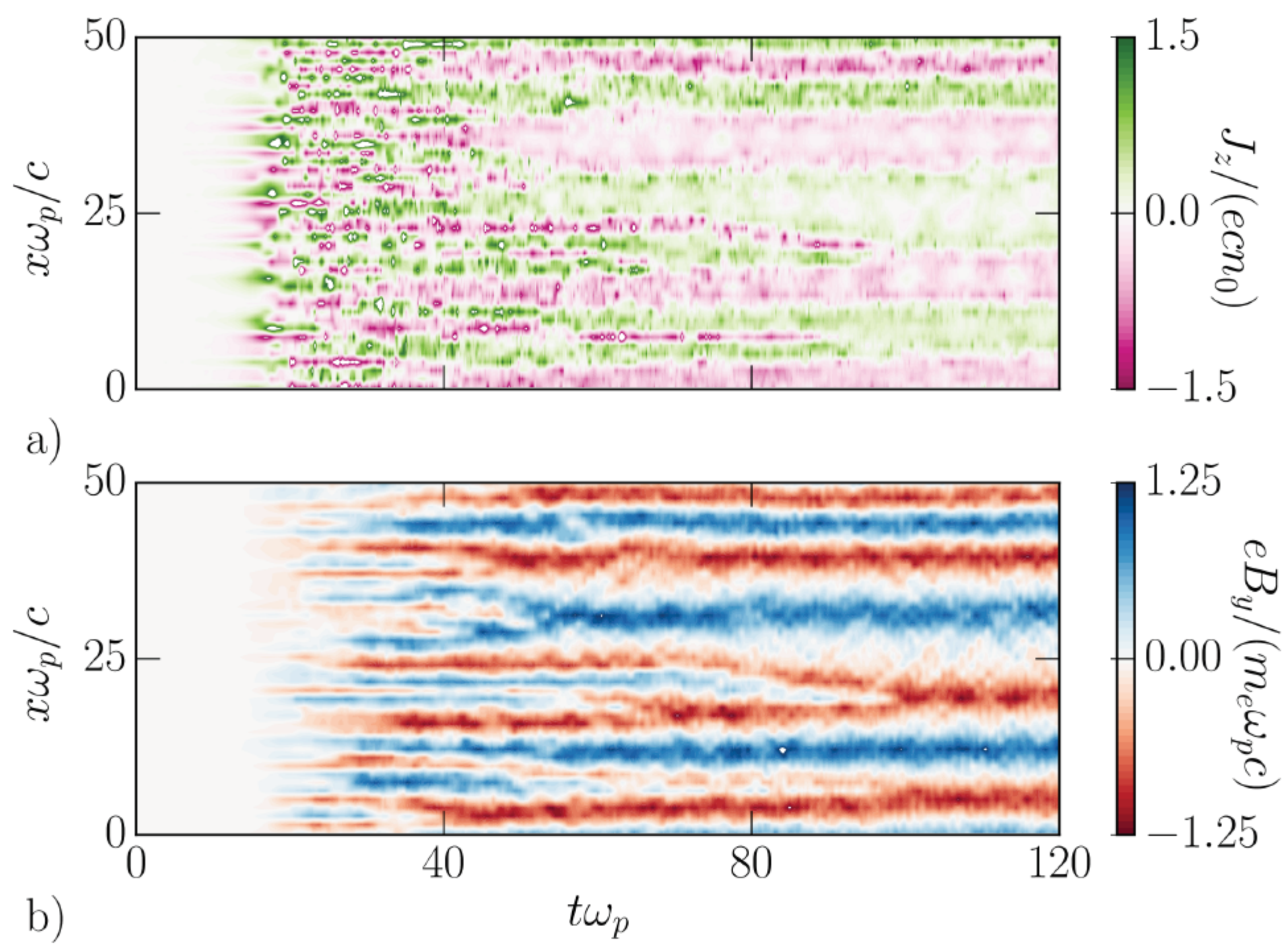

A. Grassi *et al.*, Phys. Rev. E **95**, 023203 (2017)

PIC codes can help design & interpret experimental campaigns

2D and 3D simulations on super-computers will be necessary here

High-harmonic generation & electron acceleration from laser-solid interaction

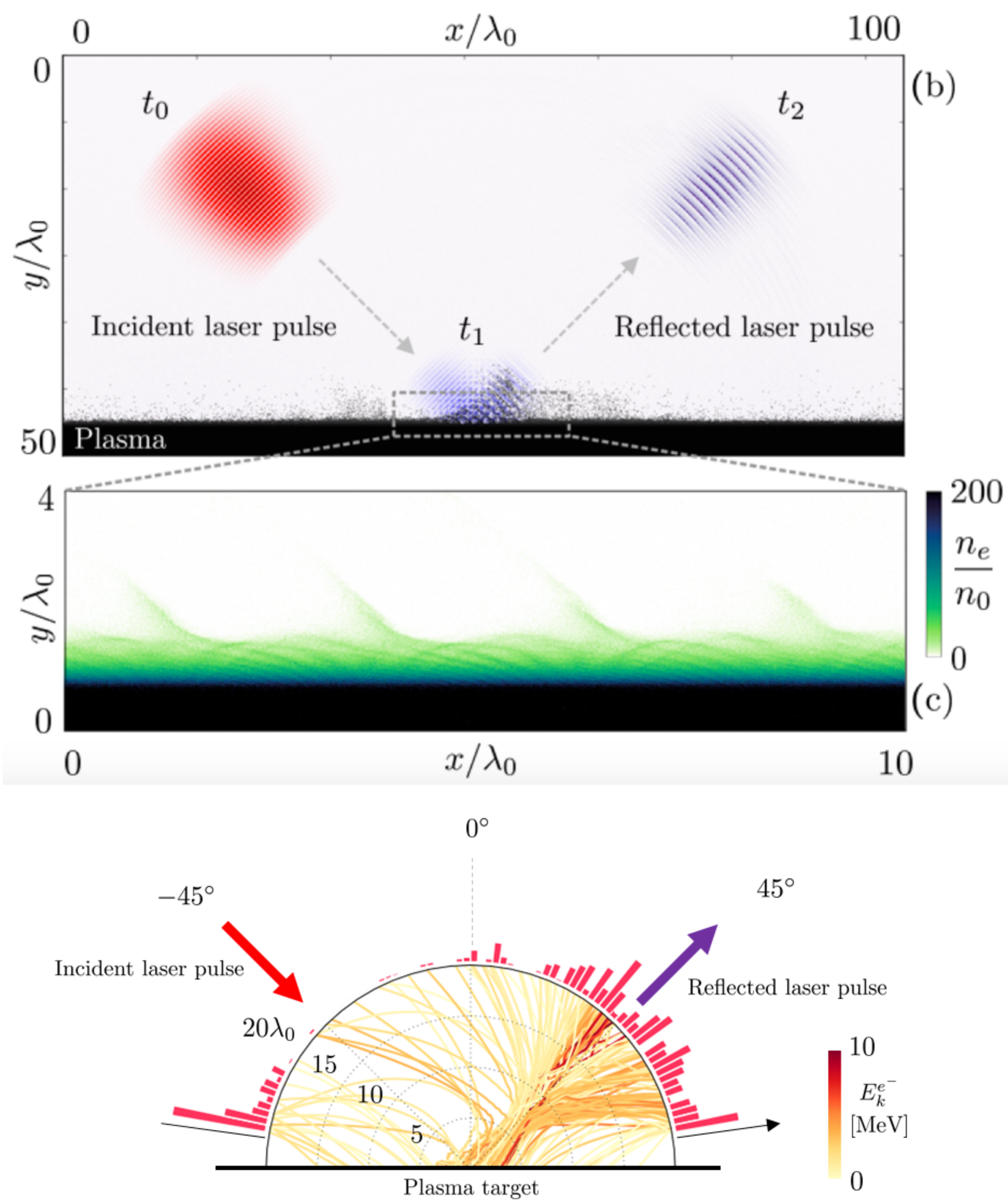

G. Bouchard, F. Quéré, CEA/IRAMIS

Laser wakefield acceleration of electrons

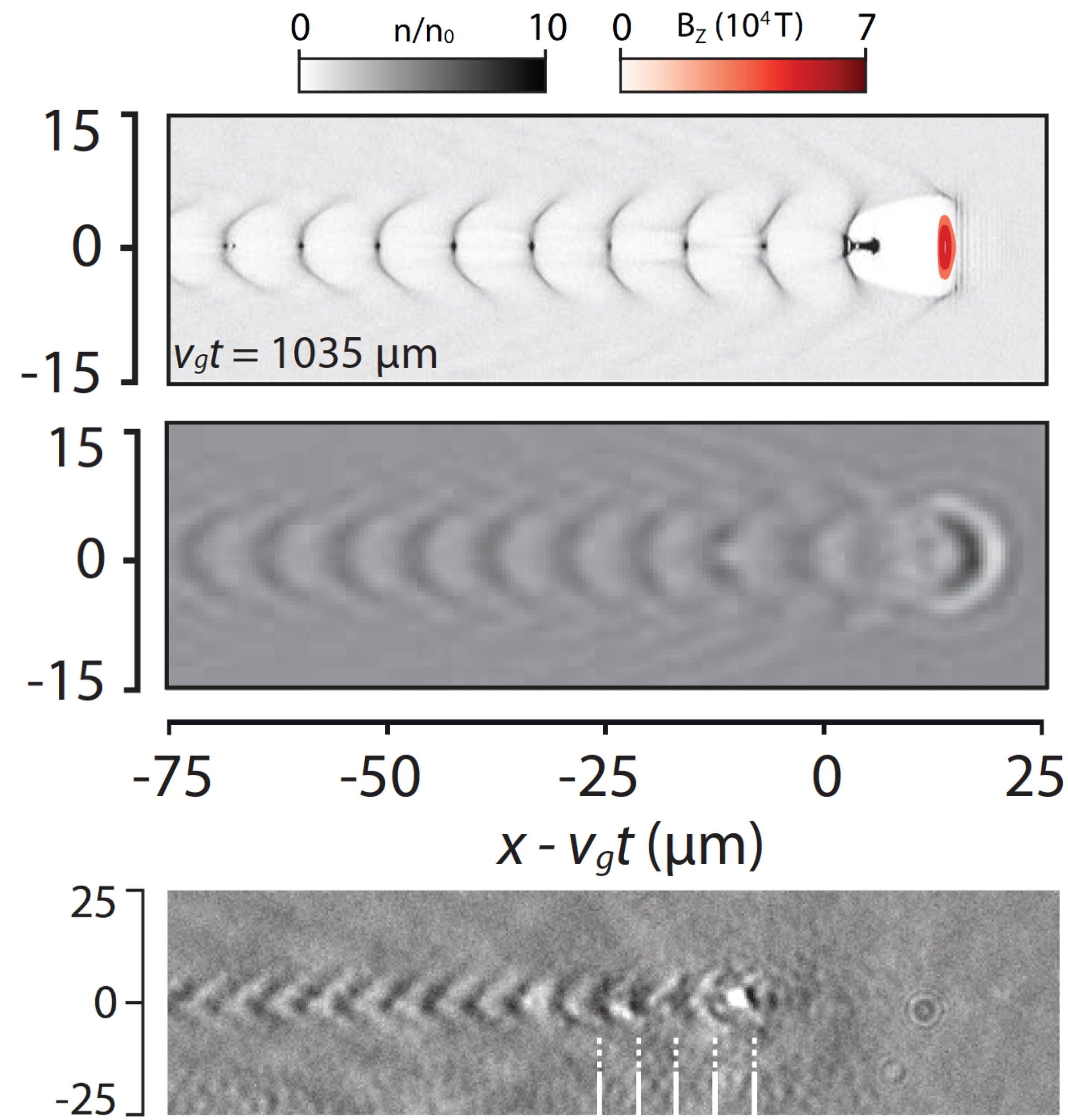

A. Sävert *et al.*, Phys. Rev. Lett. **115**, 055002 (2015)

PIC codes are very versatile: they can be applied to a wide range of physical scenarii, from laser-plasma interaction to astrophysics

Pair production on multi-petawatt laser facilities

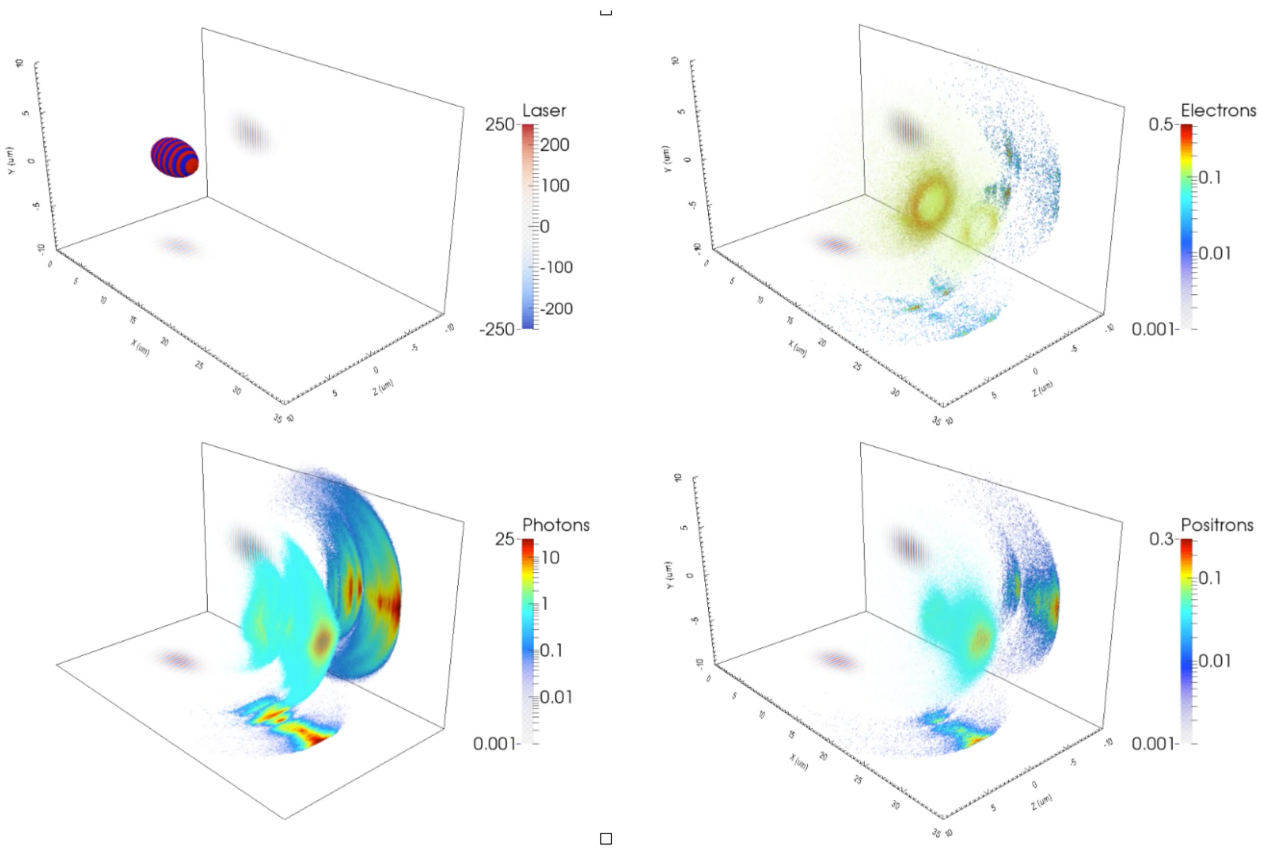

M. Lobet *et al.*, Phys. Rev. STAB **20**, 043401 (2017)

Relativistic shocks in electron-positron plasmas

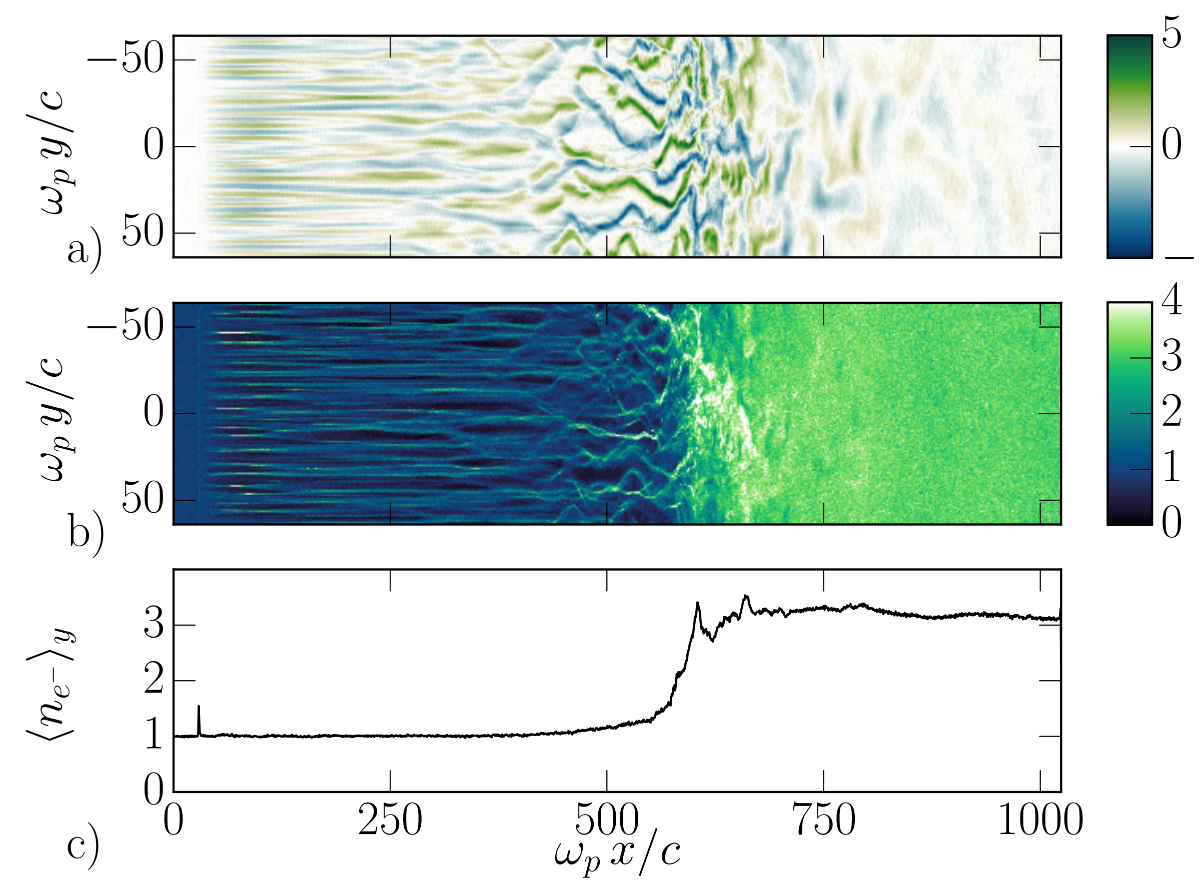

Plotnikov, Grassi & Grech, MNRAS **477**, 5238 (2018)

Beyond the electromagnetic PIC code ...

Space plasmas & astrophysics

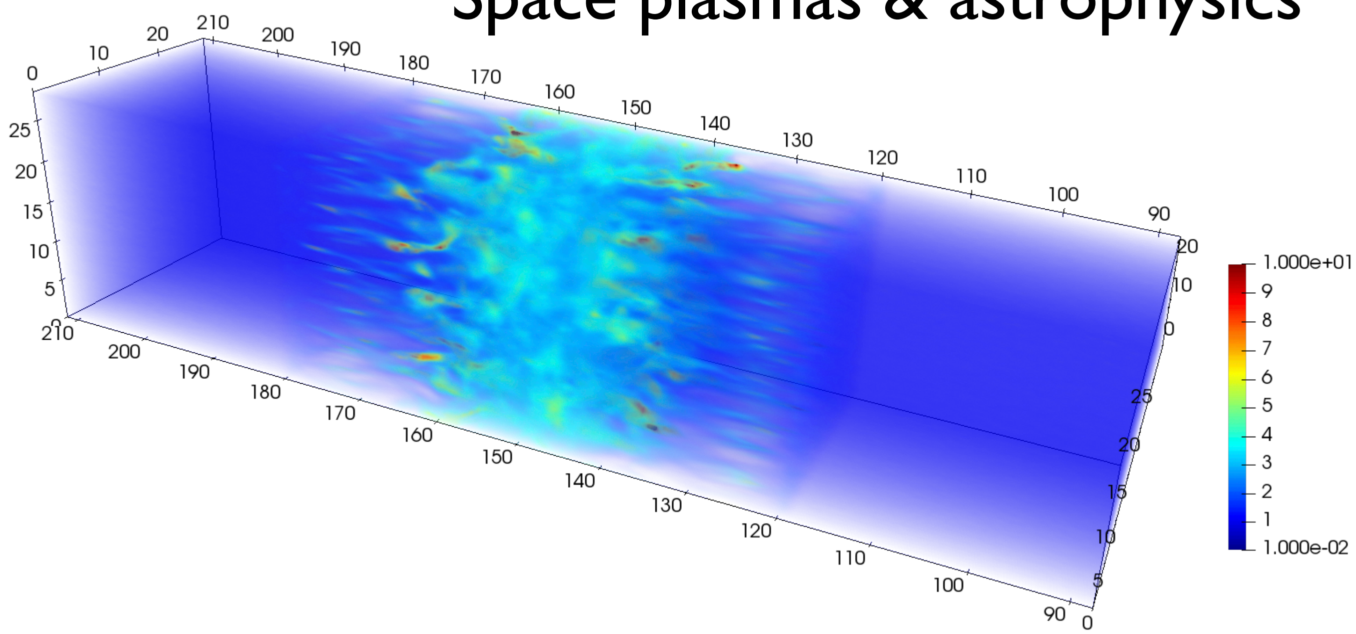

source: SMILEI dev-team

Laser plasma interaction

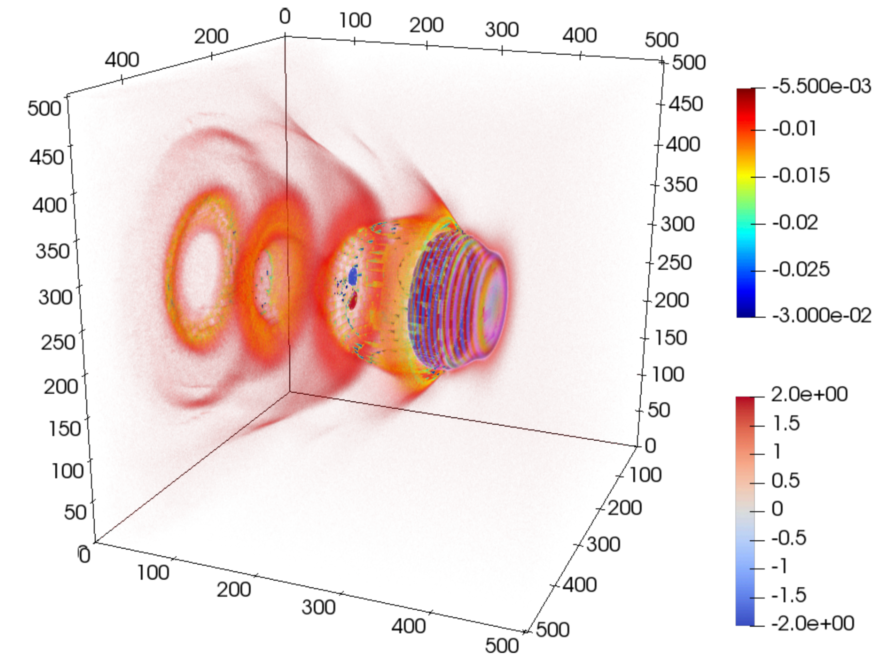

source: SMILEI dev-team

Space propulsion (Plasma thruster)

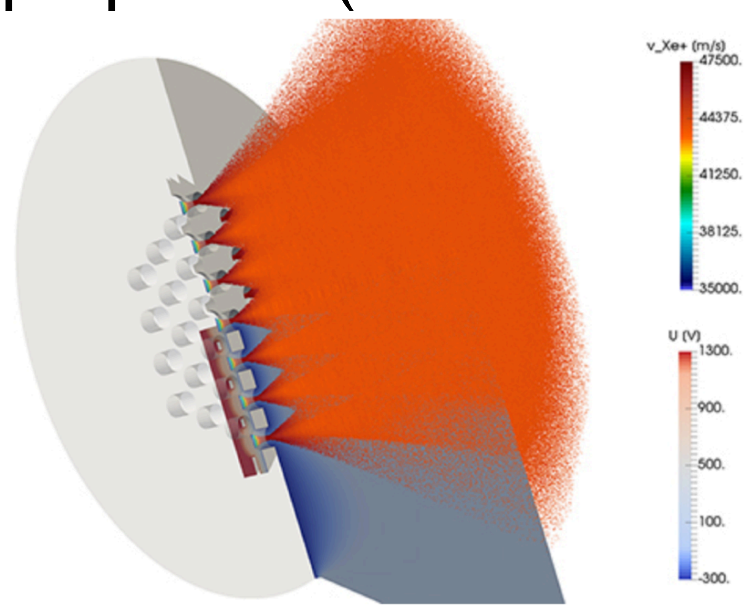

source: Gauss Center for Supercomputing

Cosmology

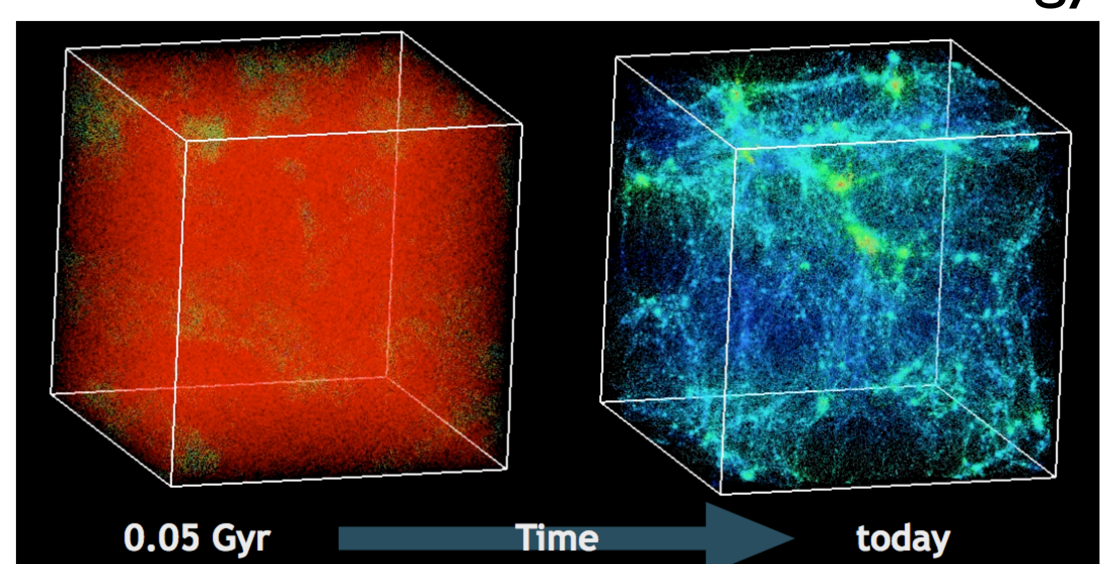

source: K. Heitmann, Argonne National Lab

Simulations of laser ion acceleration with low density targets in the ultra-high intensity regime

SMILEI: simulations performed by Iuliana Vladisavlevici (Vladisavlevici et al. submitted 2022)

Qualitative illustration of proton acceleration

$a_0 = 85$ ($I = 10^{22}$ W/cm^2); $\tau = 20$fs
$n_e = 10n_c$; $L_x = 15\mu$m

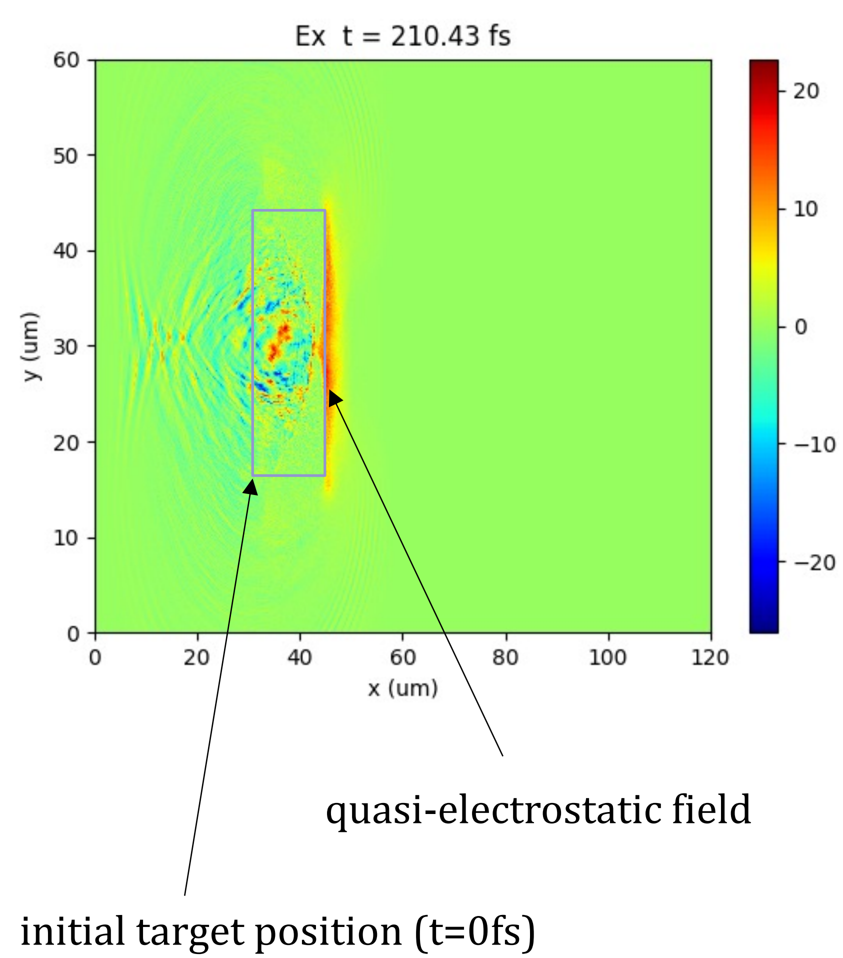

Electrons

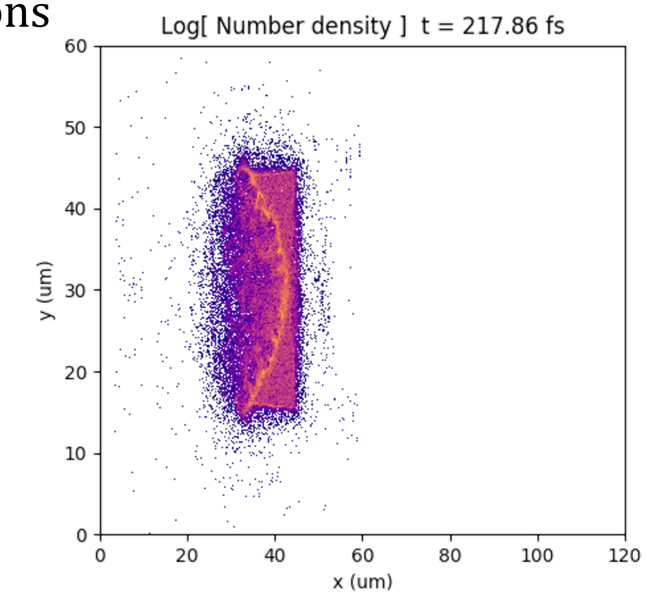

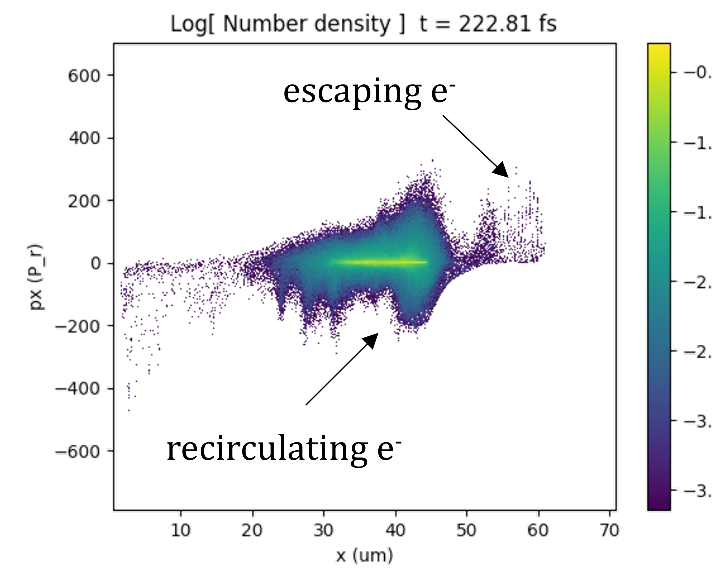

Protons

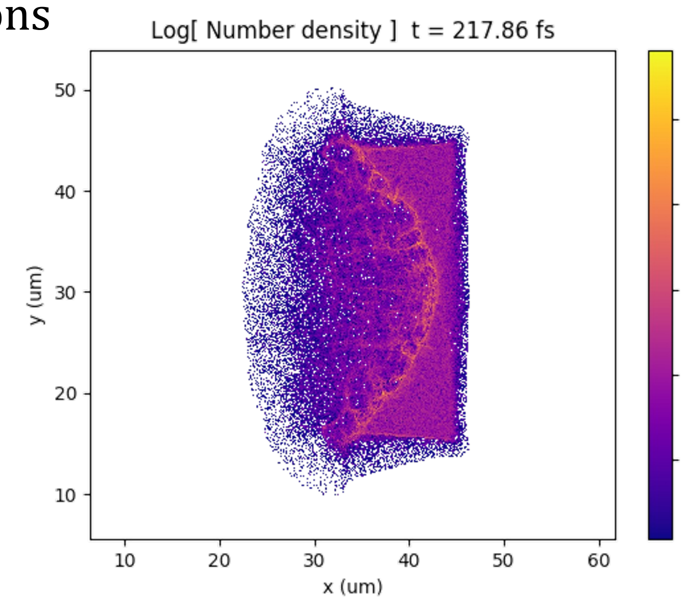

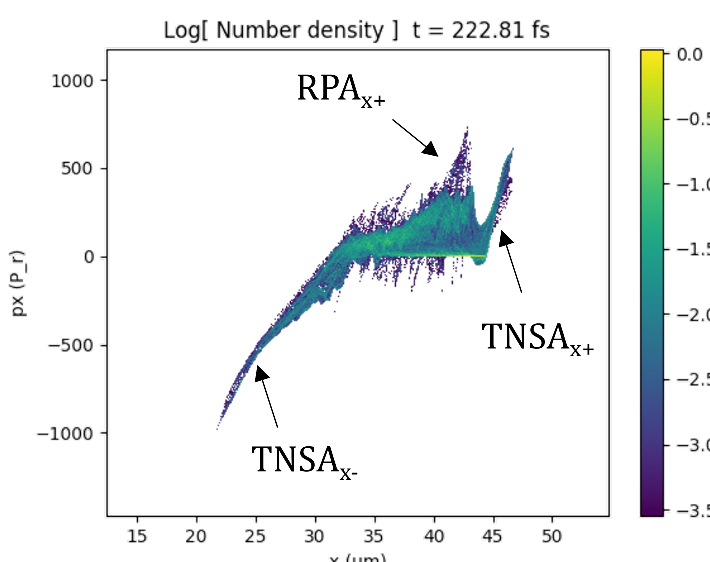

Simulations of laser ion acceleration with low density targets in the ultra-high intensity regime

Calder: Monte Carlo emission and pair production modules have been implemented (M. Lobet et al. arXiv.1311.1107v2)

Energy time evolution for I=10^{22} W/cm^2 (left) and for I = I=10^{23} W/cm^2 (right) for a 2 n_c, 190 microns long cos^2 target. The laser comes from the left side of the simulation box.

I=10^{22} W/cm^2

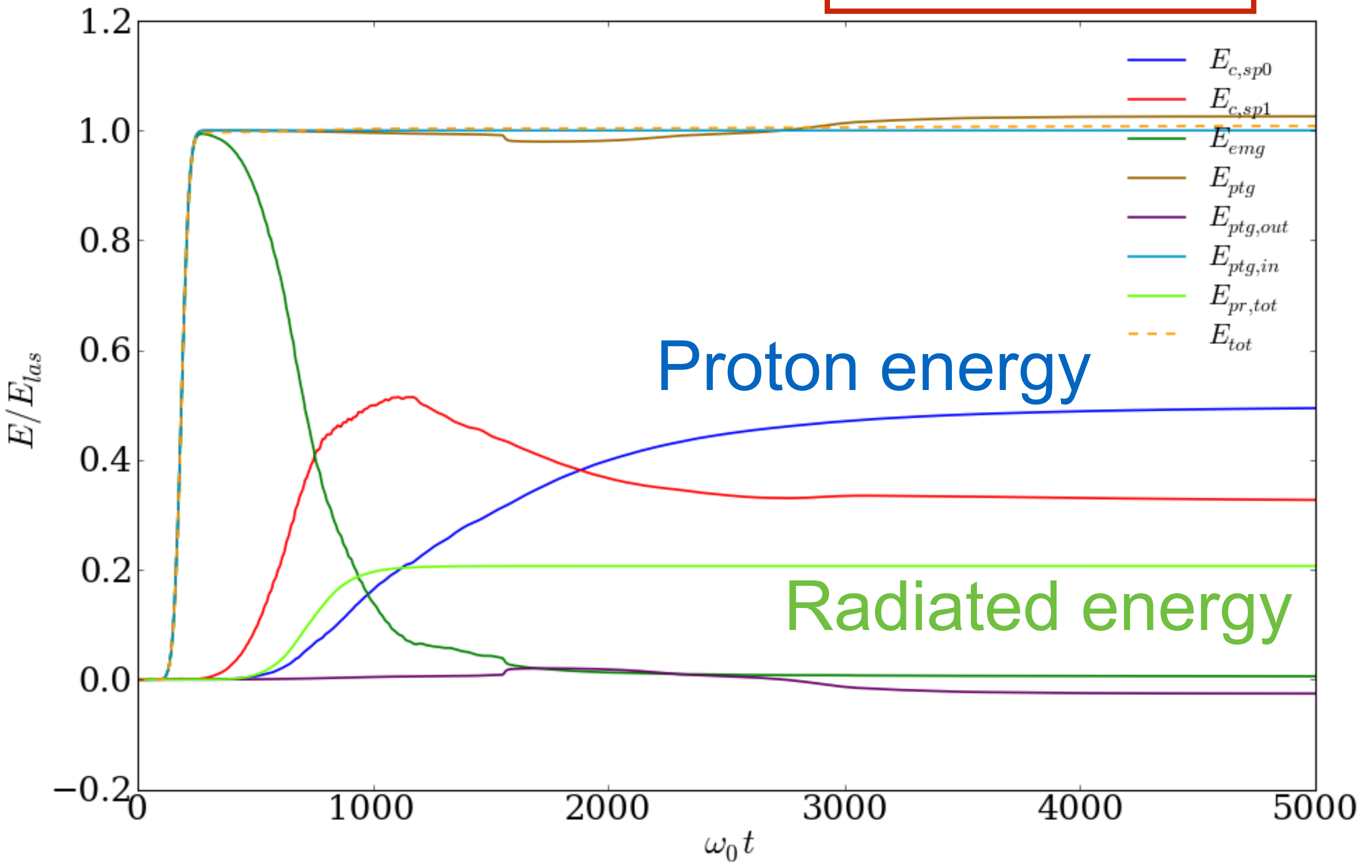

I=10^{23} W/cm^2

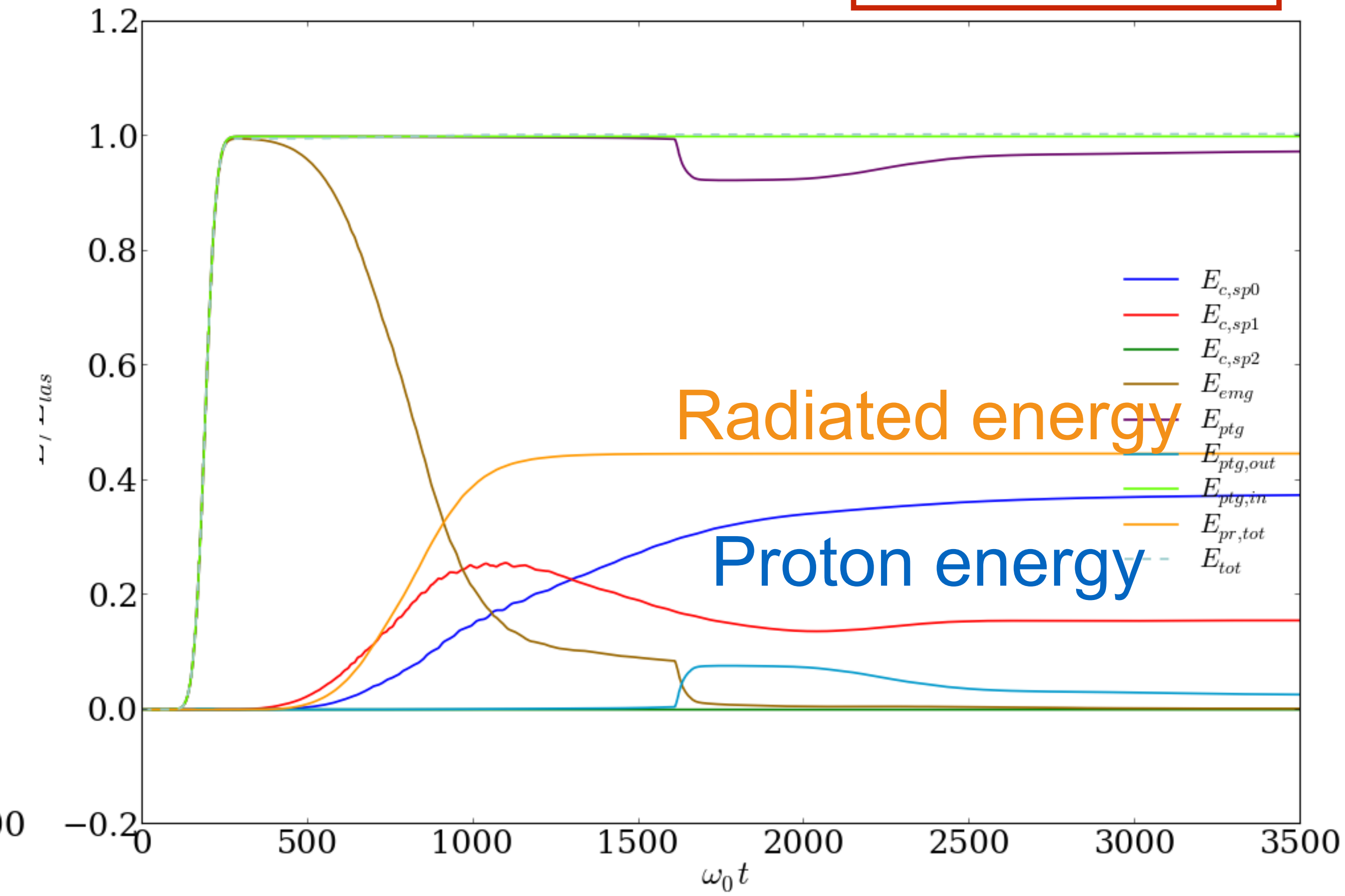

→ Competition with radiation emission

Simulations of laser ion acceleration with low density targets in the ultra-high intensity regime

Calder: Monte Carlo emission and pair production modules have been implemented

Energy time evolution and proton phase space for I $=5\times10^{23}$ W/cm^2 for a 4 n_c, 190 microns long cos^2 target. The laser comes from the left side of the simulation box.

I=5×10^{23} W/cm^2

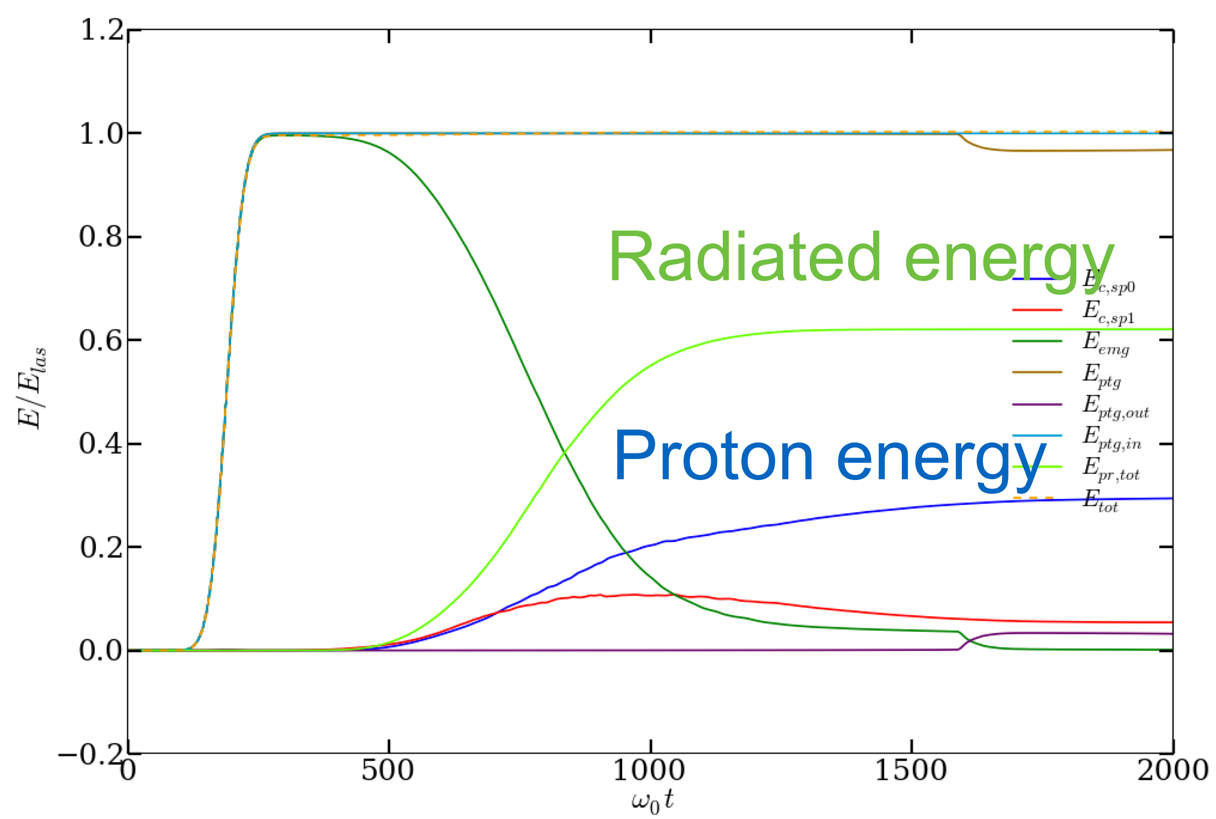

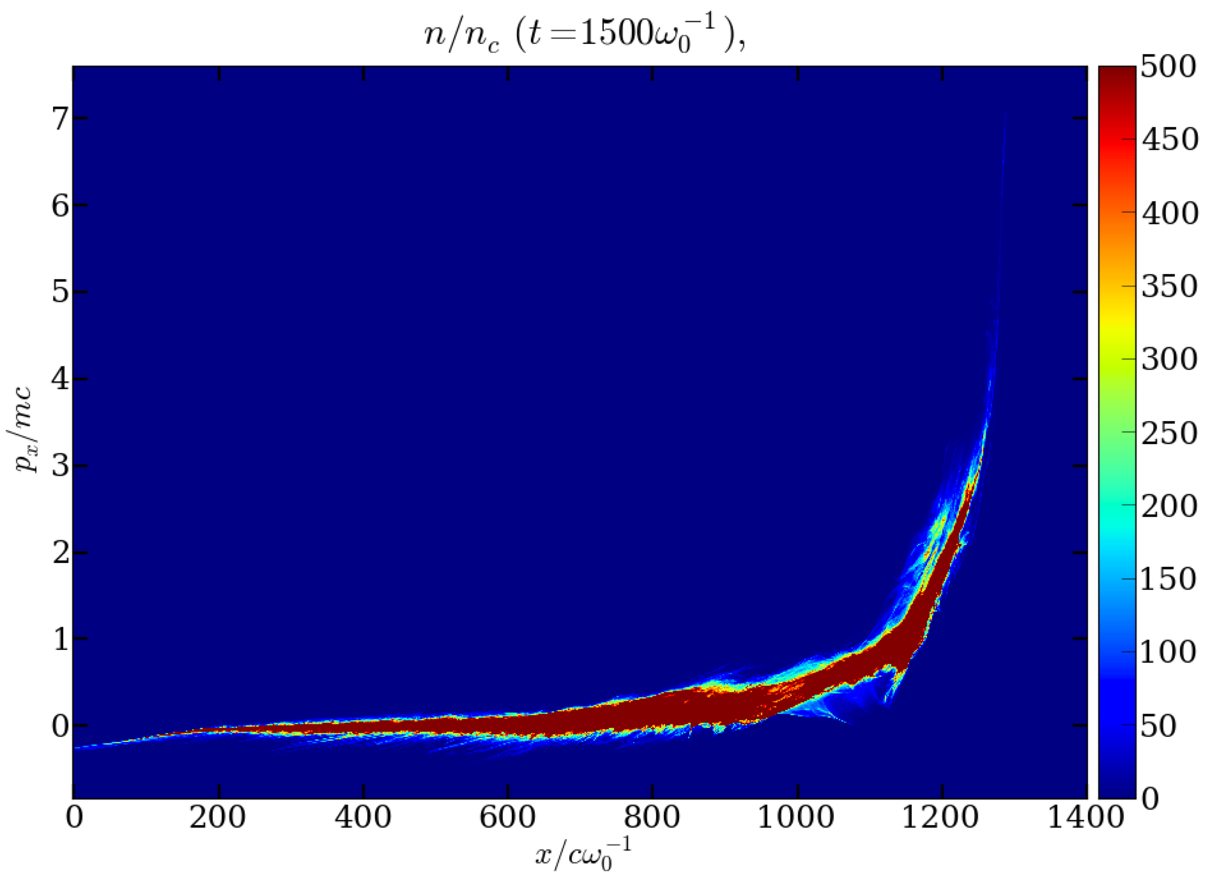

→ Competition with radiation emission

Maximum proton energy through shock acceleration: 6.25 GeV

Simulation results: collision between a GeV electron beam with a counter-propagating laser

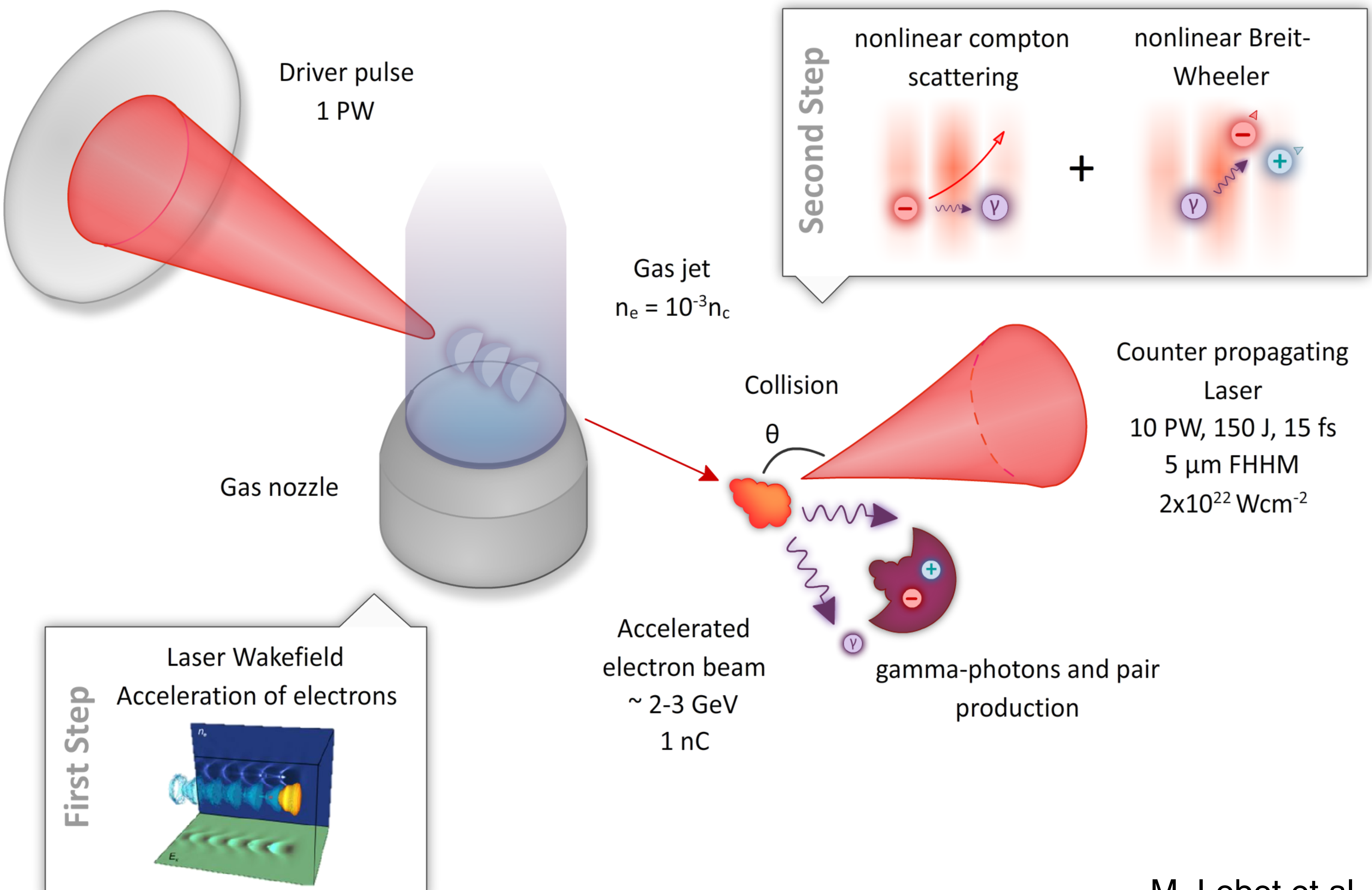

M. Lobet et al. PRAB 2017

First step: Optimizing the electron energy, acceleration up to 3 GeV in a LWFA with a 15 J laser

- $\lambda = 0.8\ \mu m$, $E = 15\ J$, $T = 30\ fs$, $W_{FWHM} = 23\ \mu m$, $P_0 = 460\ TW$, $a_0 = 6$
- $n_e = 0.001 n_c = 1.7 \times 10^{18}\ cm^{-3}$
- LWFA scaling laws [2]: 2 GeV, 1 nC, 1 cm

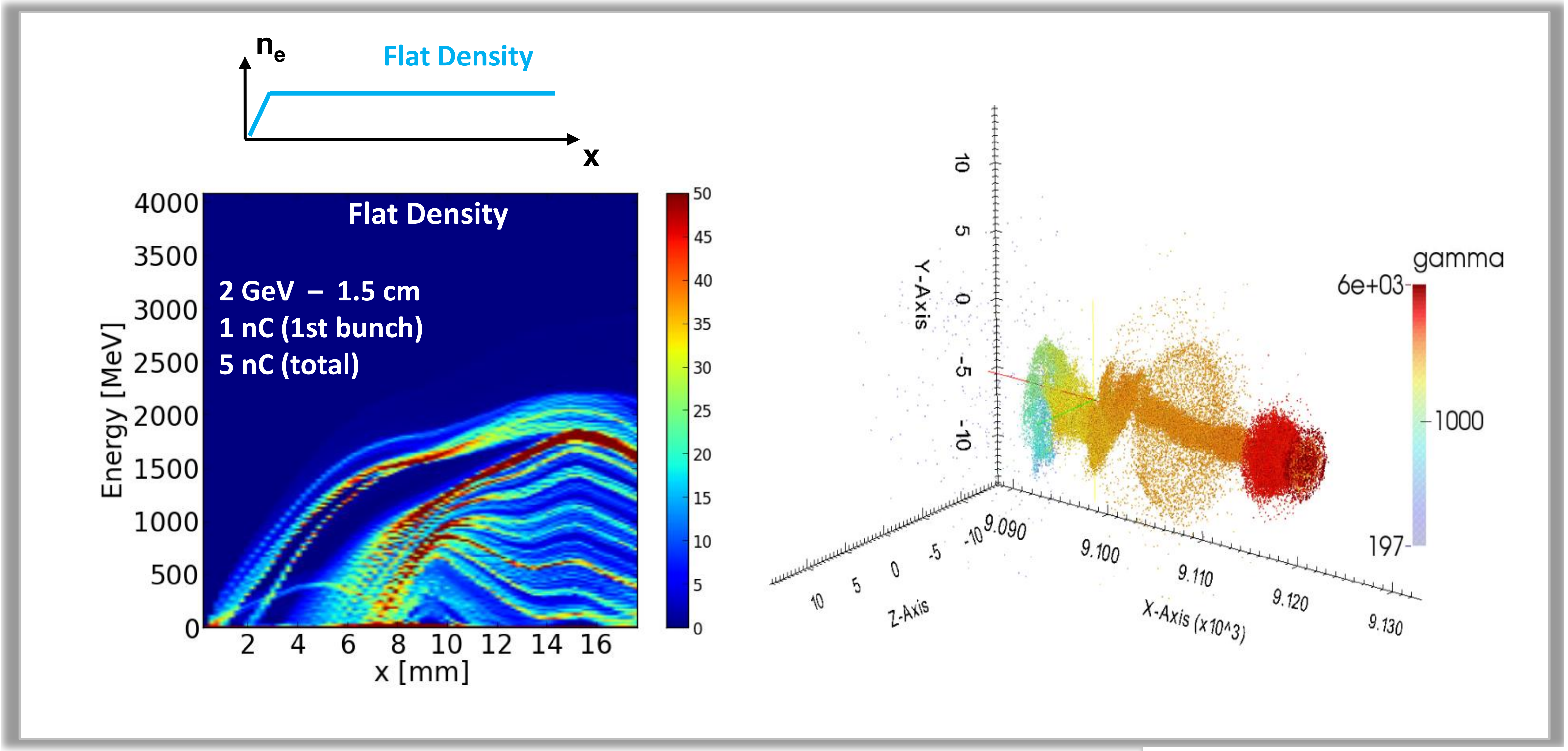

[1] A. Lifschitz *et al.*, JoCP 228, 1803-1814 (2009), [2] Lu et al., PRSTAB 10, 061301 (2007)

Second step: collision with a counter-propagating laser pulse, the γ-photon emission

- First simulation case: P_0 = 4.7 PW, W_{FWHM} = 2 µm, a_0 = 219, $I_0 = 10^{23}$ W/cm^2
- Strong deceleration of the electron beam with generation of GeV photons before the maximal laser intensity

Electron longitudinal phase space:

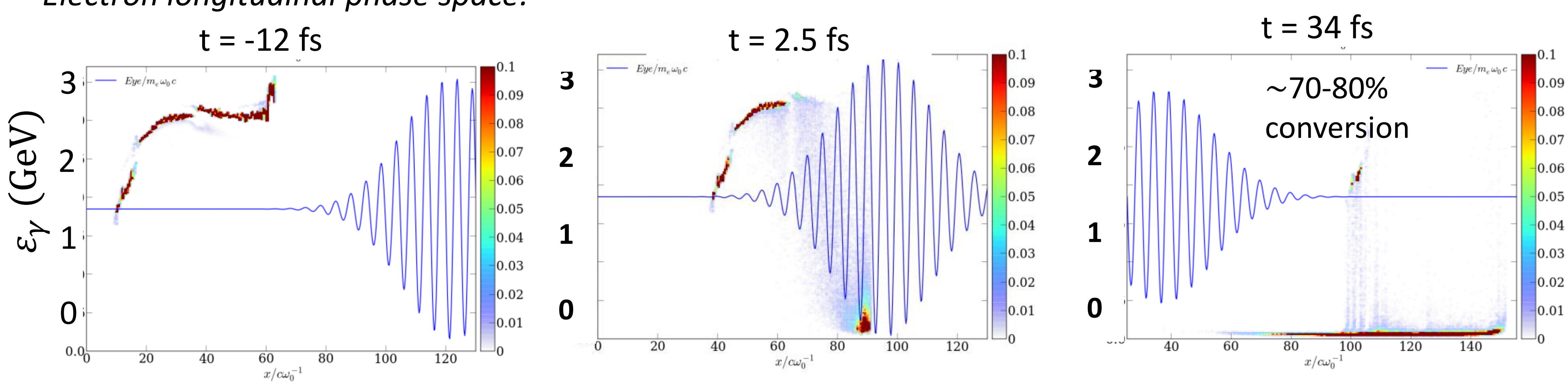

Photon distribution (longitudinal phase space):

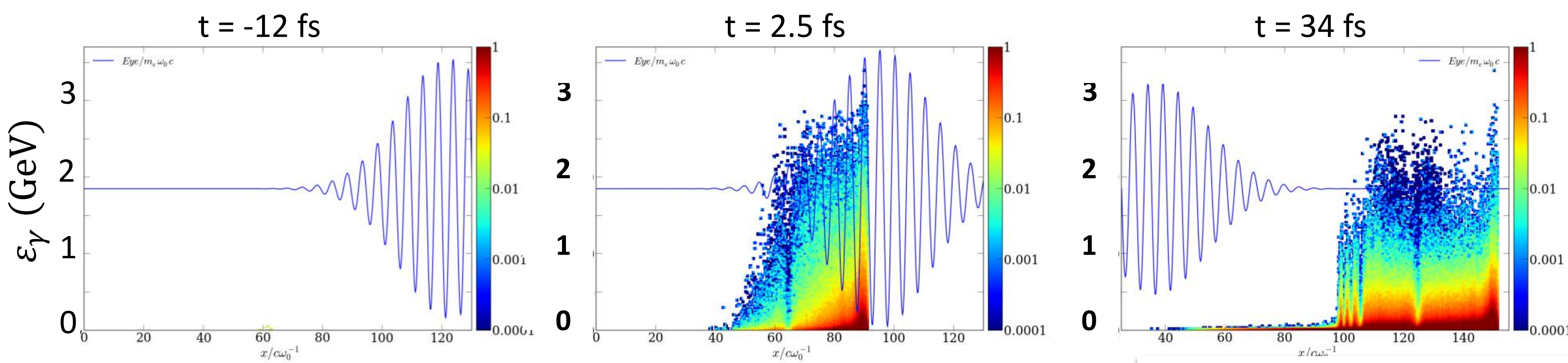

Second step, collision with a counter-propagating laser pulse: pair production and energy distribution

- The pairs are created few femtoseconds after the photon emission, near the intensity peak of the wave, and loss their energy by radiation in the tail of the laser

Electron longitudinal phase space:

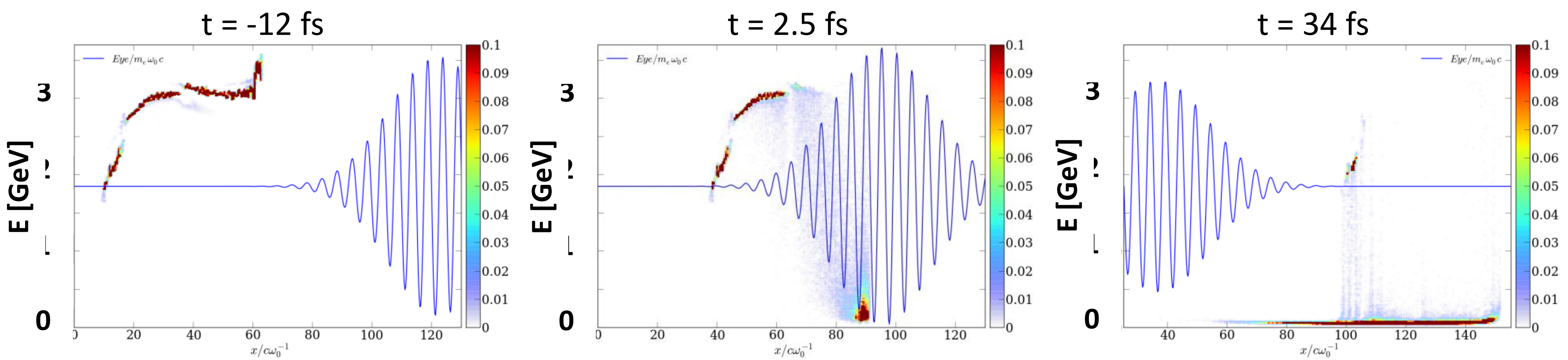

Positron longitudinal phase space:

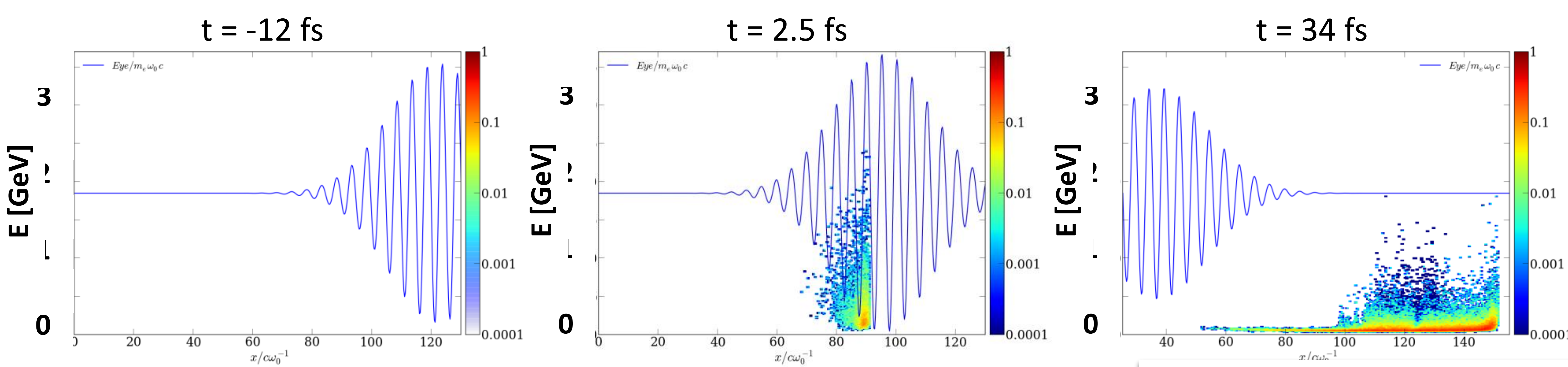

Two-target configuration for the study of the Weibel instability in colliding e^-e^+ jets

Could be transposed to e^-p plasma collisions using low density targets

- High laser intensity necessary to generate sufficiently dense pair plasmas
- Large focal spot necessary to minimize transverse spreading of pair plasma and generate many filaments

$\Rightarrow$ Total laser energy > 200 kJ

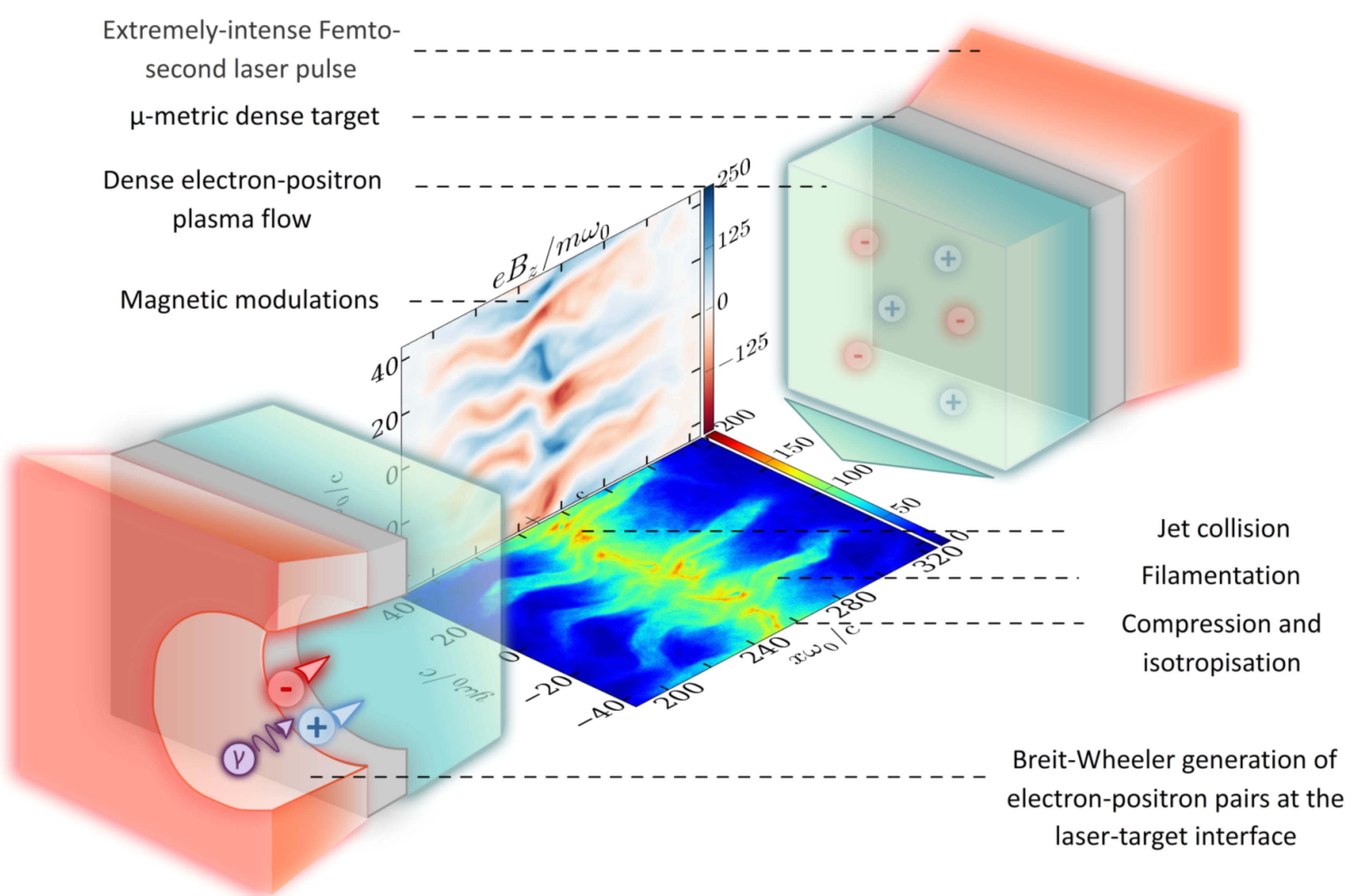

CALDER PIC Simulation

- **Laser:** plane wave, wavelength $\lambda_0 = 1\ \mu m$, Gaussian profile of $125\omega_0^{-1}$ (65 fs) FWHM, linear polarization, amplitude $a_0 = 800$ ($I \sim 8.9 \times 10^{23}\ \mathrm{Wcm^{-2}}$)
- **Target:** fully-ionized Al^{13+} slab of $32c\omega_0^{-1}$ ($5\ \mu m$) thickness + preplasma of $12.5c\omega_0^{-1}$ ($2\ \mu m$) thickness

M. Lobet et al. PRL 2015

Saturated magnetic fluctuations exceed 10^6 T!

- Formation of magnetic and density filaments
- At saturation time,

$$B_z \simeq 150\,\frac{m_e\omega_0}{e} \simeq 1.5\times 10^6\mathrm{T}\ !$$

- Estimate of the saturated magnetic field (in the Alfvén limit)

$$B_{z,sat} = (2\gamma\_n\_/n_c)^{1/2} \sim 100 m_e\omega_0/e$$

- Estimate of the filament size

$$\lambda \sim 2\pi(n_c\gamma\_/n\_)^{1/2} \sim 20c/\omega_0$$

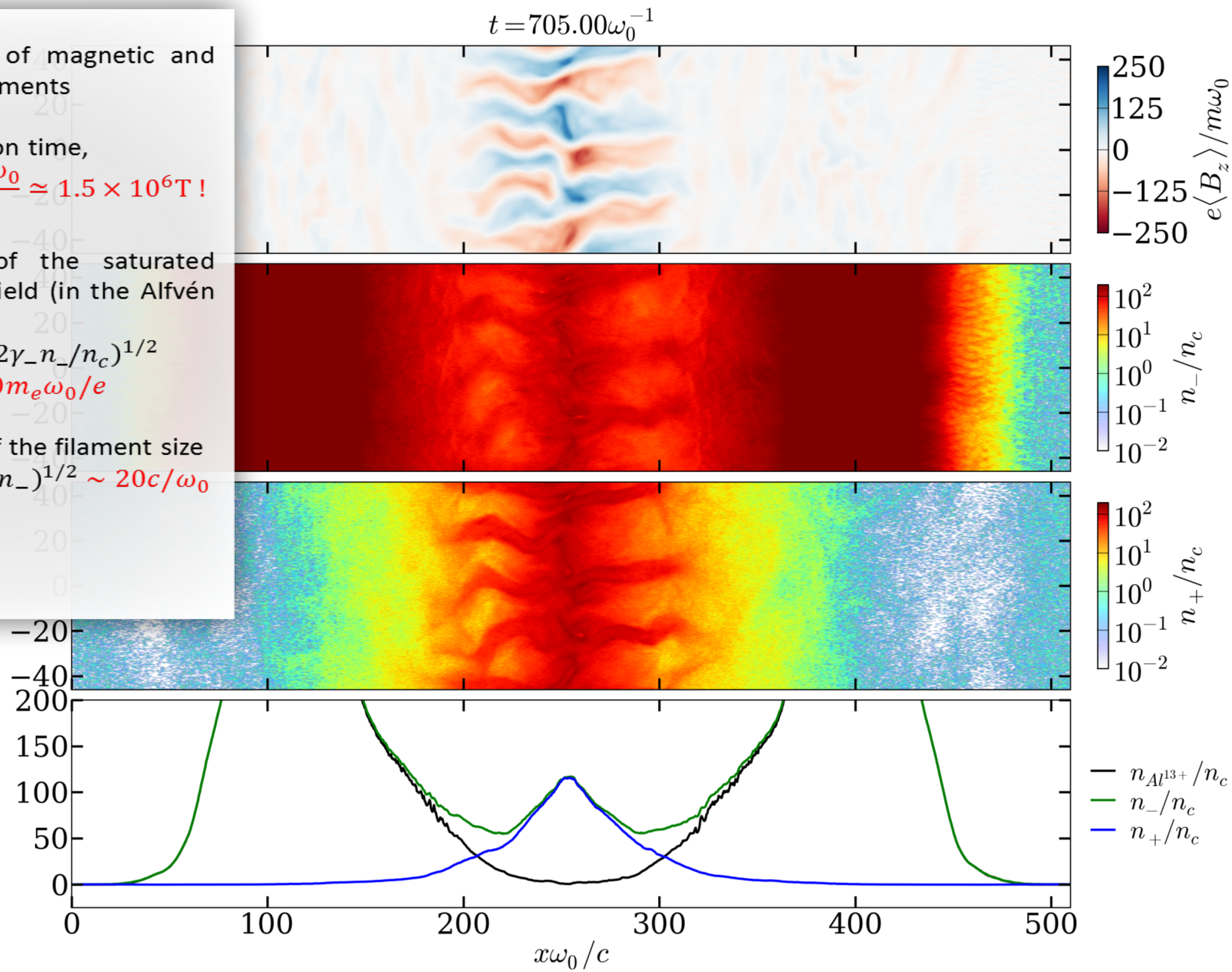

Simulation of the generation of Doppler-boosted beams (WARP-X)

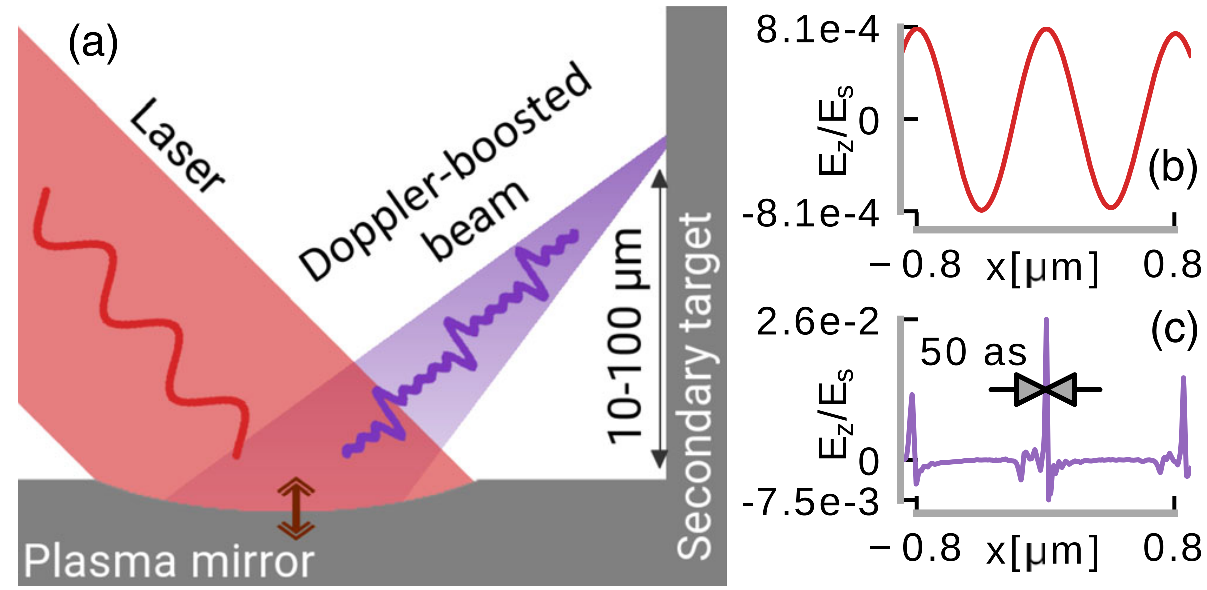

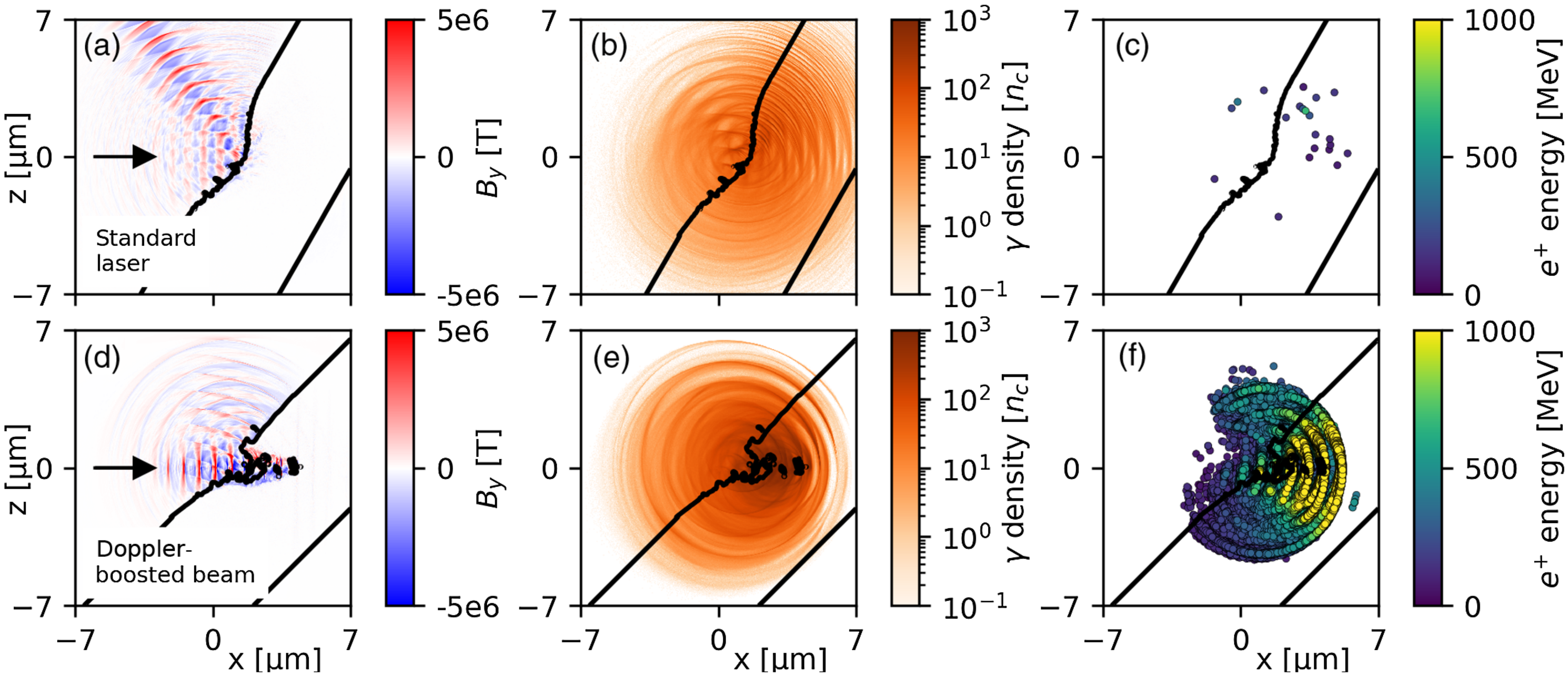

Luca Fedeli et al. 2021 Phys. Rev. Lett. 127, 114801
Luca Fedeli et al. 2022 New J. Phys. 24 025009 PICSAR-QED

Attosecond pulse interaction with matter
PIC simulations

Electron density (t= 40T_L = 1.2 fs)

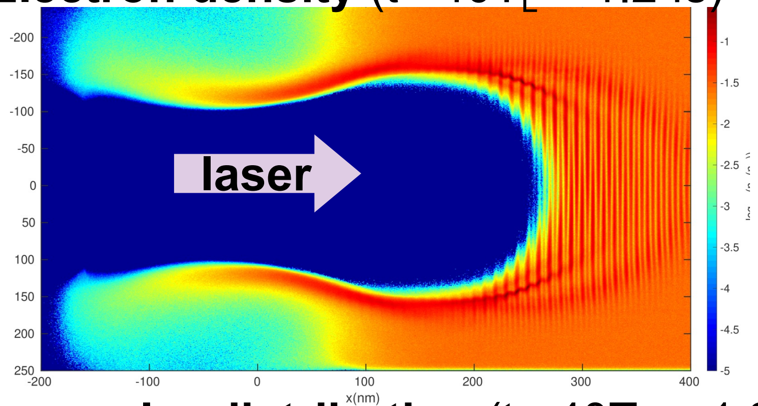

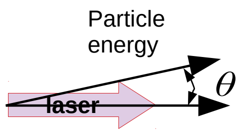

Energy angular distribution (t= 40T_L = 1.2 fs)

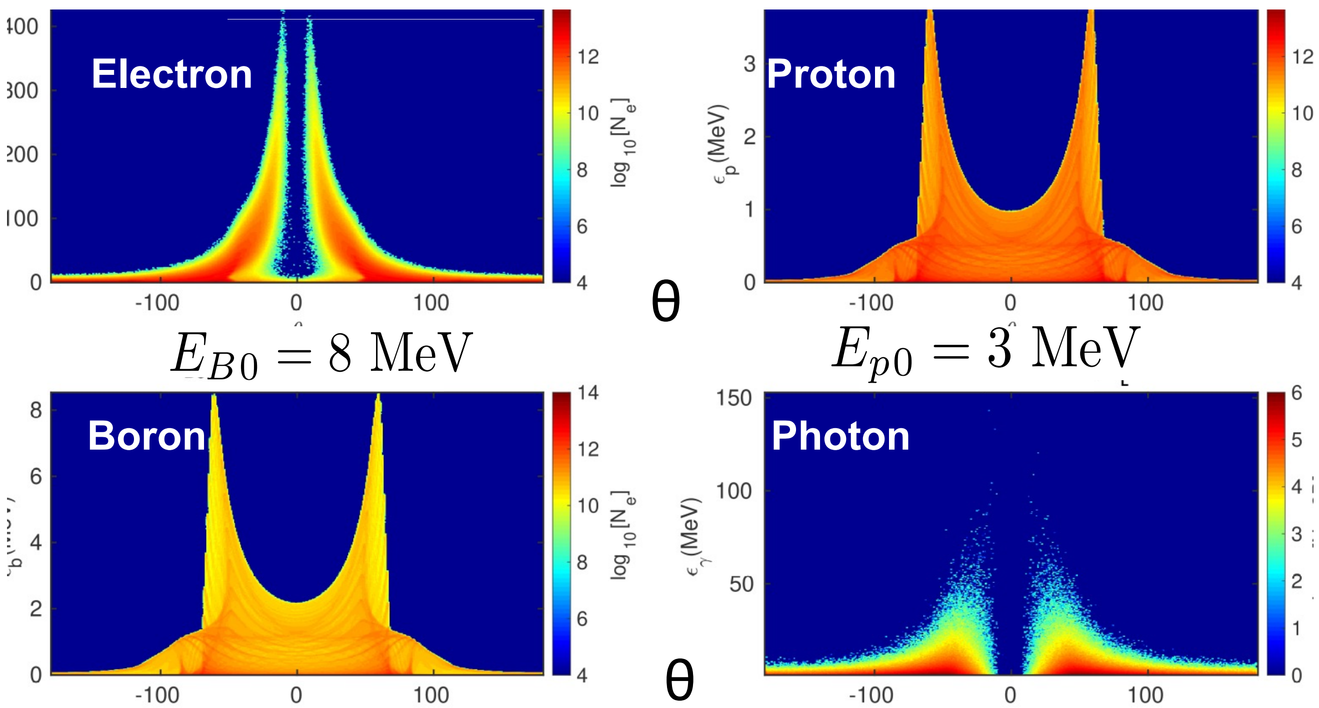

2D PIC Simulations with EPOCH

Current parameters

$\boldsymbol{\lambda_L} = \mathbf{10\ nm}$ $\quad I_L = 2.71 \times 10^{26}\ \mathrm{W.cm}^{-2}$

$a_L = 140$

$\mathrm{FWHM}_{(\mathrm{intensity})} = 330$ as & $\mathrm{Spot} = 10\lambda_L$

$\mathcal{E}_L = 10$ J

Solid pB target

B & H target $n_{e0} = 3 \times 10^{23}\ \mathrm{cm}^{-3} \simeq 0.03 n_c$

- Electron are swept out of the channel
- Proton and Boron ions are accelerated mainly transversely to several MeV and also longitudinally to MeV

X. Ribeyre et al. Scientific Reports 12:4665 (2022)

EPOCH: simulations performed by Rémi Capdessus

Available tutorials

Smilei) Overview Understand Use More

Smilei)

v4.7

Smilei is a Particle-In-Cell code for plasma simulation. Open-source, collaborative, user-friendly and designed for high performances on super-computers, it is applied to a wide range of physics studies: from relativistic laser-plasma interaction to astrophysics.

Download GitHub Chat Partners Publications Tutorials

https://smileipic.github.io/Smilei/

A high-performance PIC code

running on various supercomputers worldwide

with dedicated **post-processing tools** (Happi) and an ensemble of **benchmarks** (Easi, for continuous integration)

An extensive documentation

with online tutorials

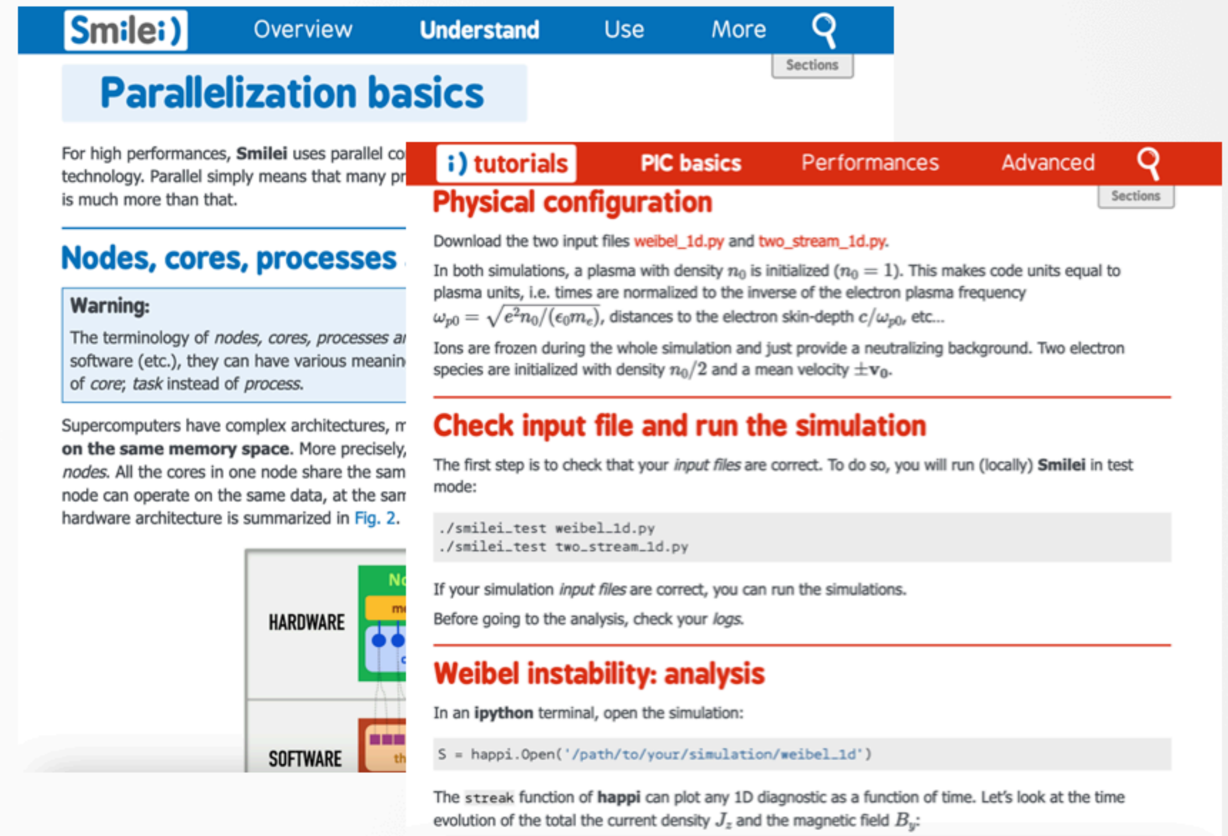

and a collaborative community

Github
sources, issues

Element
chat

SMILEI tutorials

tutorials | PIC basics | Performances | Advanced

Smilei tutorials

This website provides tutorials for learning how to use the PIC code Smilei and its post-processing tool **happi**.

Choose among the available tutorials in the top menu.

Links to Smilei's documentation:

- Smilei units
- Smilei input syntax
- Smilei post-processing
- Smilei tutorials source

Site index   Last updated on Mar 08, 2022   Powered by Sphinx 4.4.0

https://smileipic.github.io/tutorials/index.html#

SMILEI tutorials

i) tutorials | PIC basics | Performances | Advanced

- Setup
- Laser Propagation in vacuum
- Thermal plasma
- Weibel and two-stream instabilities
- Units

Sm… torials

This website provides tutorials for learning how to use the PIC code Smilei and its post-processing tool **happi**.

Choose among the available tutorials in the top menu.

Links to Smilei's documentation:

- Smilei units
- Smilei input syntax
- Smilei post-processing
- Smilei tutorials source

Site index Last updated on Mar 08, 2022 Powered by Sphinx 4.4.0

SMILEI tutorials

tutorials | PIC basics | Performances | Advanced

Parallel computing
Patch arrangement

Smilei tutorials

This website provides tutorials for learning how to use the PIC code Smilei and its post-processing tool **happi**.

Choose among the available tutorials in the top menu.

Links to Smilei's documentation:

- Smilei units
- Smilei input syntax
- Smilei post-processing
- Smilei tutorials source

Site index   Last updated on Mar 08, 2022   Powered by Sphinx 4.4.0

SMILEI tutorials

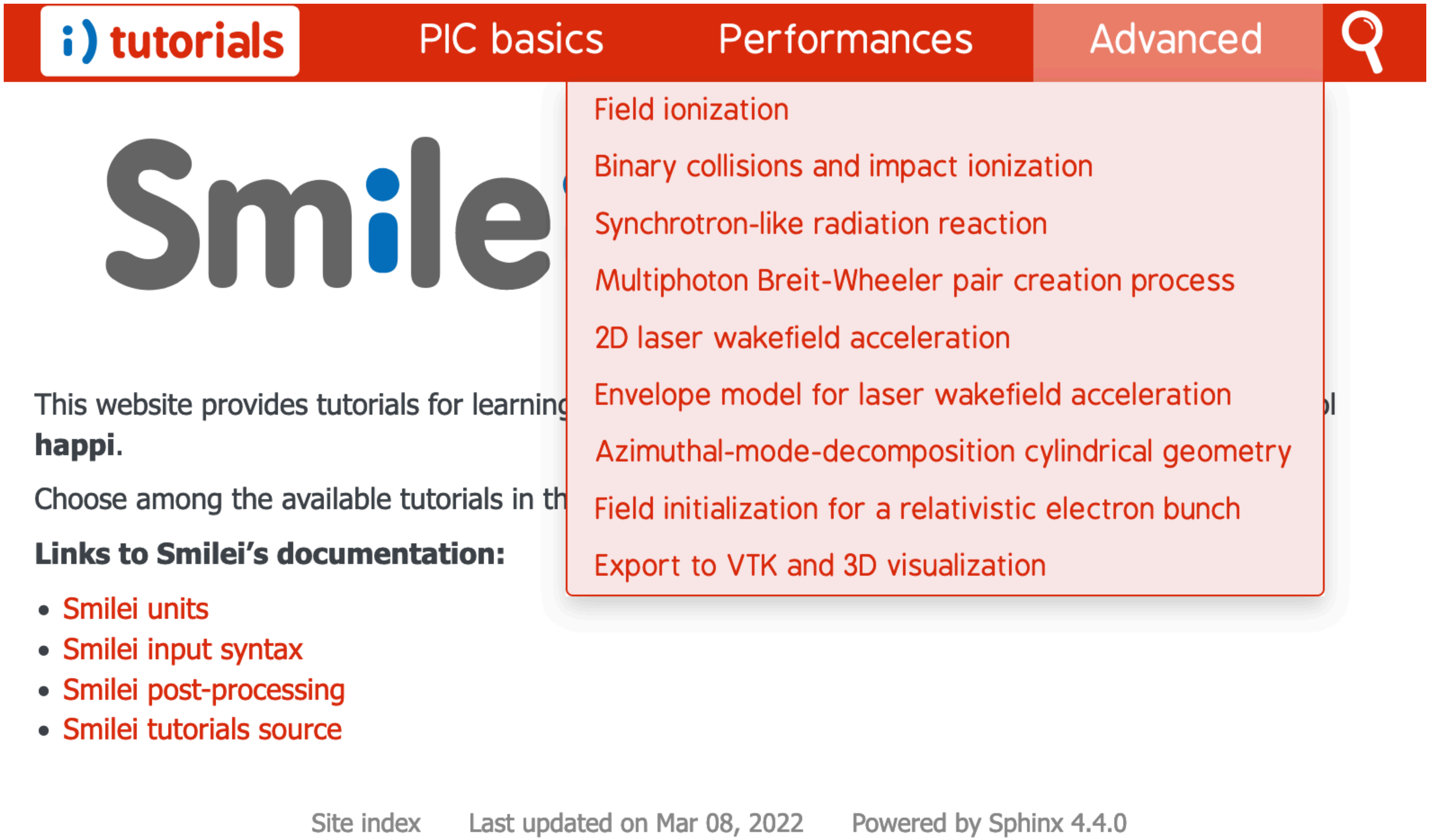

Prospects for the near future

Conclusions

- PIC codes are very useful and versatile tools for plasma simulation.
- PIC codes can be efficiently parallelized and adapted to new HPC architectures: need for HPC specialists.
- With additional physical modules a large variety of situations can be simulated: need for physicists.
- Opensource, collaborative PIC codes are available: SMILEI, EPOCH, WARP-X…
- Always be careful with your results, compare them with theory, experiments….

Perspectives

- Exascale supercomputers: more 3D simulations
- GPUs
- Pseudo-spectral codes (see WARP-X)
- AMR
- Assistance by ML tools (optimisation, data analysis…)

Thank you for your attention !

Additional slides

2nd Remark

The Particle-In-Cell method integrates Vlasov Equation along the trajectories of so-called *quasi-particles*

Injecting this *ansatz* in Vlasov Eq., multiplying by $\mathbf{p}$ and integrating over all momenta $\mathbf{p}$

$$\sum_{p=1}^{N_s} w_p \, \frac{\mathbf{p}_p}{m_s \gamma_p} \, \mathbf{p}_p \cdot \left[\partial_{\mathbf{x}_p} S(\mathbf{x}-\mathbf{x}_p) + \partial_{\mathbf{x}} S(\mathbf{x}-\mathbf{x}_p)\right]$$

$$+ \sum_{p=1}^{N_s} w_p \, S(\mathbf{x}-\mathbf{x}_p) \, \left[\partial_t \mathbf{p}_p - q_s \left(\mathbf{E} + \mathbf{v}_p \times \mathbf{B}\right)\right] = 0$$

Let us now integrate in space:

$$\sum_{p=1}^{N_s} w_p \, \frac{\mathbf{p}_p}{m_s \gamma_p} \, \mathbf{p}_p \cdot \cancel{\int d\mathbf{x} \left[\partial_{\mathbf{x}_p} S(\mathbf{x}-\mathbf{x}_p) + \partial_{\mathbf{x}} S(\mathbf{x}-\mathbf{x}_p)\right]}$$

$$+ \sum_{p=1}^{N_s} w_p \int d\mathbf{x} S(\mathbf{x}-\mathbf{x}_p) \, \left[\partial_t \mathbf{p}_p - q_s \left(\mathbf{E} + \mathbf{v}_p \times \mathbf{B}\right)\right] = 0$$

Finally leading to solving for all $\mathbf{p}$:

$$\partial_t \mathbf{p}_p = q_s \left(\mathbf{E}_p + \mathbf{v} \times \mathbf{B}_p\right) \quad \text{with} \quad (\mathbf{E},\mathbf{B})_p \equiv \int d\mathbf{x} \, (\mathbf{E},\mathbf{B})(\mathbf{x}) \, S(\mathbf{x}-\mathbf{x}_p)$$

3rd Remark

If one does things in a *smart way*, only Maxwell-Ampère & Maxwell-Faraday Eqs. need to be solved

Take the divergence of Maxwell-Ampère's Eq. :

$$\nabla \cdot (\partial_t \mathbf{E} + \mathbf{J} = \nabla \times \mathbf{B})$$
$$\Leftrightarrow$$
$$\partial_t \nabla \cdot \mathbf{E} + \nabla \cdot \mathbf{J} = 0$$

Assume charge is conserved, i.e., $\partial_t \rho + \nabla \cdot \mathbf{J} = 0$

One gets: $\partial_t (\nabla \cdot \mathbf{E} - \rho) = 0$

If at time t=0, Poisson & Gauss Eqs. are satisfied,
and if current deposition is made in a way that conserve charge,

then solving only Maxwell-Ampère & Maxwell-Faraday ensures that both Eqs. remain satisfied at later time.

Step 4

The Finite-Difference Time-Domain (FDTD) method is a popular method for solving Maxwell's Equations

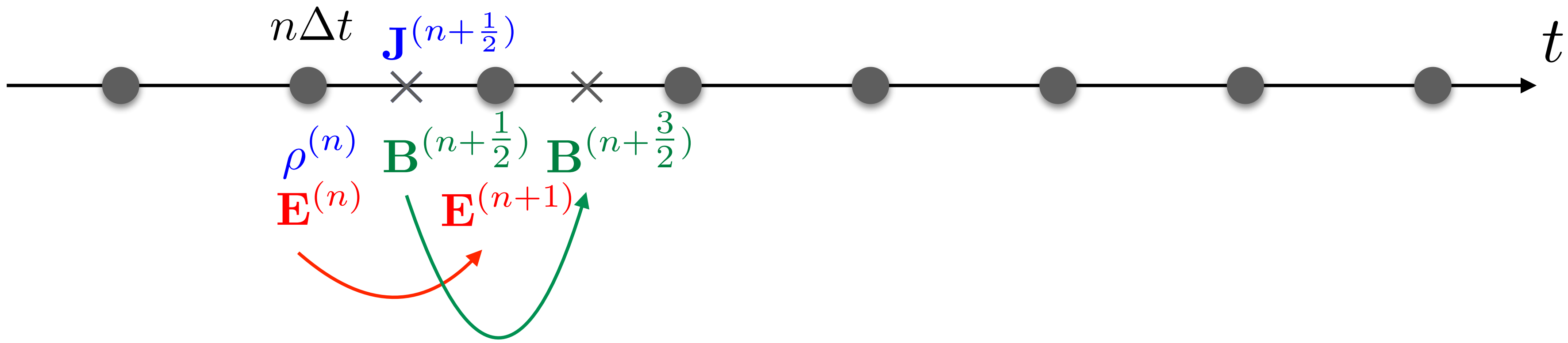

Solving Ampère's equation: $\partial_t E_y = -J_y - \partial_x B_z$

time-centering
$$\frac{(E_y)^{(n+1)} - (E_y)^{(n)}}{\Delta t} = -J_y^{(n+\frac{1}{2})} - (\partial_x B_z)^{(n+\frac{1}{2})}$$

space-centering
$$\frac{(E_y)_i^{(n+1)} - (E_y)_i^{(n)}}{\Delta t} = -(J_y)_i^{(n+\frac{1}{2})} - \frac{(B_z)_{i+\frac{1}{2}}^{(n+\frac{1}{2})} - (B_z)_{i+\frac{1}{2}}^{(n-\frac{1}{2})}}{\Delta x}$$

Solving Faraday's equation: $\partial_t B_z = \partial_x E_y$

space/time-centering
$$\frac{(B_z)_{i+\frac{1}{2}}^{(n+\frac{3}{2})} - (B_z)_{i+\frac{1}{2}}^{(n+\frac{1}{2})}}{\Delta t} = \frac{(E_y)_{i+1}^{(n+1)} - (E_y)_i^{(n+1)}}{\Delta x}$$

A. Taflove, *Computation electrodynamics: The finite-difference time-domain method*, 3rd Ed. (2005)

Step 4

Numerical analysis of the FDTD solvers gives you access to the numerical dispersion relation & CFL condition

The *numerical* electromagnetic wave equation in a vacuum

$$\partial_t^N \mathbf{E} = +\nabla^N \times \mathbf{B}$$
$$\partial_t^N \mathbf{B} = -\nabla^N \times \mathbf{E}$$

with:

$$\partial_t^N F = \Delta t^{-1}\left[F^{(n+\frac{1}{2})} - F^{(n-\frac{1}{2})}\right]$$
$$\partial_\mu^N F = \Delta \mu^{-1}\left[F_{i+\frac{1}{2}} - F_{i-\frac{1}{2}}\right]$$

Using the standard technique to derive the wave equation leads to:

$$\partial_{tt}^N \mathbf{E} + \sum_\mu \partial_{\mu\mu}^N \mathbf{E} = 0$$

Looking for *numerical* solution in the form:

$$(E_y)^{(n)}_{i,j+\frac{1}{2},k} = E_{y0}\,\exp\{\imath\left[ik_x\Delta x + (j+\tfrac{1}{2})k_y\Delta y \right.$$
$$\left. + kk_z\Delta z - n\omega\Delta t\right]\}$$

Nuter et al., Eur. Phys. J. D (2014); All papers by B. Godfrey, from the 70's up to now !!!

Full relativistic collision model of *PICLS*

Binary collision model (Takizuka & Abe, J. Comp. Phys., 1977)
Weakly relativistic collision model (Sentoku et al., J. Phys. Soc. Jpn, 1998)

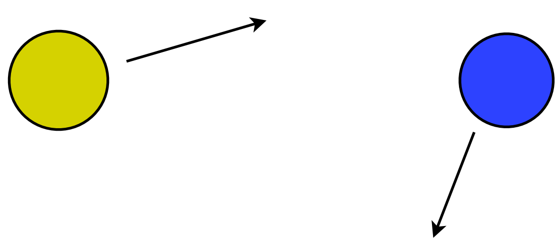

laboratory frame

$\longleftrightarrow$

Lorentz transform

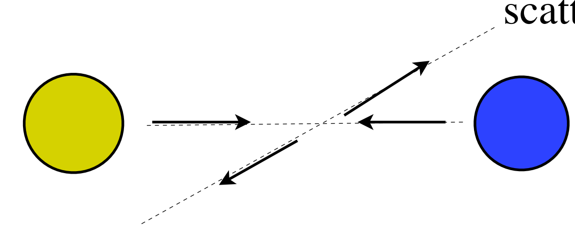

center of mass frame, γ_{cm}

$$\tan\theta_{cm} = \frac{\sin\theta_L}{\gamma_{cm}(\cos\theta_L - \beta_{cm}/\beta)}$$

evaluate the collision frequency on the one particle at rest frame.

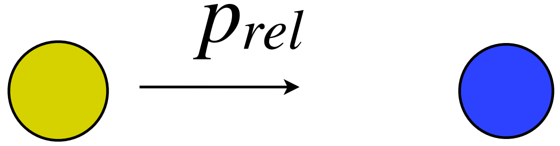

one particle at rest frame

$$\nu_{\alpha\beta} = \frac{4\pi(e_\alpha e_\beta)^2 n_l L}{p_{rel}^2 v_{rel}}$$

$$L = \ln(\lambda_D p_{rel}/\hbar)$$

$$\langle \tan^2\theta_L/2 \rangle = \nu_{\alpha\beta}\Delta t$$

Lorentz transform

Full relativistic collision model of *PICLS*

collision between different weighted particles

Nanbu and Yonemura, J. Comp. Phys., 1998

particle α

particle β

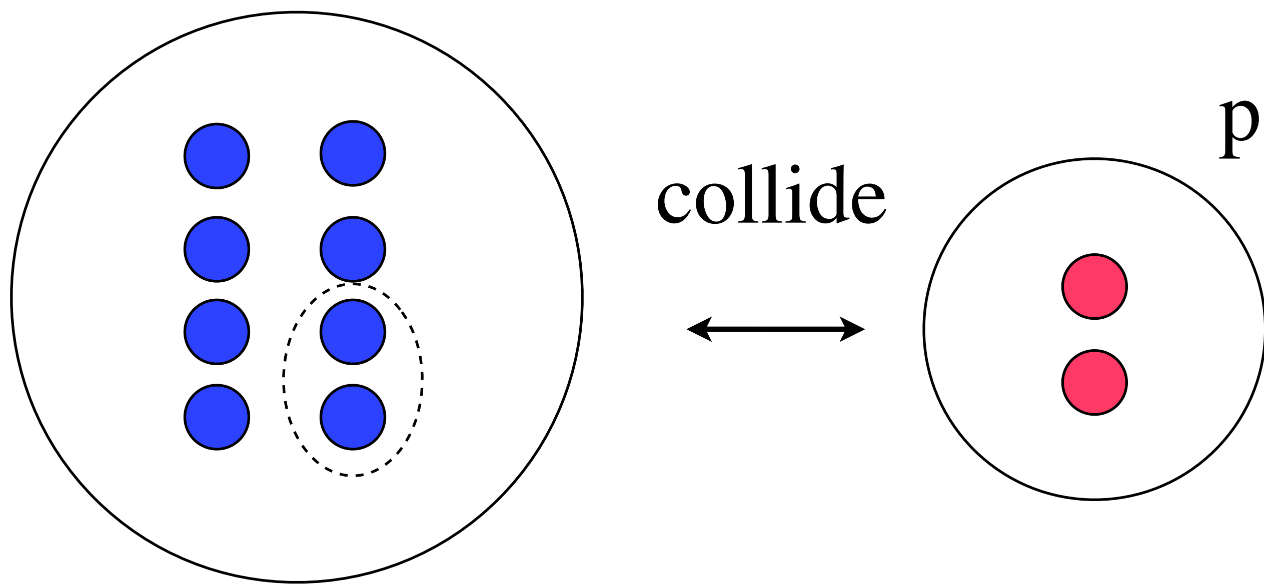

weight = 8

$P_\alpha = 2/8 = 0.25$

weight = 2

$P_\beta = 2/2 = 1$

Collision time is also modified to set a common time increment per real particle.

$$\Delta t_c = (w_\alpha / w_\beta)\Delta t_0 = 4\,\Delta t_0$$

Particle α has a collision with probability $P_\alpha = 0.25$.
Particle β collides every time step.

This model does not conserve energy and momentum in an individual collision, but it conserves the momentum and energy statistically.

+ Collisional ionization (Thomas-Fermi, Saha and impact ionization with Lotz model)
+ Radiation cooling by Bremsstrahlung

Energy transfer rate from hot electrons to ions

- test simulation of relativistic collision model (I) -

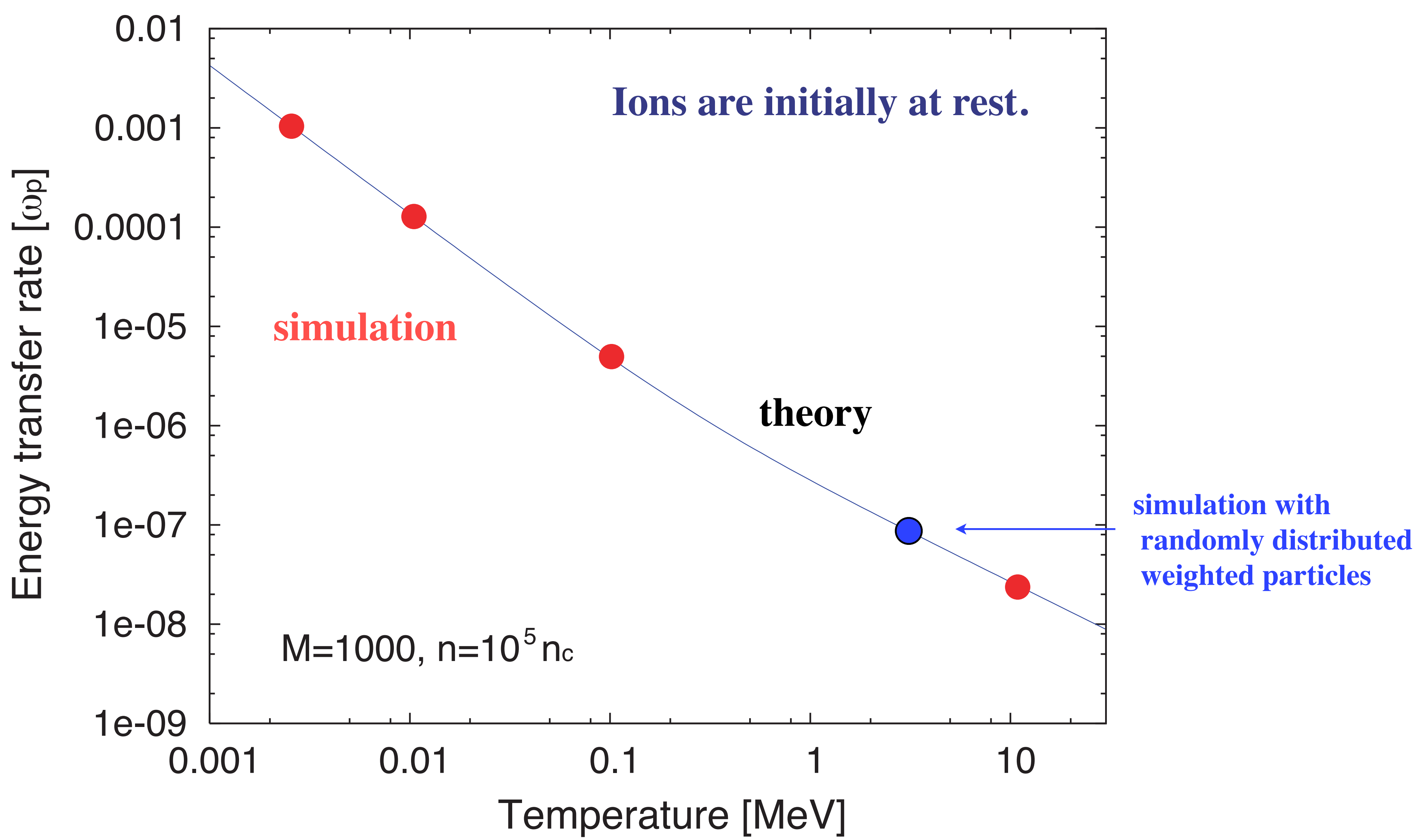

theory (Lifshitz, 1981)

$$\frac{d(E_i/E_e)}{dt} = \frac{8\pi z^2 e^4 nL}{Mm_e c^3(\gamma - 1)}$$

Electron stopping power in hydrogen plasma

- test simulation of relativistic collision model (II) -

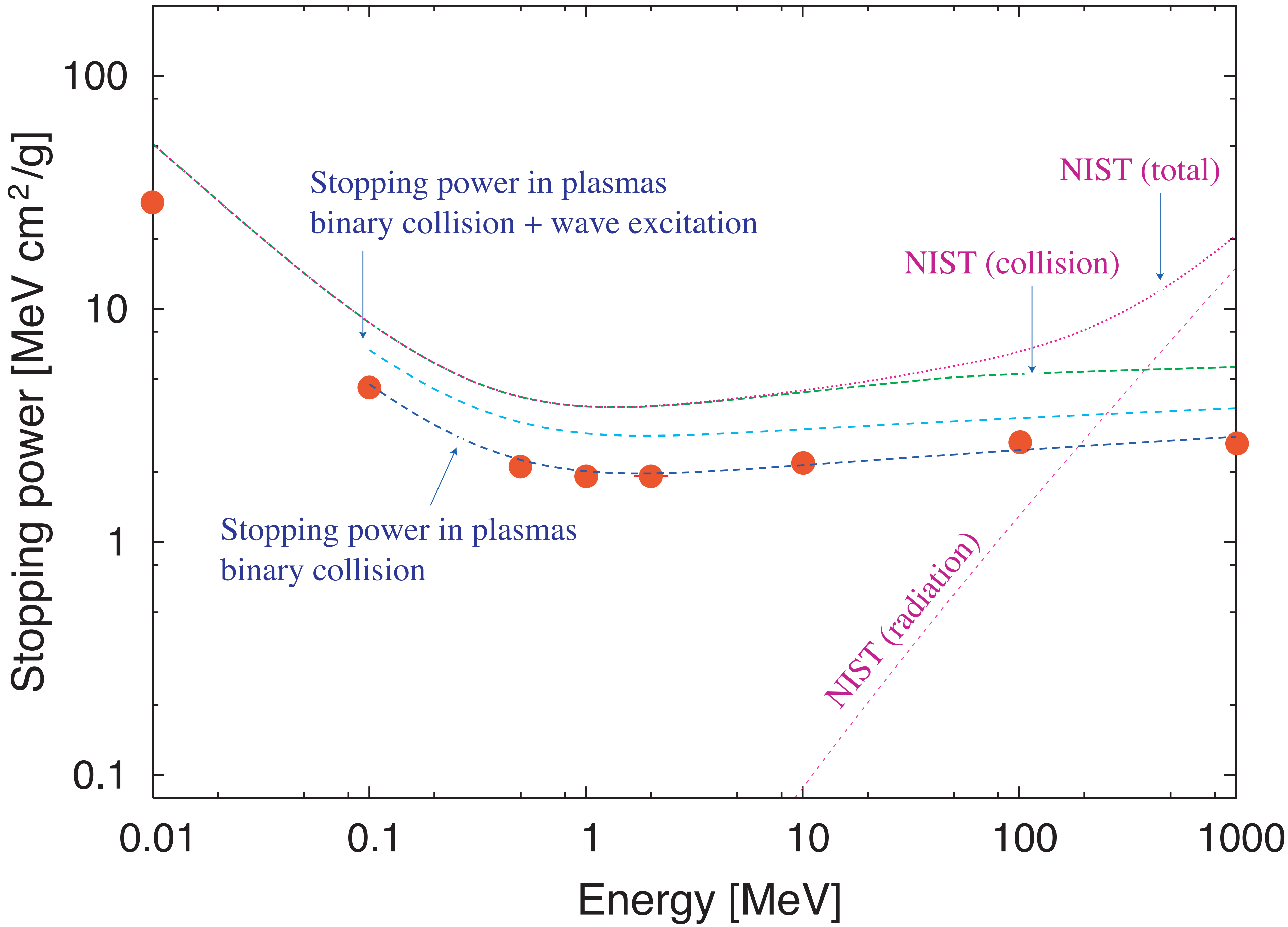

Plasma
12.5g/cc
T=5keV

NIST database: electron stopping power in hydrogen gas

advection solved by CIP method

The RT code solves the following **radiation transfer advection equation**:

$$\left(\frac{1}{c}\frac{\partial}{\partial t} + \mathbf{n}\cdot\nabla\right) I = \eta - \chi I$$

- *I(r,Ω,hν,t)* : intensity of radiation
- *η(r,hν,t)* : emissivity
- *χ(r,hν,t)* : opacity

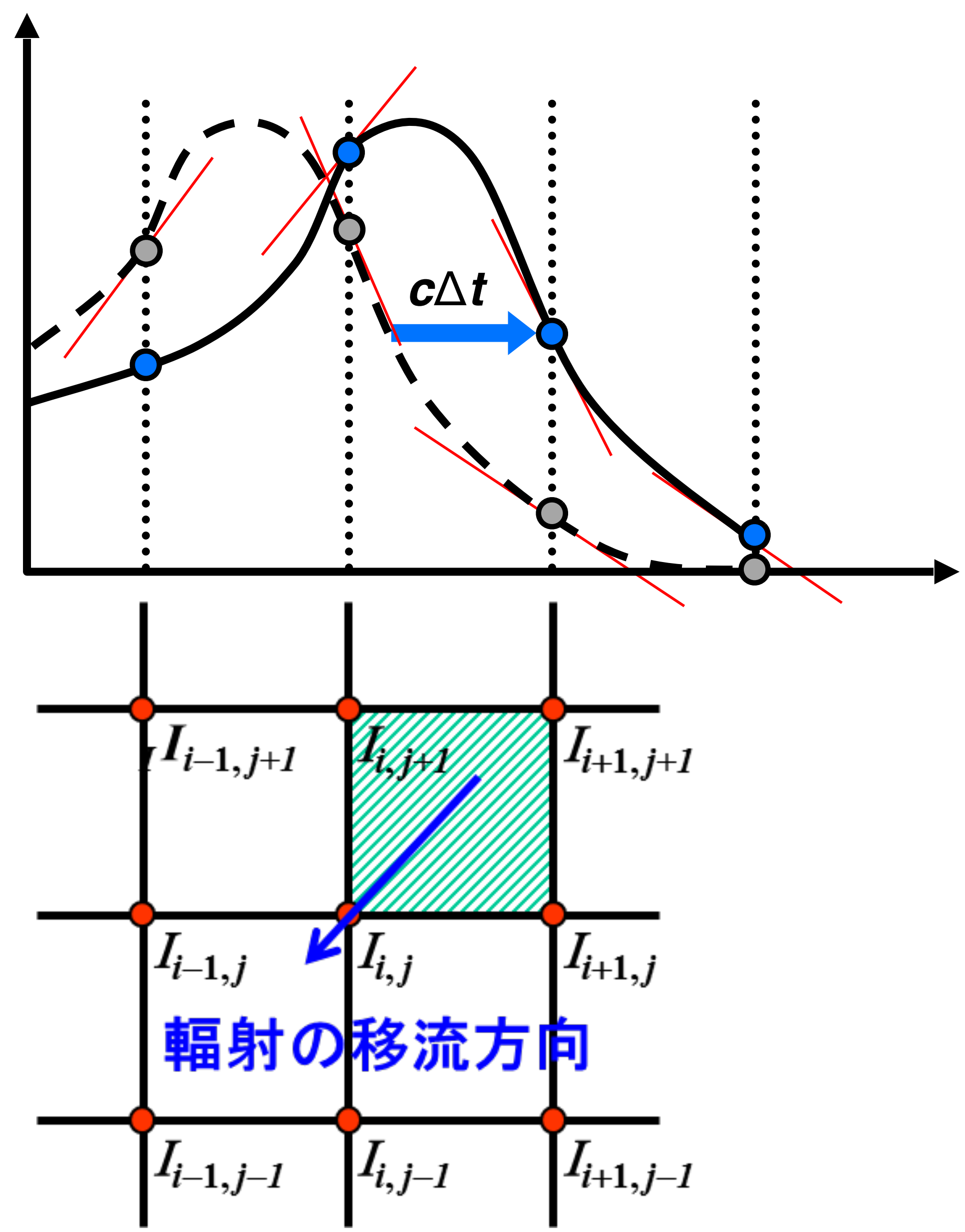

- The constrained interpolation profile (CIP) scheme is used, which solves the profile together with its gradient
- CIP method gives 3rd-order spatial accuracy to advection term
- This explicit method is suitable for MPI parallelization

T. Yabe, et al., CPC **66** (1991) 233.; F. Xiao et al., CPC **93** (1996) 1; F. Xiao et al., CPC **94** (1996) 103.

pre-calculated databases of NLTE *η* and *χ*

The non-equilibrium, collisional-radiative atomic kinetics 0-D code FLYCHK[1] is used to pre-calculate a database of non-LTE emissivity (η) and opacity (χ) as a function of temperature, density and photon energy

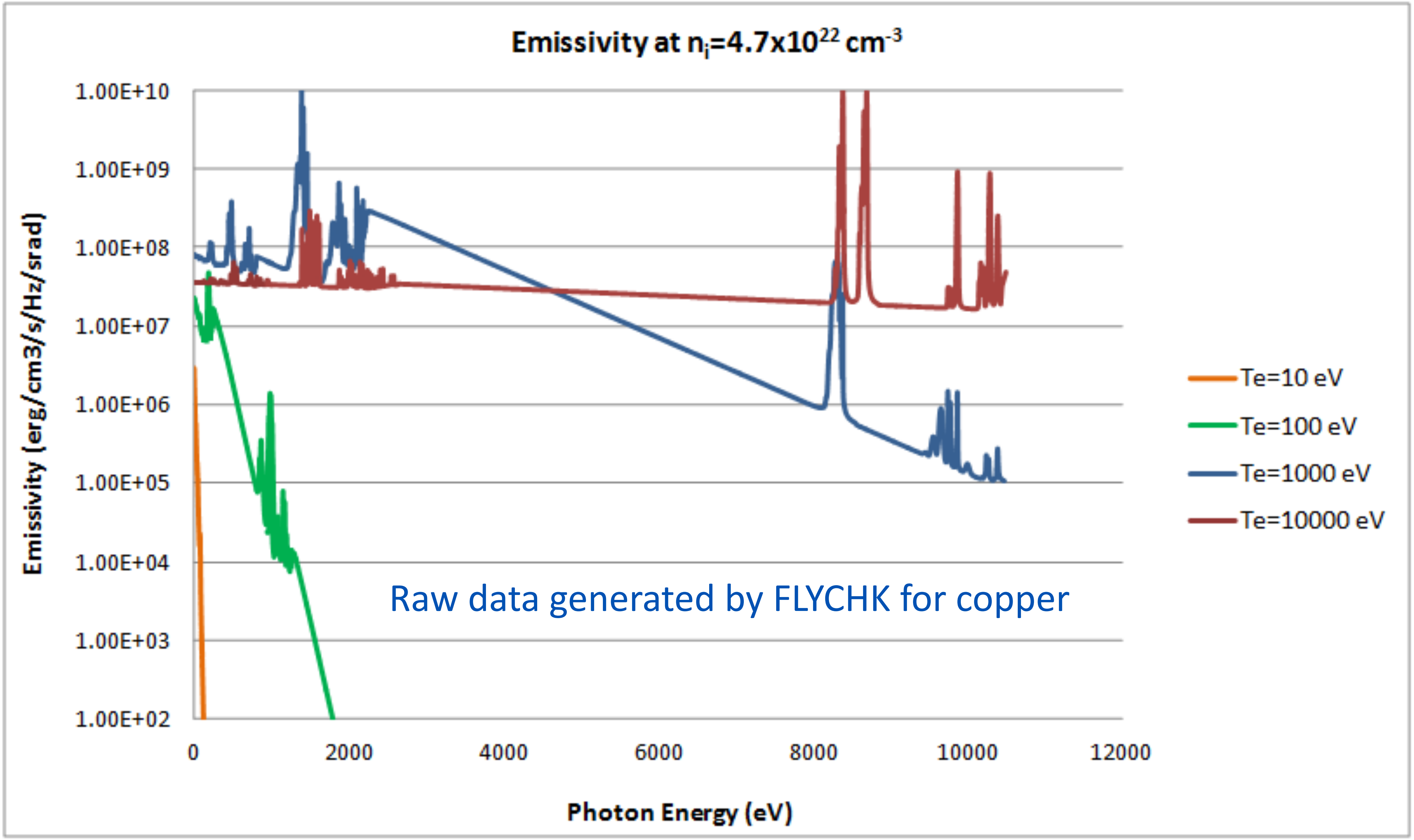

[1] H. K. Chung, M. H. Chen, W. L. Morgan, Y. Ralchenko, and R. W. Lee, High Energy Density Phys. 1, 3 (2005)

multi-group method for photon energies

- Radiation energy is divided into groups of finite energy width ΔE_g
- The transport equation (I, η, χ) is integrated over ΔE_g and then solved to obtain the radiation intensity I_g for each group.
- Groups are adaptively selected to better capture important spectral features

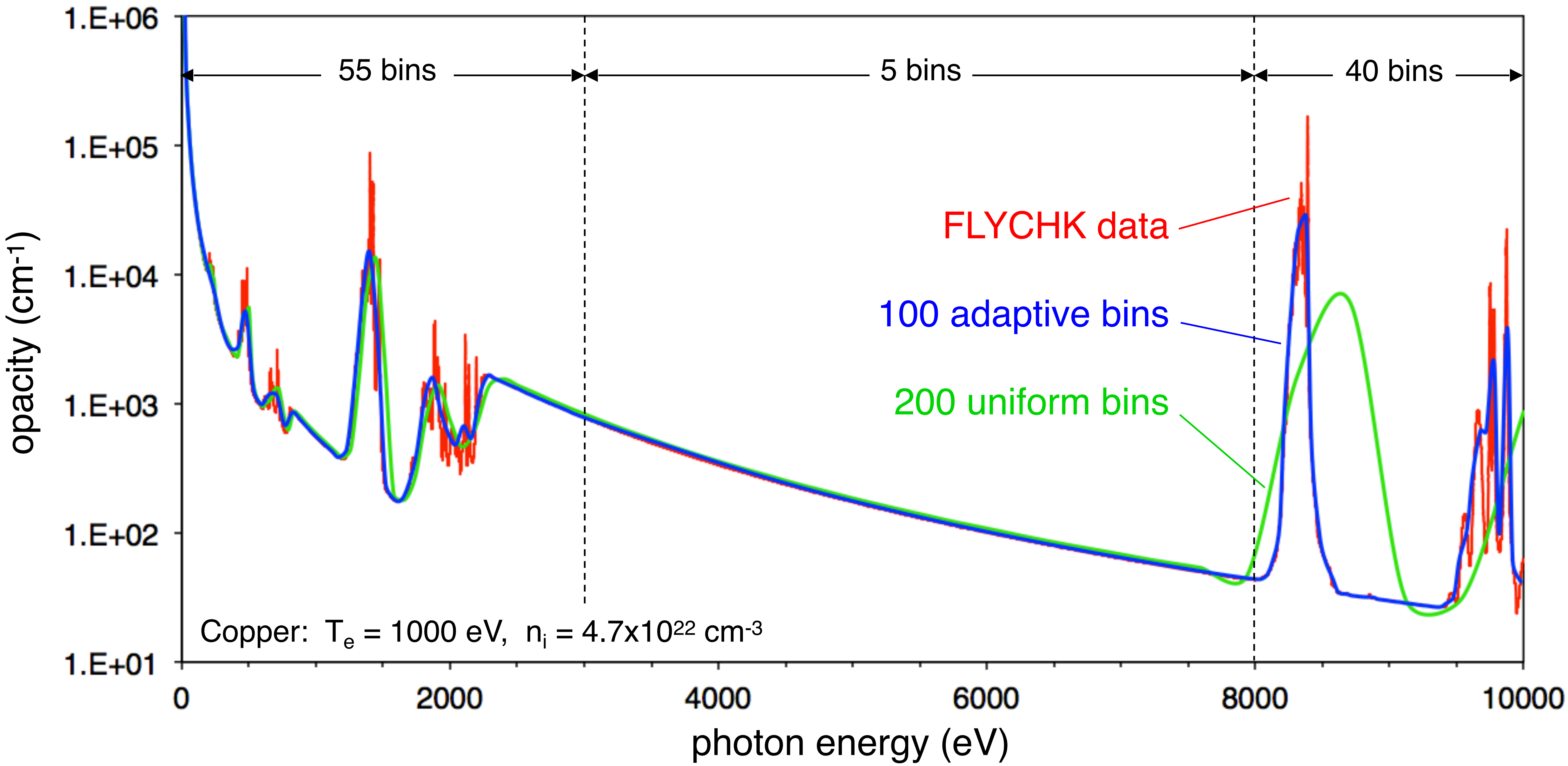

S_N method for angular directions

- For the angular variables (θ, ω), we apply the discrete ordinate S_N method
- The transport equation is solved for each discrete direction (m, n) to obtain the radiation intensity $I_{m,n}$ in that direction
- Typically, the 2π solid angle for the upper hemisphere is discretized into ~150 directions, while the lower hemisphere is assumed symmetric

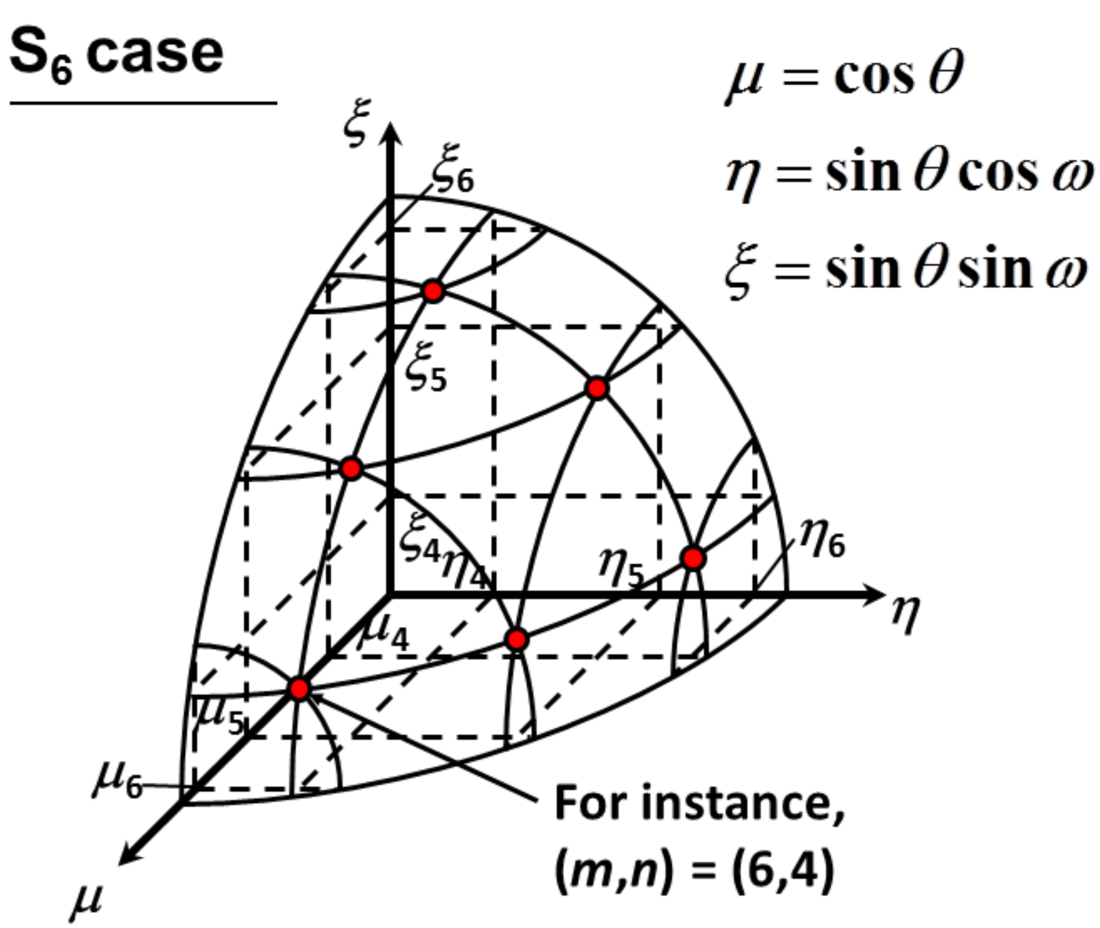

Lee, C.E., Los Alamos Scientific Laboratory Report LA-2595, 1962

The self-force is implemented in the code PICLS

PICLS, ref: Y.Sentoku and A. kemp, J. Comput. Phys. **227**, 6846 (2008)

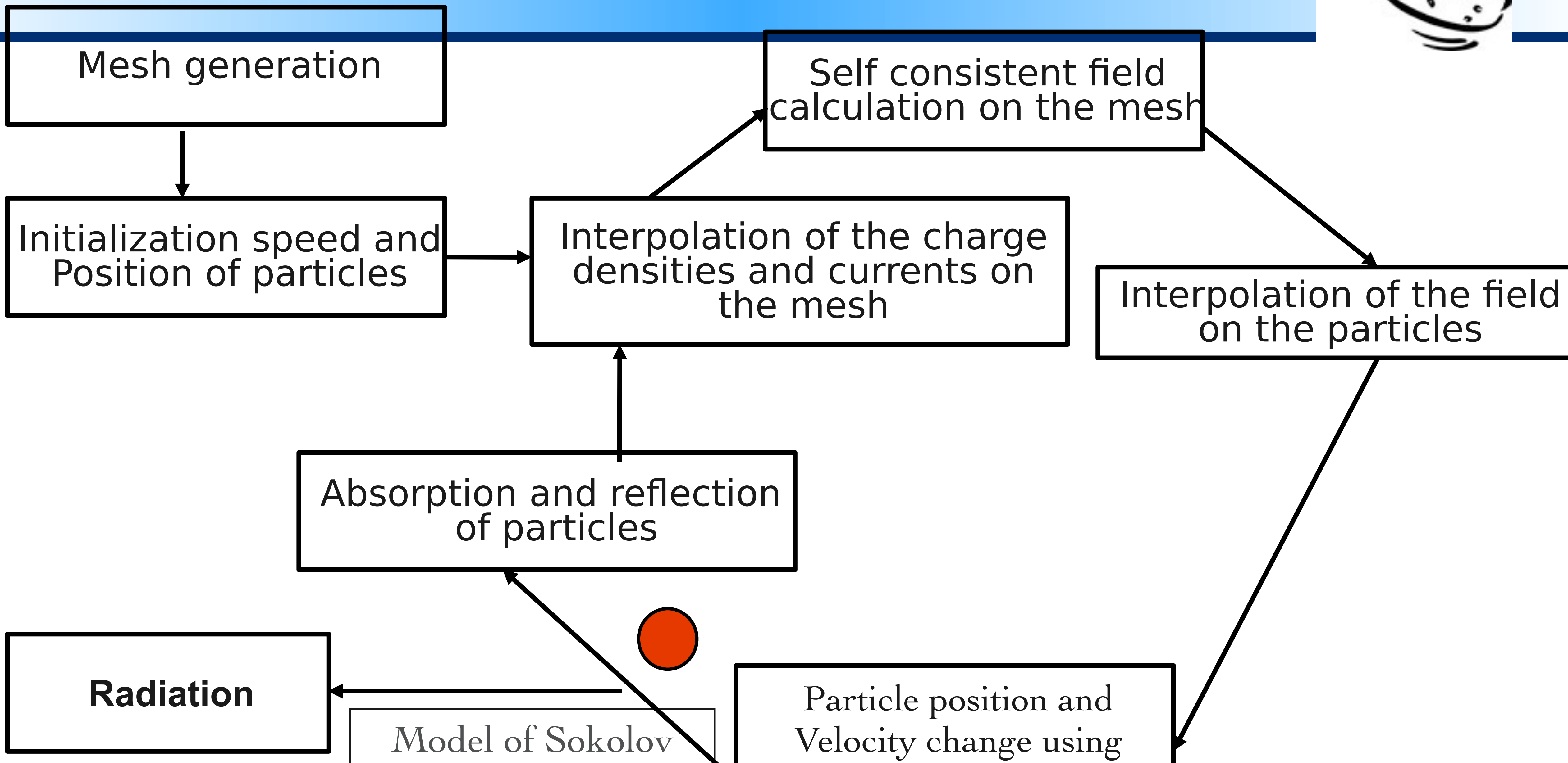

$$\frac{d\mathbf{p}_e}{dt} = \mathbf{f}_L - e\,\delta\mathbf{v}_e \times \mathbf{B} - \gamma_e^2(\mathbf{f}_L \cdot \delta\mathbf{v}_e)\mathbf{v}_e/c^2,$$

$$\frac{d\mathbf{x}_e}{dt} = \mathbf{v}_e + \delta\mathbf{v}_e, \quad \delta\mathbf{v}_e = \frac{\tau_0}{m_e}\frac{\mathbf{f}_L - \mathbf{v}_e(\mathbf{v}_e \cdot \mathbf{f}_L)/c^2}{1 + \tau_0(\mathbf{v}_e \cdot \mathbf{f}_L)/mc_e^2}$$

I.V. Sokolov and al, arXiv : 1102.3685v

R. Capdessus et al. PRE 2012

Underdense targets with a $\cos^2$ density profile

a_0=107.6, 8 T0, 6λ transverse FWHM, 3.66 n_c, H plasma, 60λ FWHM target. I=2.5×10^{22} W/cm^2

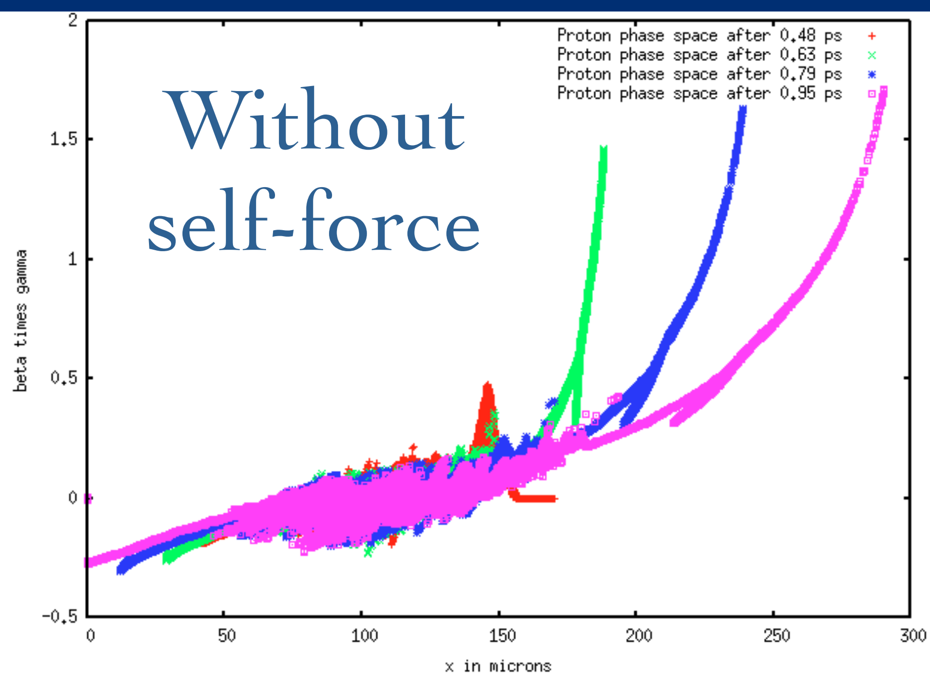

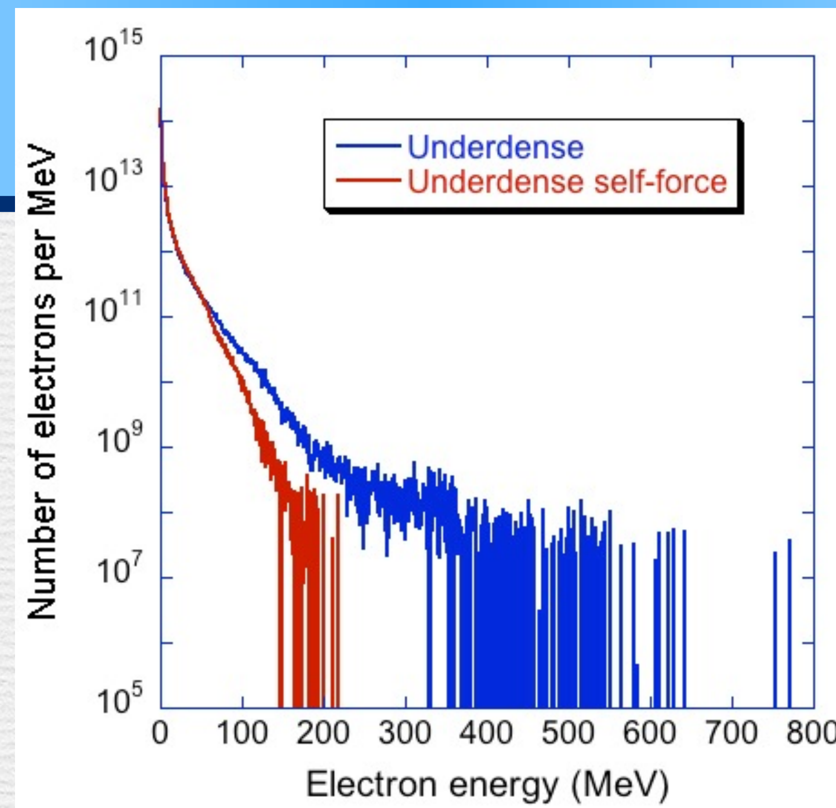

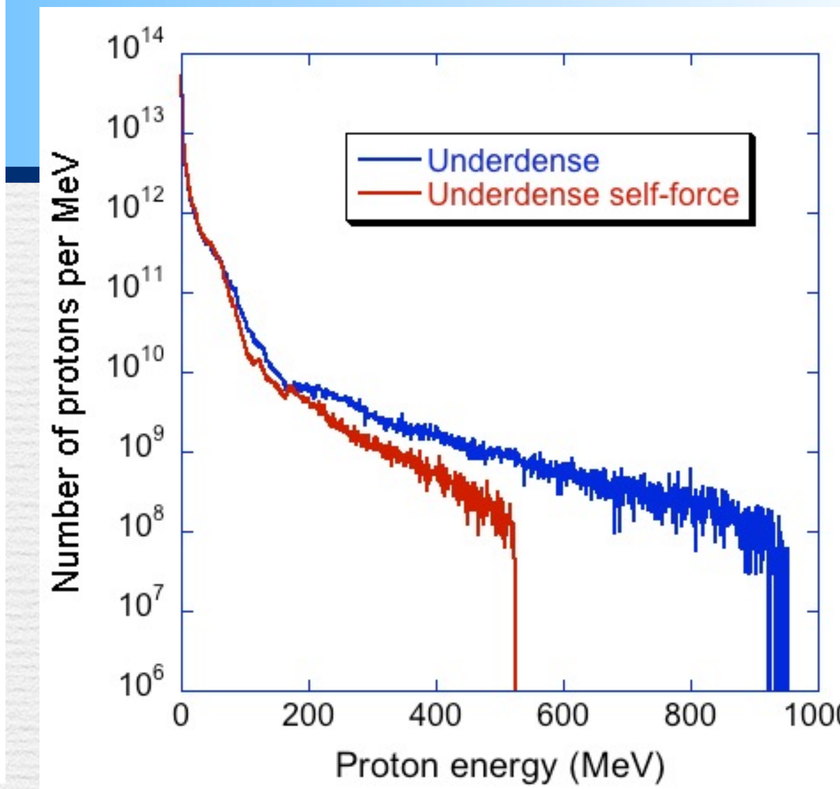

Proton phase space

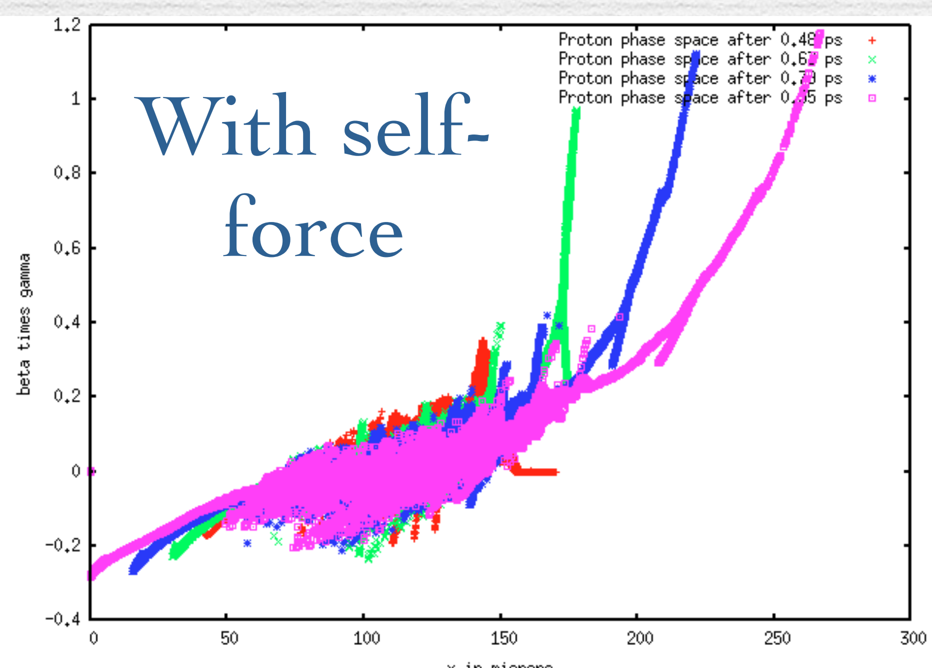

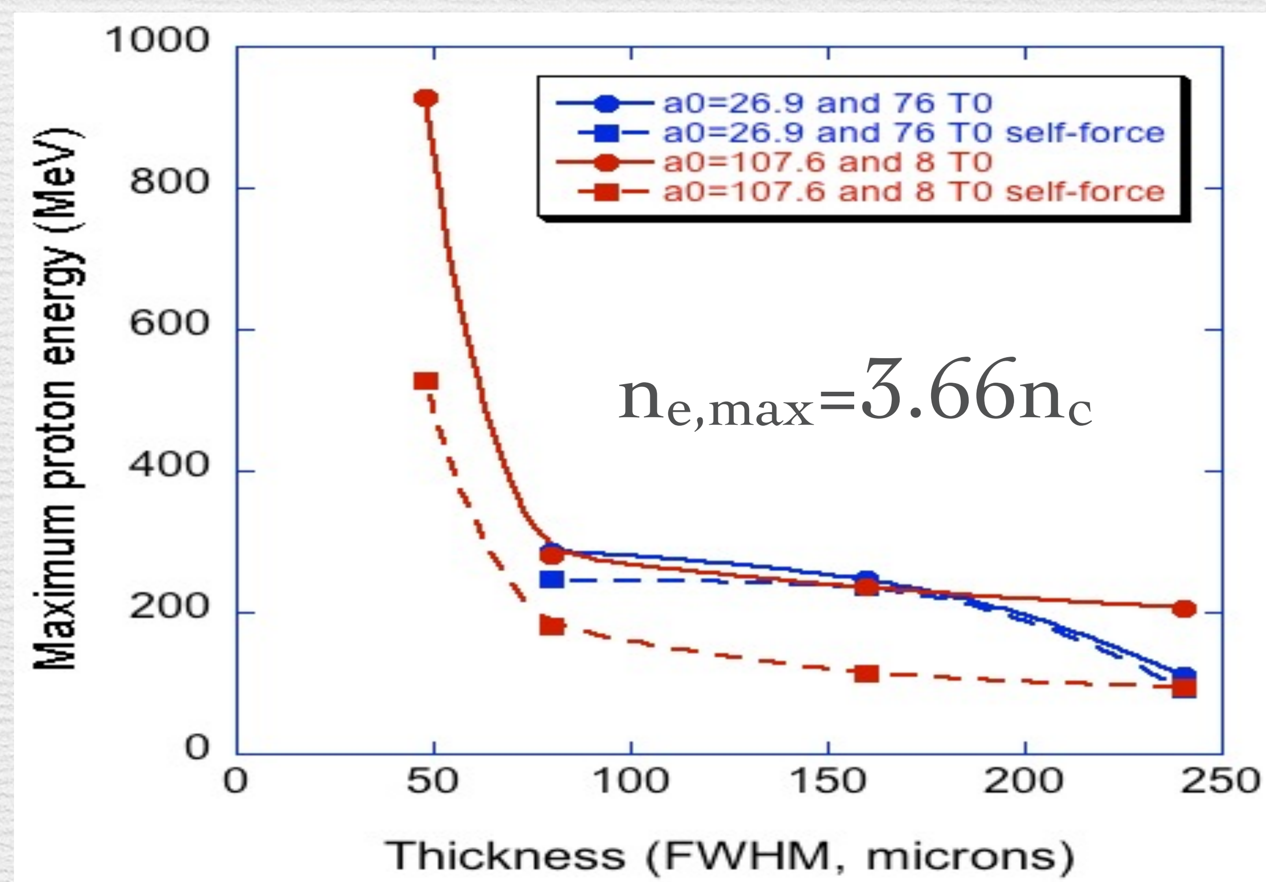

E. d'Humières et al. EPJ WoC 2013